Lecture Notes

-

Progettazione Assistita di Organi di Macchina
Progettazione del Telaio
FEM Fundamentals and Chassis Design

Enrico Bertocchi

June 7, 2019

Chapter 1

Spatial beam structures

1.1 Beam axis and cross section definition

A basic necessary condition for identifying a deformable body as a beam – and hence applying the associated framework – is that its centroidal curve be at least loosely recognizable.

Once such centroidal line has been roughly defined, locally perpendicular planes may be derived whose intersection with the body itself defines the local beam cross section.

Then, the G center of gravity position may be computed for each of the local cross sections, leading to a refined, potentially iterative definition for the beam centroidal axis[1].

A local cross-sectional reference system may be defined by aligning the normal z axis with the beam centroidal curve, and by employing, as the first in-section axis, namely x, the projection of a given global $\underline{v}$ vector, which is assumed not to be parallel to the beam axis.

The second in-section axis y may be then derived, in order to obtain a $Gxyz$ right-handed coordinate system, whose unit vectors are $\hat{i}, \hat{j}, \hat{k}$.

If a thin walled profile is considered in place of a solid cross section member – i.e., the section wall midplane is recognizable too (see paragraph XXX), then a curvilinear coordinate $0 \leq s \leq l$ may be defined that spans the in-cross-section wall midplane, along with a local through-wall-thickness coordinate $-t(s)/2 \leq r \leq +t(s)/2$.

Such s, r, in-section coordinates based on the profile wall may be employed in place of their cartesian x, y counterparts, if favourable.

Beam axis may be discontinuous at sudden body geometry changes; a rigid body connection is ideally assumed to restrict the relative motion of the proximal segments. Such rigid joint modeling may be extended to more complex n-way joints; if the joint finite stiffness is to be taken into account, it has to be described through the entries of a rank $6(n-1)$ symmetric square matrix [2].

At joints or beam axis angular points the cylindrical bodies swept by the cross sections do usually overlap, besides they only loosely mimic the actual deformable body geometry; the results obtained through the local application of the elementary beam theory may at most be

---

[1]Here, centroidal curve, centroidal line, centroidal axis, or simply beam axis are treated as synonyms.

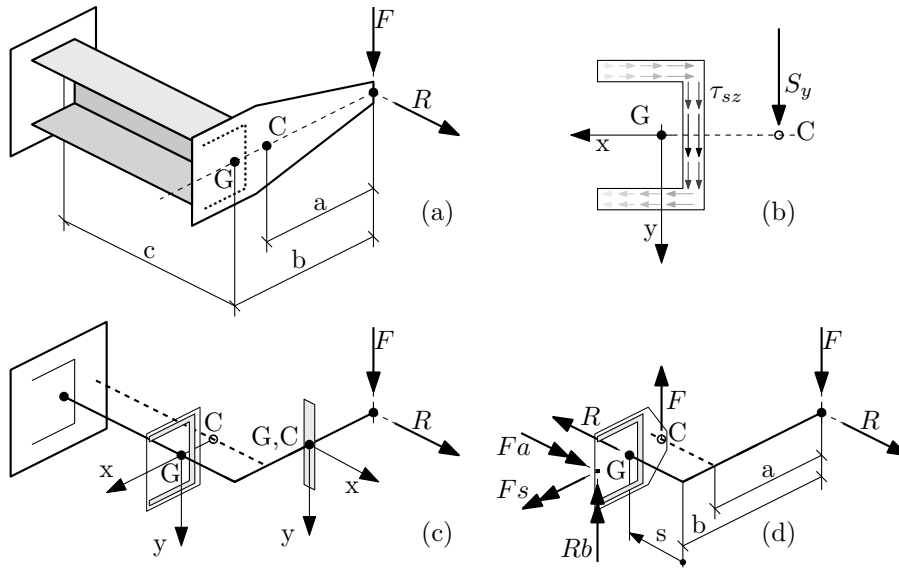[2]i.e., joint stiffness is unfortunately not a scalar value.

Figure 1.1: A beam structure.

employed to scale the triaxial local stress/strain fields[3], which have to be evaluated resorting to more complex modelings.

1.1.1 A worked example

See Figure 1.1. TODO.

1.2 Cross-sectional resultants for the spatial beam

At any point along the axis the beam may be notionally split, thus obtaining two facing cross sections, whose interaction is limited to three components of interfacial stresses, namely the axial normal stress σ_{zz} and the two shear components τ_{yz}, τ_{zx}.

Three force resultant components may be defined by integration along the cross section area, namely the normal force, the y- and the

---

[3]The peak stress values obtained through the elementary beam theory may be profitably employed as *nominal stresses* within the stress concentration effect framework.

x- oriented shear forces, respectively defined as

$$N = \int_A \sigma_{zz} dA$$

$$S_y = \int_A \tau_{yz} dA$$

$$S_x = \int_A \tau_{zx} dA$$

Three moment resultant components may be similarly defined, namely the x- and y- oriented bending moments, and the torsional moment. However, if the centroid is the preferred fulcrum for evaluating the bending moments, the below discussed C shear center is employed for evaluating the torsional moment. We hence define

$$M_x \equiv M_{(G,x)} = \int_A \sigma_{zz} y dA$$

$$M_y \equiv M_{(G,y)} = -\int_A \sigma_{zz} x dA$$

$$M_t \equiv M_{(C,z)} = \int_A \left[\tau_{yz}(x - x_C) - \tau_{zx}(y - y_C) \right] dA$$

The applied vector associated to the normal force component $(G, N\hat{k})$ is located at the section center of gravity , whereas the shear force $(C, S_x\hat{i} + S_y\hat{j})$ is supposed to act at the shear center; such convention decouples the energy contribution of force and moment components for the straight beam.

Cross section resultants may be obtained, based on equilibrium for a statically determinate structure. The ordinary procedure consists in

- notionally splitting the structure at the cross section whose resultants are under scrutiny;

- isolating a portion of the structure that ends at the cut, whose locally applied loads are all known; the structure has to be preliminarily solved for the all the constraint reactions that act on the isolated portion;

- setting the equilibrium equations for the isolated substructure, according to which the cross-sectional resultants are in equilibrium with whole loading.

1.3 Axial load and uniform bending

It is preliminarily noted that the elementary extensional-flexural solution is exact with respect to the Theory of Elasticity if the following conditions hold:

- beam constant section;

- beam rectilinear axis;

- absence of locally applied loads;

- absence of shear resultants[4] (i.e. constant bending moments);

- principal material directions of orthotropy are uniform along the section, and one of them is aligned with the beam axis;

- the ν_{31} and the ν_{32} Poisson's ratios[5] are constant along the section, where 3 means the principal direction of orthotropy aligned with the axis. Please note that $E_i \nu_{ji} = E_j \nu_{ij}$, and hence $\nu_{ji} \neq \nu_{ij}$ for a generally orthotropic material.

Most of the above conditions are in fact violated in many textbook structural calculations, thus suggesting that the elementary beam theory is robust enough to be adapted to practical applications, i.e. limited error is expected if some laxity is used in circumscribing its scope[6].

The extensional-flexural solution builds on the basis of the following simplifying assumptions:

- the in-plane[7] stress components $\sigma_x, \sigma_y, \tau_{xy}$ are null;

- the out-of-plane shear stresses τ_{yz}, τ_{zx} are also null;

---

[4] A locally pure shear solution may be in fact superposed; such solution may however not be available for a general cross section.

[5] We recall that ν_{ij} is the Poisson's ratio that corresponds to a contraction in direction j, being a unitary extension applied in direction i in a manner that the elastic body is subject to a uniaxial stress state.

[6] Measures for both the error and the violation have to be supplied first in order to quantify the approximation.

[7] Both the *in-plane* and the *out-of-plane* expressions for the characterization of the stress/strain components refer to the cross sectional plane.

- the axial elongation ϵ_z linearly varies along the cross section, namely

$$\epsilon_z = a + bx + cy \qquad (1.1)$$

or, equivalently[8], each cross section is assumed to remain planar in the deformed configuration.

The three general constants a, b and c possess a physical meaning; in particular a represents the axial elongation $\bar{\epsilon}$ as measured at the centroid[9], c represents the $1/\rho_x$ curvature[10] whereas b represent the $1/\rho_y$ curvature, apart from its sign.

Figure 1.2 (c) justifies the equality relation $c = 1/\rho_x$; the beam axial fibers with a Δz initial length are elongated by the curvature up to a $\Delta\theta\,(\rho_x + y)$ deformed length, where $\Delta\theta\rho_x$ equates Δz based on the length of the unextended fibre at the centroid. By evaluating the axial strain value for a general fiber, it follows that $\epsilon_z = 1/\rho_x\,y$.

In addition, Figure 1.2 (c) relates the $1/\rho_x$ curvature to the displacement component in the local y direction, namely v, and to the section rotation angle with respect to the local x axis, namely θ, thus obtaining

$$\frac{d\theta}{dz} = \frac{1}{\rho_x}, \quad \theta = -\frac{dv}{dz}, \quad \frac{d^2v}{dz^2} = -\frac{1}{\rho_x} \qquad (1.2)$$

Following analogous considerations, see 1.2 (e), we may similarly obtain

$$\frac{d\phi}{dz} = \frac{1}{\rho_y}, \quad \phi = +\frac{du}{dz}, \quad \frac{d^2u}{dz^2} = +\frac{1}{\rho_y} \qquad (1.3)$$

where ϕ is the cross section rotation about the local y axis, and u is the x displacement component.

According to the assumptions in the preamble, a uniaxial stress state is assumed, where the only nonzero σ_z stress component may be determined as

$$\sigma_z = E_z\epsilon_z = E_z\left(\bar{\epsilon} - \frac{1}{\rho_y}x + \frac{1}{\rho_x}y\right) \qquad (1.4)$$

---

[8]The axial, out-of-plane displacement $\Delta w = \int_{\Delta l} \epsilon_z dz = \Delta_l\,(a + bx + cy)$ accumulated between two contiguous cross sections with an Δl initial distance, is consistent with that of a relative rigid body motion.

[9]or, equivalently, the average elongation along the section, in an integral sense.

[10]namely the inverse of the beam curvature radii as observed with a line of sight aligned with the x axis. Curvature is assumed positive if the associated θ section rotation grows with increasing z, i.e. $d\theta/dz > 0$.
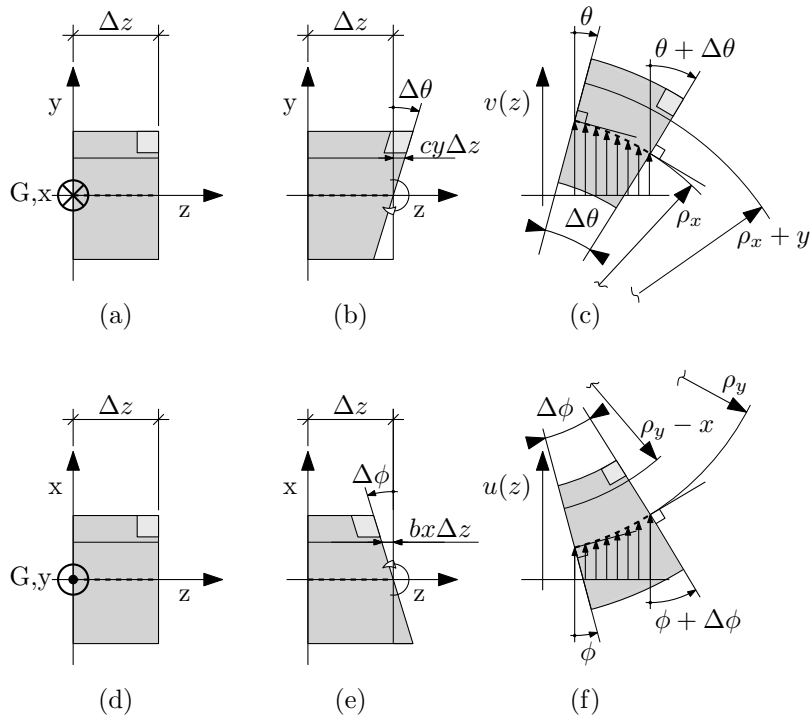
Figure 1.2: A differential fibre elongation proportional to the y coordinate induces a curvature $1/\rho_x$ on the normal plane with respect to the x axis. A differential fibre contraction proportional to the x coordinate induces a curvature $1/\rho_y$ on the normal plane with respect to the y axis. The didascalic trapezoidal deformation modes (b) and (e) clearly associate the differential elongation/contraction with the positive relative end rotation; they are however affected by a spurious shear deformation as evidenced by the skewed corner.
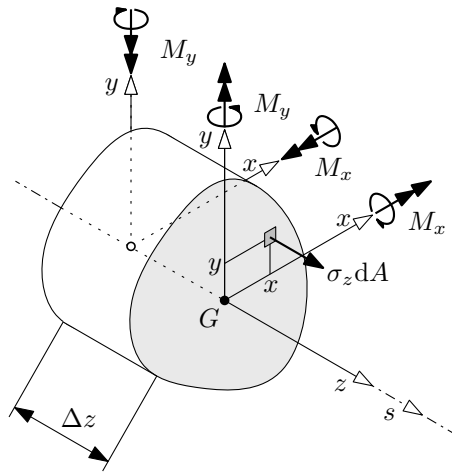
Figure 1.3: Positive x and y bending moment components adopt the same direction of the associated local axes at the beam segment end showing an outward-oriented arclength coordinate axis; at beam segment ends characterized by an inward-oriented local z axis, the same positive bending moment components are locally counter-oriented to the respective axes.

Stress resultants may easily be evaluated based on Fig. 1.3 as

$$N = \iint_A E_z \epsilon_z dA = \overline{EA}\bar{\epsilon} \tag{1.5}$$

$$M_x = \iint_A E_z \epsilon_z y dA = \overline{EJ}_{xx}\frac{1}{\rho_x} - \overline{EJ}_{xy}\frac{1}{\rho_y} \tag{1.6}$$

$$M_y = -\iint_A E_z \epsilon_z x dA = -\overline{EJ}_{xy}\frac{1}{\rho_x} + \overline{EJ}_{yy}\frac{1}{\rho_y} \tag{1.7}$$

where the combined material/cross-section stiffness moduli

$$\overline{EA} = \iint_A E_z(x,y)\, dA \tag{1.8}$$

$$\overline{EJ}_{xx} = \iint_A E_z(x,y)yy\, dA \tag{1.9}$$

$$\overline{EJ}_{xy} = \iint_A E_z(x,y)yx\, dA \tag{1.10}$$

$$\overline{EJ}_{yy} = \iint_A E_z(x,y)xx\, dA \tag{1.11}$$

may also be rationalized as the cross section area and moment of inertia, respectively, multiplied by a suitably averaged Young modulus, evaluated in the axial direction.

Those moduli simplify to their usual $E_z A, E_z J_{**}$ analogues, where the influence of the material and of the geometry are separated if the former is homogeneous along the beam cross section.

From Eqn. 1.5 we obtain

$$\bar{\epsilon} = \frac{N}{\overline{EA}}. \tag{1.12}$$

By concurrently solving Eqns. 1.6 and 1.7 with respect to the $1/\rho_x$ and $1/\rho_y$ curvatures, we obtain

$$\frac{1}{\rho_x} = \frac{M_x \overline{EJ}_{yy} + M_y \overline{EJ}_{xy}}{\overline{EJ}_{xx}\overline{EJ}_{yy} - \overline{EJ}_{xy}^2} \tag{1.13}$$

$$\frac{1}{\rho_y} = \frac{M_x \overline{EJ}_{xy} + M_y \overline{EJ}_{xx}}{\overline{EJ}_{xx}\overline{EJ}_{yy} - \overline{EJ}_{xy}^2} \tag{1.14}$$

$$\frac{1}{\rho_{\text{eq}}} = \sqrt{\frac{1}{\rho_x^2} + \frac{1}{\rho_y^2}} \tag{1.15}$$

Axial strain and stress components may then be obtained for any cross section point by substituting the above calculated generalized strain components $\bar{\epsilon}$, $1/\rho_x$ and $1/\rho_y$ holding for the extensional-flexural beam into Eqn. 1.4.

As an alternative, the following

thus obtaining

$$\sigma_z = E_z \epsilon_z \tag{1.16}$$
$$= \alpha M_x + \beta M_y + \gamma N \tag{1.17}$$

where

$$\alpha\left(x, y, E_z, \overline{EJ}_{**}\right) = E_z(x, y) \frac{-\overline{EJ}_{xy}x + \overline{EJ}_{yy}y}{\overline{EJ}_{xx}\overline{EJ}_{yy} - \overline{EJ}_{xy}^2} \tag{1.18}$$

$$\beta\left(x, y, E_z, \overline{EJ}_{**}\right) = E_z(x, y) \frac{-\overline{EJ}_{xx}x + \overline{EJ}_{xy}y}{\overline{EJ}_{xx}\overline{EJ}_{yy} - \overline{EJ}_{xy}^2} \tag{1.19}$$

$$\gamma\left(x, y, E_z, \overline{EA}\right) = E_z(x, y) \frac{1}{\overline{EA}}. \tag{1.20}$$

The peak axial strain is obtained at points farther from neutral axis of the stretched section; such neutral axis may be graphically defined as follows:

- the coordinate pair

$$(x_N, y_N) \equiv \left(\frac{\bar{e}\rho_x^2\rho_y}{\rho_x^2 + \rho_y^2}, -\frac{\bar{e}\rho_x\rho_y^2}{\rho_x^2 + \rho_y^2}\right);$$

  defines its nearest pass-through point with respect to the G centroid; the two points coincide in the case $\bar{\epsilon} = 0$.

- its orientation is defined by the unit vector

$$\hat{n}_\parallel = \sqrt{\rho_x^2 + \rho_y^2}\left(\frac{1}{\rho_x}, \frac{1}{\rho_y}\right),$$

  whereas the direction

$$\hat{n}_\perp = \sqrt{\rho_x^2 + \rho_y^2}\left(-\frac{1}{\rho_y}, \frac{1}{\rho_x}\right),$$

  is orthogonal to the neutral axis, and oriented towards growing axial elongations.

The cross section projection on the $(N, \hat{n}_\perp)$ line defines a segment whose ends are extremal with respect to the axial strain.

If the bending moment and the curvature component vectors are imposed to be parallel, i.e.

$$\lambda \begin{bmatrix} M_x \\ M_y \end{bmatrix} = \begin{bmatrix} \frac{1}{\rho_x} \\ \frac{1}{\rho_y} \end{bmatrix} = \underbrace{\frac{1}{EJ_{xx}EJ_{yy} - \overline{EJ}_{xy}^2} \begin{bmatrix} \overline{EJ}_{yy} & \overline{EJ}_{xy} \\ \overline{EJ}_{xy} & \overline{EJ}_{xx} \end{bmatrix}}_{[\overline{EJ}]} \begin{bmatrix} M_x \\ M_y \end{bmatrix} \quad (1.21)$$

an eigenpair problem is defined that leads to the definition of the principal directions for the cross sectional bending stiffness. In particolar, the eigenvectors of the $[\overline{EJ}]$ matrix define the two principal bending stiffness directions, and the associated $\overline{EJ}_{11}, \overline{EJ}_{22}$ eigenvalues constitute the associated bending stiffness moduli.

TODO: please elaborate...

1.4 Stresses due to the shear cross section resultants

In the presence of nonzero shear resultants, the bending moment exhibits a linear variation with the axial coordinate z in a straight beam. Based on the beam segment equilibrium we have

$$S_y = \frac{dM_x}{dz}, \quad S_x = -\frac{dM_y}{dz}, \tag{1.22}$$

as rationalized in Fig. 1.5, with $dz \to 0$ and M_x, M_y differentiable with respect to z.

The linear variation of the bending-induced curvature in z causes a likewise linear variation of the pointwise axial strain; stress variation is also linear in the case of constant E_z longitudinal elastic modulus.

In particular, the differentiation with respect to z of σ_z as espressed in Eqn. 1.17 returns

$$\frac{d\sigma_z}{dz} = \alpha\left(x, y, E_z, \overline{EJ}_{**}\right) S_y - \beta\left(x, y, E_z, \overline{EJ}_{**}\right) S_x \tag{1.23}$$

since its α, β, γ factors are constant with respect to z; the bending moment derivatives are here expressed in terms of the shear resultants, as in Eqns. 1.22.

Figure 1.4 rationalizes the axial equilibrium for an elementary volume of material; we have

$$\frac{d\tau_{zx}}{dx} + \frac{d\tau_{yz}}{dy} + \frac{d\sigma_z}{dz} + q_z = 0 \tag{1.24}$$

where, for the specific case, the distributed volumetric load q_z is zero.

It clearly emerges from such relation that the shear stresses τ_{zx}, τ_{yz}, that were null within the uniform bending framework, are non-uniform along the section – and hence not constantly zero – in the presence of shear resultants.

A treatise on the pointwise solution of a) the equilibrium equations 1.24, once coupled with b) the compatibility conditions and with c) the the material elastic response, is beyond the scope of the present contribution, although it has been derived for selected cross sections in e.g. [1].
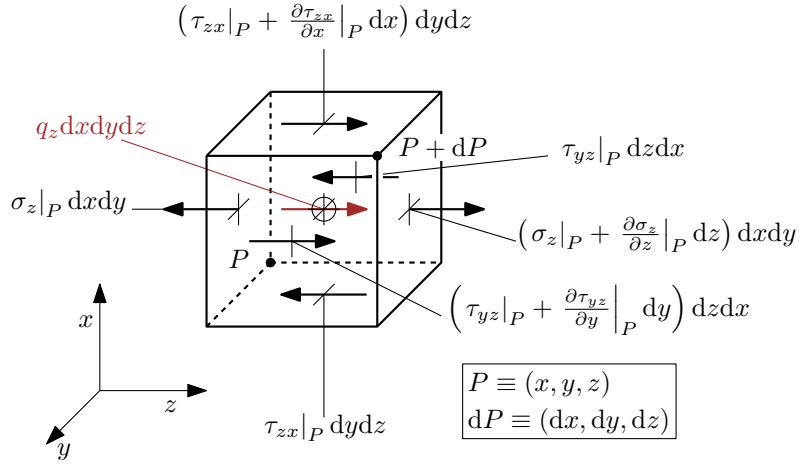
Figure 1.4: Equilibrium conditions with respect to the axial z translation for the infinitesimal volume extracted from the beam. In the case under scrutiny, the distributed volume action q_z is null.

1.4.1 The Jourawsky approach and its extension for a general section

The aforementioned axial equilibrium condition, whose treatise is cumbersome for the infinitesimal volume, may be more conveniently dealt with if a finite portion of the beam segment is taken into account, as in Figure 1.5.

A beam segment is considered whose axial extent is dz; the beam cross section is partitioned based on a (possibly curve, see Fig. 1.6) line that isolates an area portion A^* – and the related beam segment portion – for further scrutiny; axial equilibrium equation may then be stated for the isolated beam segment portion as follows

$$\bar{\tau}_{zi} t = \int_{A^*} \frac{d\sigma_z}{dz} dA, \qquad (1.25)$$

where

$$\bar{\tau}_{zi} = \frac{1}{t} \int_t \tau_{zi} dr \qquad (1.26)$$

is the average shear stress acting in the z direction along the cutting surface; i is the (locally normal) inward direction with respect to such
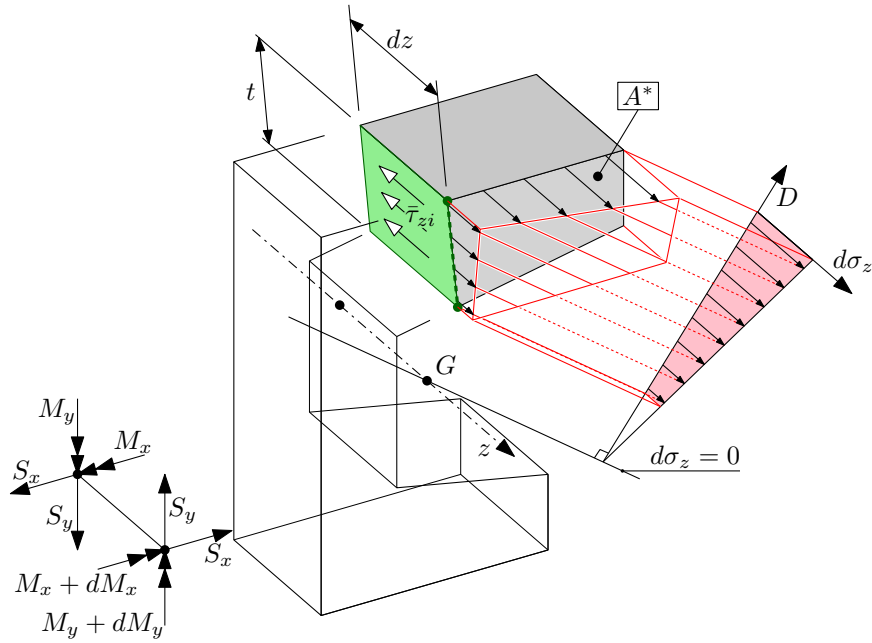
Figure 1.5: Equilibrium conditions for the isolated beam segment portion. It is noted that the null σ_z variation locus, $d\sigma_z = 0$, does not coincide with the bending neutral axis in general. Also, the depicted linear variation of $d\sigma_z$ with the D distance from such null $d\sigma_z$ locus does not hold in the case of non-uniform E_z modulus.

Figure 1.6: The curve employed for isolating the beam segment portion defines the direction of the τ_{zi} components whose average value is evaluated.

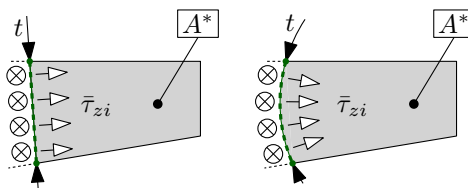a surface. Due to the reciprocal nature of the shear stresses, the same $\bar{\tau}_{zi}$ shear stress acts along the cross sectional plane, and locally at the cutting curve itself. These shear actions are assumed positive if inward directed with respect to A^*.

The $\bar{\tau}_{zi}t$ product is named *shear flow*, and may be evaluated along a general cutting curve.

It is noted that, according to Eqn. 1.25, no information is provided with regard to a) the τ_{zr} shear stress that acts parallel to the cutting curve, nor b) the pointwise variation of τ_{zi} with respect of its average value $\bar{\tau}_{zi}$. If the resorting to more cumbersome calculation frameworks is not an option, those quantities are usually just neglected; an informed choice for the cutting curve is thus critical for a reliable application of the method.

In the simplified case of a) uniform material and b) local x, y axes that are principal axes of inertia (i.e. $J_{xy} = 0$), the usual formula is obtained

$$\bar{\tau}_{zi}t = \int_{A^*} \left(\frac{yS_y}{J_{xx}} + \frac{xS_x}{J_{yy}} \right) dA = \frac{\bar{y}^* A^*}{J_{xx}} S_y + \frac{\bar{x}^* A^*}{J_{yy}} S_x, \qquad (1.27)$$

where $\bar{y}^* A^*$ and $\bar{x}^* A^*$ are the first order area moments of the A^* section portion with respect to the x and y axes, respectively[11].

1.4.2 Shear induced stresses in an open section, thin walled beam

In the case of thin walled profiles, the integral along the isolated area in Eqn. 1.25 may be performed with respect to the arclength coordinate alone; the value the $d\sigma_z/dz$ integrand assumes at the wall midplane is supposed representative of its integral average along the wall thickness, thus obtaining

$$\bar{\tau}_{zi}t = q_{zi} = \int_0^s \int_{-t/2}^{t/2} \frac{d\sigma_z}{dz} dr d\varsigma \approx \int_0^s \left. \frac{d\sigma_z}{dz} \right|_{r=0} td\varsigma. \qquad (1.28)$$

Such assumed equivalence strictly holds for a) straight wall segments[12] and b) a linear variation of the integrand along the wall, a

---

[11] According to the employed notation, $(\bar{x}^*, \bar{y}^*)$ are the centre of gravity coordinates for the A^* area.

[12] i.e. the Jacobian of the $(s, r) \mapsto (x, y)$ mapping is constant with r.

condition, the latter, that holds if the material properties are homogeneous with respect to the wall midplane[13]; in the more general case, the error incurred by this approach vanishes with vanishing thickness for what concerns assumption a), whereas if the material is inhomogeneous, through-thickness averaged $\bar{E}_z, \bar{G}_{zi}$ moduli may be employed in place of their pointwise counterpart.

If a thin walled section segment is considered such that it is not possible to infer that the interfacial shear stress is zero at at least one of its extremities, a further term needs to be considered for the equilibrium, thus obtaining

$$\bar{\tau}_{zi}(s)t(s) = q(s) = \int_a^s \frac{d\sigma_z}{dz} t d\varsigma + \underbrace{\bar{\tau}_{zi}(a)t(a)}_{q_A}. \qquad (1.29)$$

In the case of open thin walled profiles, however, such a choice for the isolated section portion is suboptimal, unless the q_A term is known.

1.4.3 Shear induced stresses in an closed section, thin walled beam

In the case of a closed thin walled, generally asymmetric section, the search for a point along the wall at which the shear flow may be assumed zero is normally not viable, and the employment of Eq. 1.29 in place of the simpler Eq. 1.28 is unavoidable.

In this case, a parametric value for the $\bar{\tau}_{iz}$ shear stress is assumed for a set of points along the cross section midcurve – one for each elementary closed loop[14] if the points are non-redundantly chosen[15].

In the multicellular cross section example shown in Figure 1.7, two elementary loops are detected; shear flows at the A, B points are parametrically defined as $\tau_A t_A$ and $\tau_B t_B$, respectively.

The $\tau(s)$ shear stress at each point along the profile wall may then be determined based on Eqn. 1.29 as a function a) of the shear resultant

---

[13]a linear $d\epsilon_z/dz$ axial strain variation is in fact associated to the curvature variation in z, and not an axial stress variation;

[14]i.e. a closed loop not enclosing any other closed loop.

[15]Redundancy may be pointed out by ideally cutting the cross section at these points: if a monolithic open cross section is obtained, the point choice is not redundant; if a portion of the section is completely isolated, and a loop remains closed, the location of these points causes redundancy.
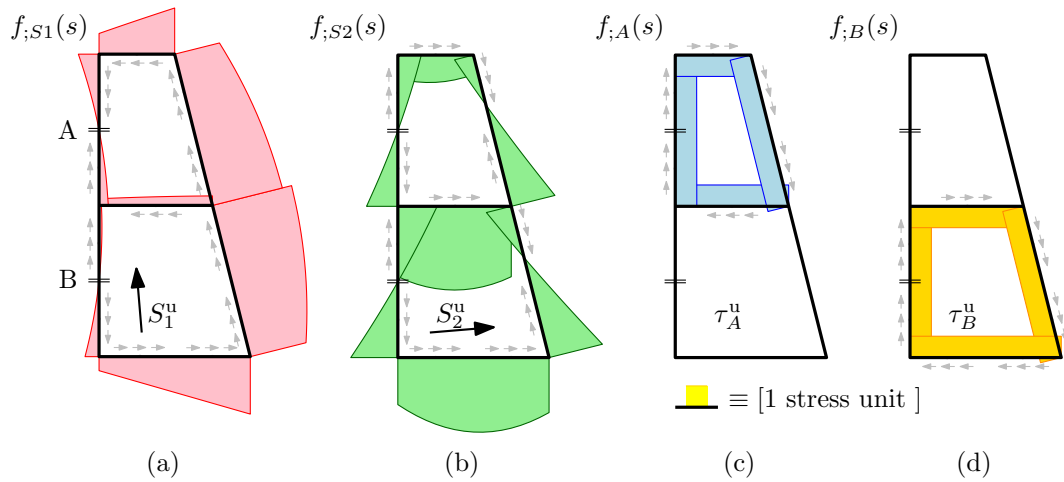
Figure 1.7: Contributions to the $\tau_{zi}(s)$ shear stress along the profile walls associated to a) a unit shear force component S_1^{u} applied along the first principal axis of inertia, whose magnitude equals the product of the cross section area and the unit stress, b) an analogous shear force component S_2^{u} aligned with the second principal axis of inertia, c) a unit shear stress τ_A^{u} applied at the opposite fictitious cut surfaces at A, and d) a unit shear stress τ_B^{u} applied at the opposite fictitious cut surfaces at B. Profile wall thickness is constant in the presented example, thus producing a continuous shear stress diagram, whereas continuity is rather aa unit shear stress τ_A^{u} applied at the opposite fictitious cut surfaces at a property of the shear flow.

components S_x and S_y, and b) of the parametrically defined shear stresses at the A,B points.

Due to the assumed linear response for the profile, superposition principle may be employed in isolating the four elementary contributions to the shear stress flow along the section.

The first two elementary contributions $f_{;Sx}(s)$ and $f_{;Sy}(s)$ are respectively due to the action alone of the x and y shear force components, whose magnitudes S_x^{u} and S_y^{u} is assumed equal the product of the stress unit (e.g. 1 MPa) and of the cross sectional area. Those forces are assumed to act in the ideal absence of shear flow at points where the latter is assumed as a parameter (points A and B in Figure 1.7).

Since the condition of zero shear flow is stress-compatible with an opening in the closed section loop, the cross section may be idealized as severed at the assumed shear flow points, and hence open. The equilibrium-based solution procedure derived for the open thin-walled section may hence be profitably applied.

A family of further elementary contributions, one for each of the assumed shear stress points, may be derived by imposing zero parametric shear flow at all the points but the one under scrutiny, and in the absence of externally applied shear resultants. The elastic problem may be rationalized as an open – initially closed, then ideally severed – thin walled profile, that is loaded by an internal constraint action whose magnitude is unity in terms of stresses. Equilibrium considerations reduce to the conservation of the shear flow due to the absence of $d\sigma_z/dz$ differential axial stress, as in the case of a closed profile under torsion discussed below.

Figures 1.7 (a) and (b) show the shear stress contributions $f_{;S1}(s)$ and $f_{;S2}(s)$ induced in the ideally opened (i.e. zero redundant shear flows at the A,B points) multicellar profile by the first and the second shear force components, respectively; due to the author distraction, such figure refers to shear components aligned with the principal directions of bending stiffness, and not to the usual x,y axes.

Figures 1.7 (c) and (d) show the shear stress contributions $f_{;A}(s)$ and $f_{;B}(s)$ associated to unity values for the parametric shear flows at the A, B segmentation points, respectively.

The cumulative shear stress distribution for the section in Figure

1.7 is

$$\tau(s) = \frac{S_1}{\mathcal{A}} f_{;S1}(s) + \frac{S_2}{\mathcal{A}} f_{;S2}(s) + \tau_A f_{;A}(s) + \tau_B f_{;B}(s) \qquad (1.30)$$

where s is a suitable arclength coordinate.

The associated elastic potential energy may then be integrated over a Δz beam axial portion, thus obtaining

$$\Delta U = \int_s \frac{\tau^2}{2G_{sz}} t \Delta z ds \qquad (1.31)$$

According to the Castigliano second theorem, the ΔU derivative with respect to the $\bar{\tau}_i$ assumed shear stress value at the i-th segmentation point equates the generalized displacement with respect to which the internal constraint reaction works, i.e. the $t\Delta z \bar{\delta}_i$ integral of the relative longitudinal displacement between the cut surfaces; we hence have

$$\frac{\partial \Delta U}{\partial \bar{\tau}_i} = \bar{\delta}_i t \Delta z \qquad (1.32)$$

The $\bar{\delta}_i$ symbol refers to the average value along the $t\Delta z$ area of such axial relative displacement.

Material continuity requires zero $\bar{\delta}_i$ value at each segmentation point, thus defining a set of equations, one for each $\bar{\tau}_i$ unknown parameter, whose solution leads to the definition of the actual shear stress distribution along the closed wall profile.

1.5 Shear stresses due to the St. Venant torsion

The classical solution for the rectilinear beam subject to uniform torsion predicts a displacement field that is composed by the superposition of a) a rigid, in-plane[16] cross section rotation about the shear centre, named twist, whose axial rate is uniform, and b) an out-of-plane *warping* displacement that is uniform in the axial direction, whereas it varies within the section; such warping displacement is zero in the case of axisymmetric sections only (e.g. solid and hollow circular cross sections).

Due to the rigid nature of the in-plane displacements, the in-plane strain components ϵ_x, ϵ_y, ϵ_{xy} are zero; the in-plane stress components σ_x, σ_y, τ_{xy}, and the normal stress σ_z are also zero if z is a direction of orthotropy for the material – as it is assumed in the following. The motion is internally restricted only due to the nonzero out-of-plane shear stresses τ_{yz} and τ_{zx}, that develop as an elastic reaction to the associated strain components.

A more in-depth treatise of the topic involves the solution of an plane, inhomogeneous Laplace partial differential equation with essential conditions imposed at the cross section boundary, which is beyond the scope of the present contribution.

However, in the case of open- and closed- section, thin walled beams, simplified solutions are available based on the assumptions that a) the out-of-plane shear stresses are locally aligned to the wall midsurface - i.e. $\tau_{zr} = 0$ leaving τ_{zs} as the only nonzero stress component[17], and b) the residual τ_{zs} shear component is either constant by moving through the wall thickness (closed section case), or it linearly varies with the through-thickness coordinate r.

1.5.1 Solid section beam

TODO.

---

[16]the rotation vector is actually normal to the cross sectional plane; the *in-plane* motion characterization refers to the associated displacement field.

[17]Here, the notation introduced in paragraph XXX for the thin walled section is employed.
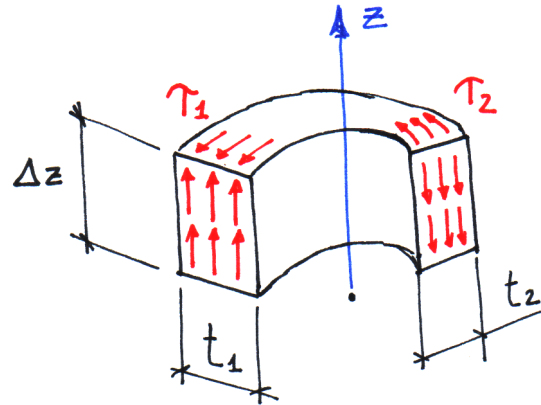
Figure 1.8: Axial equilibrium for a portion of profile wall, in the case of a closed, thin-walled profile subject to torsion.

1.5.2   Closed section, single-celled thin walled beam

The τ_{sz} component is assumed uniform along the wall thickness, or, equivalently, its deviation from the average value is neglected in calculations.

In the case the material is non-uniform across the thickness, the γ_{sz} shear strain is assumed uniform, whereas the τ_{sz} varies with the varying G_{sz} shear modulus.

In the absence of σ_z, the axial equilibrium of a portion of beam segment dictates that the shear flow $t\tau$ remains constant along the wall, i.e.

$$t_1\tau_1 = t_2\tau_2$$

as depicted in Figure 1.8.

By skipping some further interesting observations (TODO) we may just introduce the Bredt formula for the cross-section torsional stiffness

$$K_t = \frac{4A^2}{\oint \frac{1}{t}dl} \tag{1.33}$$

which is valid for single-celled, closed thin wall sections.

The peak stress is located at thinnest point along the wall, and equals

$$\tau_{\max} = \frac{M_t}{2t_{\min}A} \tag{1.34}$$

.

1.5.3   Closed section, multi-celled thin walled beam

TODO. However, a lower bound for the stiffness of the multi-celled thin walled beam may be obtained by fictitiosly severing the inner walls, thus obtaining a single cell defined by the outer wall alone.

An upper bound for the stiffness is obtained by assuming each shared inner wall as shear-rigid, and then by summing the stiffnesses of each elementary closed loop, as they constituted independent profiles. The shear-rigid nature of the inner walls is enforced by neglecting their contribution to the circuital integral at the Bredt formula denominator.

1.5.4   Open section, thin walled beam

The shear strain component γ_{zs} is assumed linearly varying across the thickness; if the G_{sz} shear modulus is assumed uniform, such linear variation characterizes the τ_{zs} stress components too.

The average value along the thickness of the τ_{zs} stress component is zero, as zero is the shear flow as defined in the previous paragraph.

For thin enough open sections of uniform and isotropic material we have

$$K_T \approx \frac{1}{3} \int_0^l t^3(s)ds \tag{1.35}$$

If the thin-walled cross section may be described as a sequence of constant thickness wall segments, the simplified formula

$$K_T \approx \frac{1}{3} \sum_i l_i t_i^3 \tag{1.36}$$

is obtained where t_i and l_i are respectively the length and the thickness of each segment.

The peak value for the τ_{zs} stress component is observed in correspondence to thickest wall section point and it equates
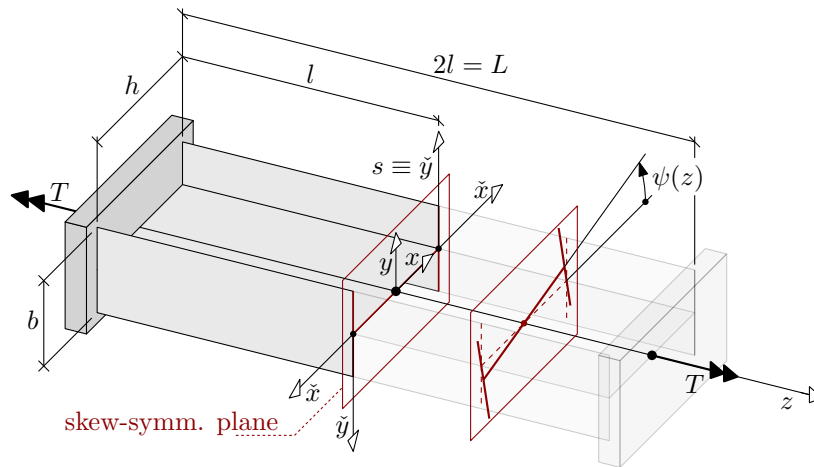
Figure 1.9: The problem under scrutiny.

$$\tau_{\max} = \frac{M_t t_{\max}}{K_T} \tag{1.37}$$

By applying the reported formulas to a rectangular section whose span length is ten times the wall thickness, the torsional stiffness is overestimated by slightly less than 7%; a similar relative error is reported in terms of shear stress underestimation.

1.5.5 Torsional stiffening due to restrained warping at profile ends: Vlasov torsion theory

As a pedagogical introduction to the restrained warping torsion, an open, thin-walled I-section beam[18] is considered whose each end is butt-welded to a massive plate, see Fig. 1.9, that locally impede the warping deformation at the base of the de Saint Venant torsion theory.

Two opposite torsional moments T are applied that induce an axial counter-rotation of the beam terminals, and hence a twist deformation of the profile, quantified this through the $\psi(z)$ section twist angle.

The cross sectional motion is limited to a twist rotation around the z axis, which is centroidal with respect to shear, plus the restrained

---

[18]also named H-section, double-T, based on normalized profile codes, e.g. IPN, IPE, or UC beams

cross-section twist — blade twist — blade widthwise displacement — blade transverse displacement
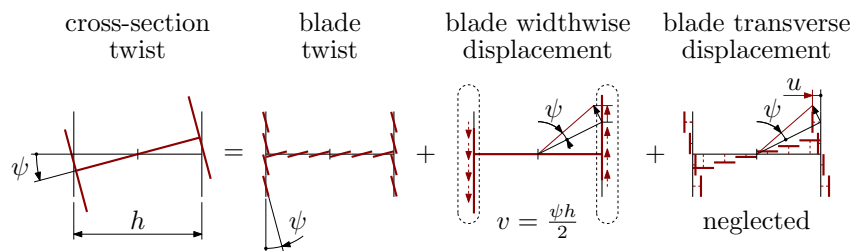
$$v = \frac{\psi h}{2}$$

neglected

Figure 1.10: XXX

warping out-of-plane displament.

In Figure 1.10 the profile walls are ideally partitioned into a set of limited width blades; the profile cross section rotation induces at the blade sections three distinct motions, i.e. a) a twist rotation, b) a widthwise translation, and c) a transverse translation with respect to the blade width.

The axial rate of the twist motion a) is at the base of the de St. Venant torsional model for open thin walled sections, which covers it exhaustively; conversely, the second order axial rate of the b) and c) translations induce bending curvatures at the blades, whose contribution to the internal energy increases the profile stiffness in torsion.

In particular, whereas the c) contribution acts along the blade bending weak axis and is usually neglected, the b) contribution is considerable and it constitutes the basis of the Vlasov restrained torsion theory for thin walled profiles. According to such a theory, blades a

Various formulas

x+ flange bending

$$V = \frac{dM_x}{dz}$$

$$T = hV = h\frac{dM_x}{dz}$$

since $\frac{M_x}{EJ_{xx}} = \frac{1}{\rho_x} = -\frac{d^2v}{dz^2}$, we substitute in the equation above $M_x = -\overline{EJ}_{xx}\frac{d^2v}{dz^2}$, thus obtaining

$$T = -h\overline{EJ}_{xx}\frac{d^3v}{dz^3}$$

24
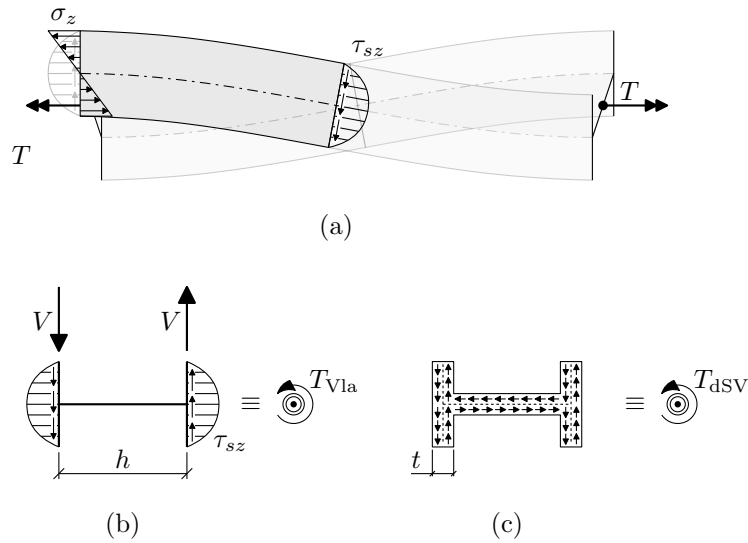
Figure 1.11: XXX

The v transverse displacement may be determined based on the local twist angle ψ as

$$v = \frac{h}{2}\psi$$

and a torque to (third derivative of) twist angle may be finally determined as

$$T = -\frac{h^2}{2}\overline{EJ}_{xx}\frac{d^3\psi}{dz^3} = -\overline{EC_w}\frac{d^3\psi}{dz^3}$$

where the $\overline{EC_w}$ cross-sectional constant for warping has been defined for the I beam as

$$\overline{EC_w} = I\frac{h^2}{2}.$$

Such T torsional moment, which is transmitted based on the flange shear load under restrained warping condition, will be referred to in the following as T_{Vla}, as opposed to its counterpart according to the de St. Venant torsion theory, i.e.

$$T_{\text{dSV}} = GK_t\frac{d\psi}{dz}.$$

Characteristic length of the cross section with respect to the Vlasov (restrained warping) torsion theory.

$$d = \sqrt{\frac{EC_w}{GK_t}}$$

The cross-sectional constant for warping may then be evaluated as

$$EC_w = d^2 GK_t$$

where GK_t is the torsional stiffness for the cross-section (material properties included) according to the free-warp, de St. Venant torsion theory.

Since the overall torsional moment is constant along the beam in the absence of distributed torsional actions, and it consists in the sums of the two T_{Vla} and T_{dSV} contributes, we have

$$0 = \frac{dT}{dz} = +\frac{dT_{\text{dSV}}}{dz} + \frac{dT_{\text{Vla}}}{dz} = -EC_w \frac{d^4\psi}{dz^4} + GK_t \frac{d^2\psi}{dz^2}$$

$$0 = -d^2 \frac{d^4\psi}{dz^4} + \frac{d^2\psi}{dz^2}$$

which is a 4th-order differential equation in the ψ unknown function, whose solutions take the general form

$\psi(z) = C_1 \sinh \frac{z}{d} + C_2 \cosh \frac{z}{d} + C_3 \frac{z}{d} + C_4$

In the theory of restrained torsion warping, an auxiliary, higher order resultant moment quantity named //bimoment// is introduced, that for the pedagogical I-section example is related to the flange bending moment by the identity

$$B = M_{xx} \cdot h$$

In general, we have

$$B = -EC_w \frac{d^2\psi}{dz^2};$$

axial stresses along the cross section linearly scale with the bimoment quantity, if the material behaves elastically.

Warping related boundary conditions may be stated as follows: free warping: $\frac{d^2\psi}{dz^2} = 0$, i.e. absence of bimoment, $B = 0$; no warping:
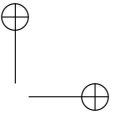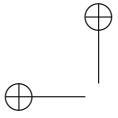
$\frac{d\psi}{dz} = 0$, i.e. absence of de St. Venant transmitted moment, $T_{\mathrm{dSV}} = 0$; Imposed rotations and imposed torsional moments complementary boundary conditions may be defined as usual.
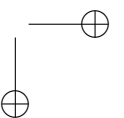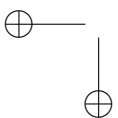
1.6 Castigliano's second theorem and its applications

Castigliano's second theorem may be employed for calculating deflections and rotations, and it states:

> If the strain energy of an elastic structure can be expressed as a function of generalised loads Q_i (namely, forces or moments) then the partial derivative of the strain energy with respect to generalised forces supplies the generalised displacement q_i (namely displacements and rotations with respect to which the generalized forces work).

In equation form,

$$q_i = \frac{\partial U}{\partial Q_i}$$

where U is the strain energy.

1.7 Internal energy for the spatial straight beam

The linear density of the elastic potential (alternatively named internal) energy for the spatial rectilinear beam may be derived as a function of its cross section resultants, namely

$$\frac{dU}{dl} = \frac{J_{\eta\eta}M_\xi^2 + J_{\xi\xi}M_\eta^2 + 2J_{\xi\eta}M_\xi M_\eta}{2E\left(J_{\xi\xi}J_{\eta\eta} - J_{\xi\eta}^2\right)} + \frac{N^2}{2EA} \tag{1.38}$$

$$+ \frac{\chi_\xi S_\xi^2 + \chi_\eta S_\eta^2 + \chi_{\xi\eta}S_\eta S_\xi}{2GA} + \frac{M_t^2}{2GK_t} \tag{1.39}$$

where

- A, $J_{\eta\eta}$, $J_{\xi\xi}$ and $J_{\xi\eta}$ are the section area and moments of inertia, respectively;

- K_t is the section torsional stiffness (**not** generally equivalent to its polar moment of inertia);
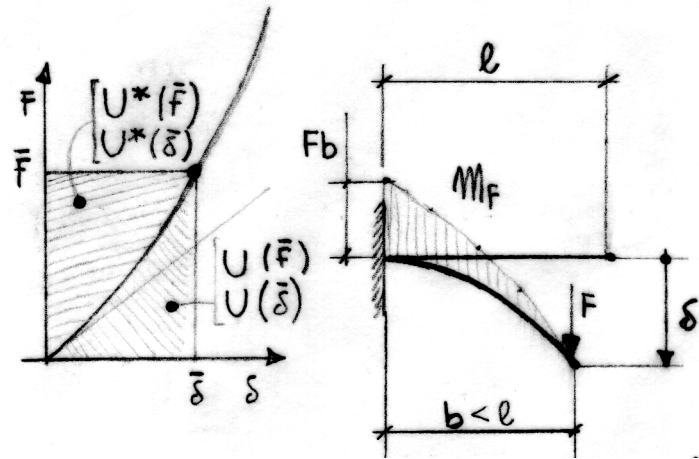
Figure 1.12: A nonlinearly elastic (namely stiffening) structure; the bending moment diagram is evaluated based on the beam portion equilibrium in its *deformed* configuration. The complementary elastic strain energy U^* is plotted for a given applied load $\bar{f}$ or assumed displacement $\bar{\delta}$, alongside the elastic strain energy U.

- E and G are the material Young Modulus and Shear Modulus, respectively; the material is assumed homogeneous, isotropic and linearly elastic.

The shear energy normalized coefficients $\chi_\eta, \chi_\xi, \chi_{\xi\eta}$ are specific to the cross section geometry, and may be collected from the expression of the actual shear strain energy due to concurrent action of the S_η, S_ξ shear forces.

In cases of elastically nonlinear structures, the second Castigliano theorem may still be employed, provided that the complementary elastic strain energy U^* is employed in place of the strain energy U, see Fig. 1.12. The two energy terms are equal for linearly behaving structures.

Chapter 2

Fundamentals of Finite Element Method for structural applications
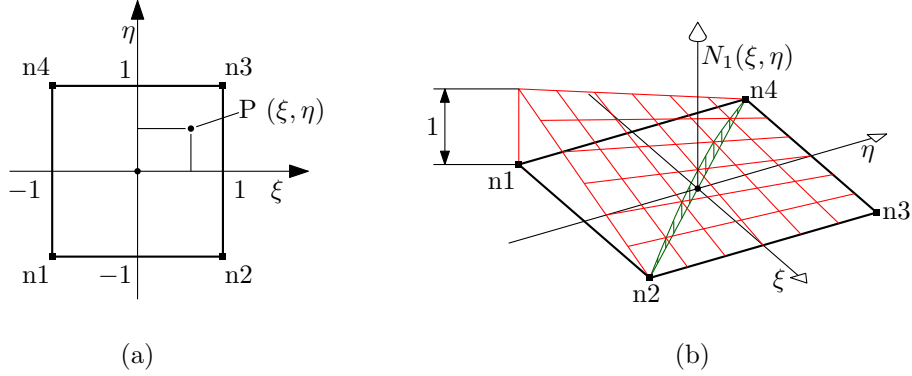
Figure 2.1: Quadrilateral elementary domain (a), and a representative weight function (b).

2.1 Preliminary results

2.1.1 Interpolation functions for the quadrilateral domain

The elementary quadrilateral domain. A quadrilateral domain is considered whose vertices are conventionally located at the $(\pm 1, \pm 1)$ points of an adimensional (ξ, η) plane coordinate system, see Figure 2.1. Scalar values f_i are associated to a set of *nodal* points $P_i \equiv [\xi_i, \eta_i]$, which for the present case coincide with the quadrangle vertices, numbered as in Figure.

A $f(\xi, \eta)$ interpolation function may be devised by defining a set of nodal influence functions $N_i(\xi, \eta)$ to be employed as the coefficients (weights) of a moving weighted average

$$f(\xi, \eta) \stackrel{\text{def}}{=} \sum_i N_i(\xi, \eta) f_i \tag{2.1}$$

Requisites for such weight functions are:

- the influence of a node is unitary at its location, whereas the influence of the others locally vanishes, i.e.

$$N_i(\xi_j, \eta_j) = \delta_{ij} \tag{2.2}$$

where δ_{ij} is the Kronecker delta function.

- for each point of the domain, the sum of the weights is unitary

$$\sum_i N_i(\xi, \eta) = 1, \ \forall[\xi, \eta] \tag{2.3}$$

Moreover, suitable functions should be continuous and straightforwardly differentiable up to any required degree.

Low order polynomials are ideal candidates for the application; for the particular domain, the nodal weight functions may be stated as

$$N_i(\xi, \eta) \stackrel{\text{def}}{=} \frac{1}{4}\left(1 \pm \xi\right)\left(1 \pm \eta\right), \tag{2.4}$$

where sign ambiguity is resolved for each i-th node by enforcing Eqn. 2.2.

The (2.3) combination of 2.4 functions turns into a general linear relation in (ξ, η) with coplanar in the ξ, η, f space – but otherwise arbitrary – nodal points.

Further generality may be introduced by *not* enforcing coplanarity.

The weight functions for the four-node quadrilateral are in fact quadratic although incomplete[1] in nature, due to the presence of the $\xi\eta$ product, and the absence of any ξ^2, η^2 term.

Each term, and the combined $f(\xi, \eta)$ function, defined as in Eqn. 2.1, behave linearly if restricted to $\xi = $ const. or $\eta = $ const. loci – namely along the four edges; quadratic behaviour may instead arise along a general direction, e.g. along the diagonals, as in Fig. 2.1b example. Such behaviour is called *bilinear*.

We now consider the $f(\xi, \eta)$ weight function partial derivatives. The partial derivative

$$\frac{\partial f}{\partial \xi} = \underbrace{\left(\frac{f_2 - f_1}{2}\right)}_{[\Delta f/\Delta \xi]_{12}} \underbrace{\left(\frac{1 - \eta}{2}\right)}_{N_1 + N_2} + \underbrace{\left(\frac{f_3 - f_4}{2}\right)}_{[\Delta f/\Delta \xi]_{43}} \underbrace{\left(\frac{1 + \eta}{2}\right)}_{N_4 + N_3} = a\eta + b \tag{2.5}$$

linearly varies from the incremental ratio value measured at the $\eta = -1$ lower edge, to the value measured at the $\eta = 1$ upper edge; the other partial derivative

$$\frac{\partial f}{\partial \eta} = \left(\frac{f_4 - f_1}{2}\right)\left(\frac{1 - \xi}{2}\right) + \left(\frac{f_3 - f_2}{2}\right)\left(\frac{1 + \xi}{2}\right) = c\xi + d. \tag{2.6}$$

---

[1] or, equivalently, *enriched linear*, as discussed above and in the following

behaves similarly, with $c = a$. However, partial derivatives in ξ, η remain constant along the corresponding differentiation direction [2].

The general quadrilateral domain. The interpolation functions introduced above for the natural quadrilateral may be profitably employed in defining a coordinate mapping between a general quadrangular domain – see Fig. 2.2a – and its reference counterpart, see Figures 2.1 and 2.2b.

In particular, we first define the $\underline{\xi}_i \mapsto \underline{x}_i$ coordinate mapping for the four vertices[3] alone, where ξ, η are the reference (or natural, or elementary) coordinates and x, y are their physical counterpart.

Then, a mapping for the inner points may be derived by interpolation, namely

$$\underline{x} = \underline{m}\left(\underline{\xi}\right) = \sum_{i=1}^{4} N_i\left(\underline{\xi}\right)\underline{x}_i \tag{2.7}$$

The availability of an inverse $\underline{m}^{-1} : \underline{x} \mapsto \underline{\xi}$ mapping is not granted; in particular, a closed form representation for such inverse is not generally available[4].

In the absence of an handy inverse mapping function, it is convenient to reinstate the interpolation procedure obtained for the natural domain, i.e.

$$f(\xi, \eta) \stackrel{\text{def}}{=} \sum_i N_i(\xi, \eta) f_i \tag{2.8}$$

The four f_i nodal values are interpolated based on the *natural* ξ, η coordinates of an inner P point, and not as a function of its physical x, y coordinates, that are never promoted to the independent variable role.

As already mentioned, the $\underline{m}$ mapping behaves linearly along $\eta =$const. and $\xi =$const. one dimensional subdomains, and in particular along

---

[2]The relevance of such partial derivative orders will appear clearer to the reader once the strain field will have been derived in paragraph XXX.

[3]The condensed notation $\underline{\xi}_i \equiv (\xi_i, \eta_i)$, $\underline{x}_i \equiv (x_i, y_i)$ for coordinate vectors is employed.

[4]Inverse relations are derived in [2], which however are case-defined and based on a selection table; for a given $\underline{\bar{x}}$ physical point, however, Newton-Raphson iterations rapidly converge to the $\underline{\bar{\xi}} = \underline{m}^{-1}(\underline{\bar{x}})$ solution if the centroid is chosen for algorithm initialization, see Section XXX

$$P \equiv (x_P(\xi,\eta), y_P(\xi,\eta)\,[,\,z_P(\xi,\eta)])$$

dA_{xy}

n1

n4

y

y_2

$N_2(\xi,\eta)$

$[z]$

1.0

C

P

η

n2

ξ

n3

x_2

x

(a)

η

n4

n3

$P \equiv (\xi,\eta)$

C

ξ_P

ξ

η_P P
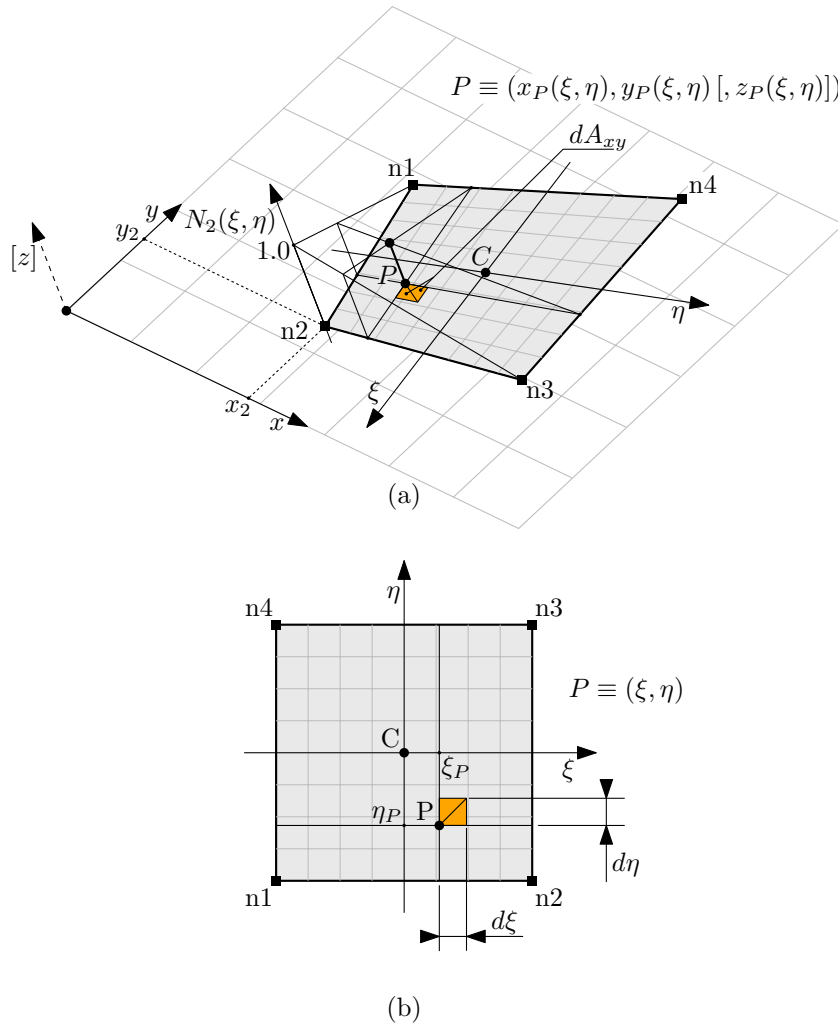
$d\eta$

n1

n2

$d\xi$

(b)

Figure 2.2: Quadrilateral general domain, (a), and its reference counterpart (b). If the general quadrangle is defined within a spatial environment, and not as a figure lying on the xy plane, limited z_i offsets are allowed at nodes with respect to such plane, which are not considered in Figure.

the quadrangle edges[5]; the inverse mapping $\underline{\mathrm{m}}^{-1}$ exists along these line segments under the further condition that their length is nonzero[6], and it is a linear function[7] . Being a composition of linear functions, the interpolation function $f(\underline{\mathrm{m}}^{-1}(x, y))$ is also linear along the aforementioned subdomains, and in particular along the quadrangle edges.

The directional derivatives of f with respect to x or y are obtained based the indirect relation

$$\begin{bmatrix} \frac{\partial f}{\partial \xi} \\ \frac{\partial f}{\partial \eta} \end{bmatrix} = \underbrace{\begin{bmatrix} \frac{\partial x}{\partial \xi} & \frac{\partial y}{\partial \xi} \\ \frac{\partial x}{\partial \eta} & \frac{\partial y}{\partial \eta} \end{bmatrix}}_{\underline{\underline{J}}'(\xi,\eta)} \begin{bmatrix} \frac{\partial f}{\partial x} \\ \frac{\partial f}{\partial y} \end{bmatrix} \tag{2.9}$$

.

The function derivatives with respect to ξ, η are obtained as

$$\begin{bmatrix} \frac{\partial f}{\partial \xi} \\ \frac{\partial f}{\partial \eta} \end{bmatrix} = \sum_i \begin{bmatrix} \frac{\partial N_i}{\partial \xi} \\ \frac{\partial N_i}{\partial \eta} \end{bmatrix} f_i. \tag{2.10}$$

The *transposed* Jacobian matrix of the mapping function that appears in 2.9 is

$$\underline{\underline{J}}'(\xi, \eta) = \begin{bmatrix} \frac{\partial x}{\partial \xi} & \frac{\partial y}{\partial \xi} \\ \frac{\partial x}{\partial \eta} & \frac{\partial y}{\partial \eta} \end{bmatrix} \tag{2.11}$$

$$= \sum_i \left(\begin{bmatrix} \frac{\partial N_i}{\partial \xi} & 0 \\ \frac{\partial N_i}{\partial \eta} & 0 \end{bmatrix} x_i + \begin{bmatrix} 0 & \frac{\partial N_i}{\partial \xi} \\ 0 & \frac{\partial N_i}{\partial \eta} \end{bmatrix} y_i \right) \tag{2.12}$$

If the latter matrix is assumed nonsingular – condition, this, that pairs the bijective nature of the $\underline{\mathrm{m}}$ mapping, equation 2.9 may be

---

[5]see paragraph XXX

[6]The case exists of an edge whose endpoints are superposed, i.e. the edge collapses to a point.

[7]A constructive proof may be defined for each edge by retrieving the non-uniform amongst the ξ, η coordinates, namely λ, as the ratio

$$\lambda = 2 \frac{(x_Q - x_i)(x_j - x_i) + (y_Q - y_i)(y_j - y_i)}{(x_j - x_i)^2 + (y_j - y_i)^2} - 1,$$

where Q is a generic point along the edge, and i,j are the two subdomain endpoints at which λ equates -1 and $+1$, respectively. A similar function may be defined for any constant ξ, η segment.

inverted, thus leading to the form

$$\begin{bmatrix} \frac{\partial f}{\partial x} \\ \frac{\partial f}{\partial y} \end{bmatrix} = \left(\underline{\underline{J}}' \right)^{-1} \begin{bmatrix} \cdots & \frac{\partial N_i}{\partial \xi} & \cdots \\ \cdots & \frac{\partial N_i}{\partial \eta} & \cdots \end{bmatrix} \begin{bmatrix} \vdots \\ f_i \\ \vdots \end{bmatrix}, \tag{2.13}$$

where the inner mechanics of the matrix-vector product are appointed for the Eq. 2.10 summation.

2.1.2 Gaussian quadrature rules for some relevant domains.

Reference one dimensional domain. The gaussian quadrature rule for approximating the definite integral of a $f(\xi)$ function over the $[-1, 1]$ reference interval is constructed as the customary weighted sum of internal function samples, namely

$$\int_{-1}^{1} f(\xi)d\xi \approx \sum_{i=1}^{n} f(\xi_i)w_i; \tag{2.14}$$

Its peculiarity is to employ location-weight pairs (ξ_i, w_i) that are optimal with respect to the polynomial class of functions. Nevertheless, such choice has revealed itself to be robust enough for for a more general employment.

Let's consider a m-th order polynomial

$$p(\xi) \stackrel{\text{def}}{=} a_m \xi^m + a_{m-1} \xi^{m-1} + \ldots + a_1 \xi + a_0$$

whose exact integral is

$$\int_{-1}^{1} p(\xi)d\xi = \sum_{j=0}^{m} \frac{(-1)^j + 1}{j + 1} a_j$$

The integration residual between the exact definite integral and the weighted sample sum is defined as

$$r\left(a_j, (\xi_i, w_i)\right) \stackrel{\text{def}}{=} \sum_{i=1}^{n} p(\xi_i)w_i - \int_{-1}^{1} p(\xi)d\xi \tag{2.15}$$

The optimality condition is stated as follows: the quadrature rule involving n sample points (ξ_i, w_i), $i = 1 \ldots n$ is optimal for the m-th order polynomial if a) the integration residual is null for general a_j values , and b) such condition does not hold for any lower-order sampling rule.

Once observed that the zero residual requirement is satisfied by any sampling rule if the polynomial a_j coefficients are all null, condition a) may be enforced by imposing that such zero residual value remains constant with varying a_j terms, i.e.

$$\left\{ \frac{\partial r\left(a_j, (\xi_i, w_i)\right)}{\partial a_j} = 0, \quad j = 0 \ldots m \right. \tag{2.16}$$

A system of $m + 1$ polynomial equations of degree[8] $m + 1$ is hence obtained in the $2n$ (ξ_i, w_i) unknowns; in the assumed absence of redundant equations, solutions do not exist if the constraints outnumber the unknowns, i.e. $m > 2n - 1$. Limiting our discussion to the threshold condition $m = 2n - 1$, an attentive algebraic manipulation of Eqns. 2.16 may be performed in order to extract the (ξ_i, w_i) solutions, which

---

[8]the $(m + 1)$-th order $w_m \xi^m$ term appears in equations

n	ξ_i	w_i
1	0	2
2	$\pm\frac{1}{\sqrt{3}}$	1
3	0	$\frac{8}{9}$
	$\pm\sqrt{\frac{3}{5}}$	$\frac{5}{9}$
4	$\pm\sqrt{\frac{3}{7} - \frac{2}{7}\sqrt{\frac{6}{5}}}$	$\frac{18+\sqrt{30}}{36}$
	$\pm\sqrt{\frac{3}{7} + \frac{2}{7}\sqrt{\frac{6}{5}}}$	$\frac{18-\sqrt{30}}{36}$

Table 2.1: Integration points for the lower order gaussian quadrature rules.

are unique apart from the pair permutations[9].

Eqns. 2.16 solutions are reported in Table 2.1 for quadrature rules with up to $n = 4$ sample points[10].

---

[9] In this note, location-weight pairs are obtained for the gaussian quadrature rule of order $n = 2$, aiming at illustrating the general procedure. The general $m = 2n - 1 = 3$rd order polynomial is stated in the form

$$p(\xi) = a_3\xi^3 + a_2\xi^2 + a_1\xi + a_0, \quad \int_{-1}^{1} p(\xi)d\xi = \frac{2}{3}a_2 + 2a_0,$$

whereas the integral residual is

$$r = a_3\left(w_1\xi_1^3 + w_2\xi_2^3\right) + a_2\left(w_1\xi_1^2 + w_2\xi_2^2 - \frac{2}{3}\right) + a_1\left(w_1\xi_1 + w_2\xi_2\right) + a_0\left(w_1 + w_2 - 2\right)$$

Eqns 2.16 may be derived as

$$\begin{cases} 0 = \frac{\partial r}{\partial a_3} = w_1\xi_1^3 + w_2\xi_2^3 & (e_1) \\ 0 = \frac{\partial r}{\partial a_2} = w_1\xi_1^2 + w_2\xi_2^2 - \frac{2}{3} & (e_2) \\ 0 = \frac{\partial r}{\partial a_1} = w_1\xi_1 + w_2\xi_2 & (e_3) \\ 0 = \frac{\partial r}{\partial a_0} = w_1 + w_2 - 2 & (e_4) \end{cases}$$

which are independent of the a_j coefficients.

By composing $\left(e_1 - \xi_1^2 e_3\right)/(w_2\xi_2)$ it is obtained that $\xi_2^2 = \xi_1^2$; e_2 may then be written as $(w_1 + w_2)\xi_1^2 = 2/3$, and then as $2\xi_1^2 = 2/3$, according to e_4. It derives that $\xi_{1,2} = \pm 1/\sqrt{3}$. Due to the opposite nature of the roots, e_3 implies $w_2 = w_1$, relation, this, that turns e_4 into $2w_1 = 2w_2 = 2$, and hence $w_{1,2} = 1$.

[10] see https://pomax.github.io/bezierinfo/legendre-gauss.html for higher

It is noted that the integration points are symmetrically distributed with respect to the origin, and that the function is never sampled at the $\{-1, 1\}$ extremal points.

General one dimensional domain. The extension of the one dimensional quadrature rule from the reference domain $[-1, 1]$ to a general $[a, b]$ domain is pretty straightforward, requiring just a change of integration variable – i.e. a mapping function $x = m(\xi)$ s.t. $a = m(-1)$ and $b = m(1)$ – to obtain the following

$$\int_a^b f(x)dx = \int_{-1}^1 f\left(m(\xi)\right) \frac{dm}{d\xi} d\xi \approx \sum_{i=1}^n f\left(m(\xi)\right) \frac{dm}{d\xi}\bigg|_{\xi = \xi_i} w_i. \quad (2.17)$$

Such a mapping function may be conveniently defined along the same lines as the weight (or shape) function based interpolation, thus obtaining

$$m(x) = \underbrace{\left(\frac{1 - \xi}{2}\right)}_{N_1} a + \underbrace{\left(\frac{1 + \xi}{2}\right)}_{N_2} b.$$

The first order derivative may be evaluated as

$$\frac{dm}{d\xi} = \frac{dN_1}{d\xi} a + \frac{dN_2}{d\xi} b = \frac{b - a}{2}$$

and it is constant along the interval, so that it may be collected outside of the summation, thus leading to

$$\int_a^b f(x)dx \approx \frac{b - a}{2} \sum_{i=1}^n f\left(\frac{b + a}{2} + \frac{b - a}{2}\xi_i\right) w_i. \quad (2.18)$$

Reference quadrangular domain. A quadrature rule for the reference quadrangular domain of Figure 2.1a may be derived by nesting the quadrature rule defined for the reference interval, see Eqn. 2.14, thus obtaining

$$\int_{-1}^1 \int_{-1}^1 f\left(\xi, \eta\right) d\xi d\eta \approx \sum_{i=1}^p \sum_{j=1}^q f\left(\xi_i, \eta_j\right) w_i w_j \quad (2.19)$$

order gaussian quadrature rule sample points.

where (ξ_i, w_i) and (η_j, w_j) are the coordinate-weight pairs of the two quadrature rules of p and q order, respectively, employed for spanning the two coordinate axes. The equivalent notation

$$\int_{-1}^{1} \int_{-1}^{1} f(\xi, \eta) \, d\xi d\eta \approx \sum_{l=1}^{pq} f\left(\underline{\xi}_l\right) w_l \qquad (2.20)$$

emphasises the characteristic nature of the pq point/weight pairs for the domain and for the quadrature rule employed; a general integer bijection[11] $\{1\ldots pq\} \leftrightarrow \{1\ldots p\} \times \{1\ldots q\}$, $l \leftrightarrow (i,j)$ may be utilized to formally derive the two-dimensional quadrature rule pairs

$$\underline{\xi}_l = (\xi_i, \eta_j), \quad w_l = w_i w_j, \quad l = 1 \ldots pq \qquad (2.21)$$

from their uniaxial counterparts.

General quadrangular domain. The rectangular infinitesimal area $dA_{\xi\eta} = d\xi d\eta$ in the neighborhood of a ξ_P, η_P location, see Figure 2.2b, is mapped to the quadrangle of Figure 2.2a, which is composed by the two triangular areas

$$dA_{xy} = \frac{1}{2!} \begin{vmatrix} 1 & x(\xi_P, \eta_P) & y(\xi_P, \eta_P) \\ 1 & x(\xi_P + d\xi, \eta_P) & y(\xi_P + d\xi, \eta_P) \\ 1 & x(\xi_P + d\xi, \eta_P + d\eta) & y(\xi_P + d\xi, \eta_P + d\eta) \end{vmatrix} +$$

$$+ \frac{1}{2!} \begin{vmatrix} 1 & x(\xi_P + d\xi, \eta_P + d\eta) & y(\xi_P + d\xi, \eta_P + d\eta) \\ 1 & x(\xi_P, \eta_P + d\eta) & y(\xi_P, \eta_P + d\eta) \\ 1 & x(\xi_P, \eta_P) & y(\xi_P, \eta_P) \end{vmatrix}. \qquad (2.22)$$

---

[11] e.g.

$$\{i - 1; j - 1\} = (l - 1) \bmod (p, q), \quad l - 1 = (j - 1)q + (i - 1)$$

where the operator

$$\{a_n; \ldots; a_3; a_2; a_1\} = m \bmod (b_n, \ldots, b_3, b_2, b_1)$$

consists in the extraction of the n least significant a_i digits of a mixed radix representation of the integer m with respect to the sequence of b_i bases, with $i = 1 \ldots n$.

The determinant formula for the area of a triangle, shown below along with its n-dimensional symplex hypervolume generalization,

$$
\mathcal{A} = \frac{1}{2!} \begin{vmatrix} 1 & x_1 & y_1 \\ 1 & x_2 & y_2 \\ 1 & x_3 & y_3 \end{vmatrix}, \quad \mathcal{H} = \frac{1}{n!} \begin{vmatrix} 1 & \underline{\mathbf{x}}_1 \\ 1 & \underline{\mathbf{x}}_2 \\ \vdots & \vdots \\ 1 & \underline{\mathbf{x}}_{n+1} \end{vmatrix} \tag{2.23}
$$

has been employed above.

By operating a local multivariate linearization of the 2.22 matrix terms, the relation

$$
dA_{xy} \approx \quad \frac{1}{2!} \begin{vmatrix} 1 & x & y \\ 1 & x + x_{,\xi} d\xi & y + y_{,\xi} d\xi \\ 1 & x + x_{,\xi} d\xi + x_{,\eta} d\eta & y + y_{,\xi} d\xi + y_{,\eta} d\eta \end{vmatrix} +
$$

$$
+ \frac{1}{2!} \begin{vmatrix} 1 & x + x_{,\xi} d\xi + x_{,\eta} d\eta & y + y_{,\xi} d\xi + y_{,\eta} d\eta \\ 1 & x + x_{,\eta} d\eta & y + y_{,\eta} d\eta \\ 1 & x & y \end{vmatrix}
$$

is obtained, where $x, y, x_{,\xi}, x_{,\eta}, y_{,\xi}$, and $y_{,\eta}$ are the x, y functions and their first order partial derivatives, sampled at the (ξ_P, η_P) point; infinitesimal terms of order higher than $d\xi, d\eta$ are neglected.

After some matrix manipulations[12], the following expression is ob-

---

[12] In the first determinant, the second row is subtracted from the third one, and the first row is subtracted from the second one. The $d\xi$, $d\eta$ factors are then collected from the second and the third row respectively. In the second determinant, the second row is subtracted from the first one, and the third row is subtracted from the second one. The $d\xi$, $d\eta$ factors are then collected from the first and the second row respectively. We now have

$$
dA_{xy} = \frac{1}{2} \begin{vmatrix} 1 & x & y \\ 0 & x_{,\xi} & y_{,\xi} \\ 0 & x_{,\eta} & y_{,\eta} \end{vmatrix} d\xi d\eta + \frac{1}{2} \begin{vmatrix} 0 & x_{,\xi} & y_{,\xi} \\ 0 & x_{,\eta} & y_{,\eta} \\ 1 & x & y \end{vmatrix} d\xi d\eta
$$

The first column of both the determinants contains a single, unitary, nonzero term, whose row and column indexes are even once added up; the determinants of the associated complementary minors hence equate their whole matrix counterpart. We hence obtain

$$
dA_{xy} = \frac{1}{2} \begin{vmatrix} x_{,\xi} & y_{,\xi} \\ x_{,\eta} & y_{,\eta} \end{vmatrix} d\xi d\eta + \frac{1}{2} \begin{vmatrix} x_{,\xi} & y_{,\xi} \\ x_{,\eta} & y_{,\eta} \end{vmatrix} d\xi d\eta
$$

from which Eq.2.24 may be straightforwardly derived.

tained

$$dA_{xy} = \underbrace{\begin{vmatrix} x_{,\xi} & y_{,\xi} \\ x_{,\eta} & y_{,\eta} \end{vmatrix}}_{|J^{\mathrm{T}}(\xi_P, \eta_P)|} dA_{\xi\eta} \qquad (2.24)$$

that equates the ratio of the mapped and of the reference areas to the determinant of the transformation (transpose) Jacobian matrix[13].

After the preparatory passages above, we obtain

$$\iint_{A_{xy}} g(x,y) dA_{xy} = \iint_{-1}^{1} g\left(x\left(\xi,\eta\right), y\left(\xi,\eta\right)\right) |J(\xi,\eta)| \, d\xi d\eta, \quad (2.25)$$

thus reducing the quadrature over a general domain to its reference domain counterpart, which has been discussed in the paragraph above.

Based on Eqn. 2.20, the quadrature rule

$$\iint_{A_{xy}} g(\underline{x}) dA_{xy} \approx \sum_{l=1}^{pq} g\left(\underline{x}\left(\underline{\xi}_l\right)\right) |J(\underline{\xi}_l)| \, w_l \qquad (2.26)$$

is derived, stating that the definite integral of a g integrand over a quadrangular domain pertaining to the physical x, y plane (x, y are dimensional quantities, namely lengths) may be approximated as follows:

1. a reference-to-physical domain mapping is defined, that is based on the vertex physical coordinate interpolation;

2. the function is sampled at the physical locations that are the images of the Gaussian integration points previously obtained for the reference domain;

3. a weighted sum of the collected samples is performed, where the weights consist in the product of i) the adimensional w_l Gauss point weight (suitable for integrating on the reference domain), and ii) a dimensional area scaling term, that equals the determinant of the transformation Jacobian matrix, locally evaluated at the Gauss points.

---

[13]The Jacobian matrix for a general $\underline{\xi} \mapsto \underline{x}$ mapping is in fact defined according to

$$[J(\underline{\xi}_P)]_{ij} \stackrel{\mathrm{def}}{=} \left.\frac{\partial x_i}{\partial \xi_j}\right|_{\underline{\xi}=\underline{\xi}_P} \qquad i, j = 1 \ldots n$$

being i the generic matrix term row index, and j the column index

2.2 Basic formulation for plates and shells

A necessary condition for applying the plate/shell model framework to a deformable body is that a geometrical midsurface might be, if only loosely, recognized for such a body. Then, an iterative refinement procedure[14] may be applied to such tentative midsurface guess.

Then, material should be observed as *[piecewise-]*homogeneous, or slowly varying in mechanical properties while moving at a fixed distance from the midsurface.

Of the two outer surfaces, one has to be defined as the *upper* or *top* surface, whereas the other is named lower ot *bottom*, thus implicitly orienting the midsurface normal towards the top.

Finally, the body should result fully determined based on a) its midsurface, b) its pointwise thickness, and c) the through-thickness distribution of the constituent materials.

Actually, the geometrical midsurface is of little significance if the material distribution is not symmetric[15]; such midsurface, in fact, exhibits no relevant properties in general. Its definition is nevertheless pretty straighforward.

In the present treatise, a more general *reference* surface definition is preferred to its median geometric counterpart; in particular, an *offset* term is considered that pointwisely shifts the geometric midsurface with respect to the reference surface. A positive offsets shifts the midsurface towards the top.

With the introduction of the offset term, the reference surface may be arbitrarily positioned with respect to the body itself; as an example, an offset set equal to plus or minus half the thickness makes the reference surface correspondent to the bottom or top surfaces, respectively.

Such offset term becomes fundamental in the Finite Element (FE) shell implementation, where, in fact, the reference plane is uniquely defined by the position of the nodes, whereas the offset arbitrarily shifts the geometrical midsurface.

---

[14]Normal segments may be cast from each point along the midsurface, that end on the outer body surfaces. The midpoint locus of these segments redefines the midsurface itself.

[15]If the unsimmetric laminate is composed by isotropic layers, a reference plane may be obtained for which the $\underline{\underline{B}}$ membrane-to-bending coupling matrix vanishes; a similar condition may not be verified in the presence of orthotropic layers.

In the case of limited[16] curvatures, and for considerations whose scope is local, the tangent reference plane may be employed in place of the possibly curve reference surface, thus locally reducing the general shell treatise to its planar, plate counterpart.

The P displacement components may be defined as a function of the motion of its projection on the reference plane Q. Such Q point is named *reference point* for the through-thickness segment it belongs to.

$$u_P = u + z\,(1 + \check{\epsilon}_z)\sin\varphi \tag{2.27}$$

$$v_P = v - z\,(1 + \check{\epsilon}_z)\sin\theta \tag{2.28}$$

$$w_P = w + z\,((1 + \check{\epsilon}_z)\cos(\varphi)\cos(\theta) - 1) \tag{2.29}$$

The $\check{\epsilon}_z$ average z strain term is defined based on the accumulation of the Poisson shrinkage (or elongation) along the PQ segment, i.e.

$$\check{\epsilon}_z(z) = \frac{1}{z}\int_0^z \epsilon_z\, d\varsigma \tag{2.30}$$

$$= \frac{1}{z}\int_0^z -\frac{\nu}{1-\nu}\,(\epsilon_x + \epsilon_y)\, d\varsigma \tag{2.31}$$

The stress component σ_z which is normal to the reference surface is assumed to be either zero or negligible[17].

Such displacement components may be linarized with respect to the small rotations and small ϵ_z strain hypotheses, thus obtaining

---

[16]with respect to thickness

[17]Such assumption is coherent with the free surface conditions at the top and the bottom skins, and with the moderate thickness of the elastic body, that allows only a narrow deviation from the boundary values.

In fact, the equilibrium of a partitioned, through-thickness material segment requires that

$$\sigma_z(z) = -\int_{-h/2+o}^z \frac{\partial \tau_{zx}}{\partial x} + \frac{\partial \tau_{yz}}{\partial y}\,dz = +\int_z^{+h/2-o} \frac{\partial \tau_{zx}}{\partial x} + \frac{\partial \tau_{yz}}{\partial y}\,dz,$$

where τ_{zx}, τ_{yz} are the interlaminar, out-of-plane shear stress components, whose in-plane gradient is limited.
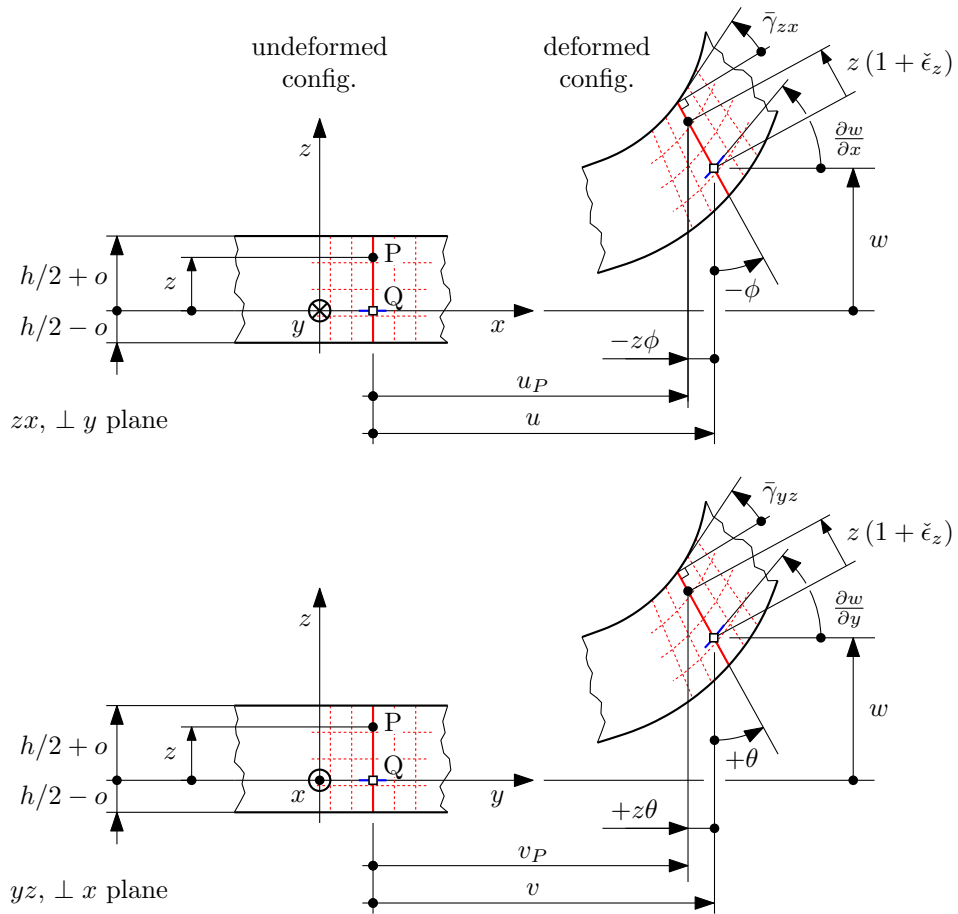
Figure 2.3: Relevant dimensions for describing the deformable plate kinematics.

$$u_P = u + z\varphi \tag{2.32}$$

$$v_P = v - z\theta \tag{2.33}$$

$$w_P = w \tag{2.34}$$

According to such linearized expression, the kinematic of the P points originally[18] laying on a through-thickness segment that is normal at Q to the reference surface may be described as that of a rigid body. The natural shear related warping is either excluded or neglected, along with the motion of the P points along the segment due to $\check{\epsilon}_z$.

Also, the behaviour of such a segment is coherent with its rigid body modeling from the external loads point of view; in particular the external actions act on the plate deformable body only through their through-thickness resultants, and no stress/strain components or work are associated by the shell framework to wall squeezing actions, e.g. laminations.

Relation between the normal displacement x, y gradient (i.e. the deformed plate slope), the rotations and the out-of-plane, interlaminar, averaged shear strain components.

$$\frac{\partial w}{\partial x} = \bar{\gamma}_{zx} - \varphi \tag{2.35}$$

$$\frac{\partial w}{\partial y} = \bar{\gamma}_{yz} + \theta \tag{2.36}$$

Strains at point P.

$$\epsilon_x = \frac{\partial u_P}{\partial x} = \frac{\partial u}{\partial x} + z\frac{\partial \varphi}{\partial x} \tag{2.37}$$

$$\epsilon_y = \frac{\partial v_P}{\partial y} = \frac{\partial v}{\partial y} - z\frac{\partial \theta}{\partial y} \tag{2.38}$$

$$\gamma_{xy} = \frac{\partial u_P}{\partial y} + \frac{\partial v_P}{\partial x} \tag{2.39}$$

$$= \left(\frac{\partial u}{\partial y} + \frac{\partial v}{\partial x}\right) + z\left(+\frac{\partial \varphi}{\partial y} - \frac{\partial \theta}{\partial x}\right) \tag{2.40}$$

---

[18]i.e. in the undeformed configuration

Generalized plate strains: membrane strains

$$\bar{\underline{\epsilon}} = \begin{pmatrix} \frac{\partial u}{\partial x} \\ \frac{\partial v}{\partial y} \\ \frac{\partial u}{\partial y} + \frac{\partial v}{\partial x} \end{pmatrix} = \begin{pmatrix} \bar{\epsilon}_x \\ \bar{\epsilon}_y \\ \bar{\gamma}_{xy} \end{pmatrix} \tag{2.41}$$

Generalized plate strains: curvatures.

$$\underline{\kappa} = \begin{pmatrix} +\frac{\partial \varphi}{\partial x} \\ -\frac{\partial \theta}{\partial y} \\ +\frac{\partial \varphi}{\partial y} - \frac{\partial \theta}{\partial x} \end{pmatrix} = \begin{pmatrix} \kappa_x \\ \kappa_y \\ \kappa_{xy} \end{pmatrix} \tag{2.42}$$

Compact form for the strain components at P.

$$\underline{\epsilon} = \bar{\underline{\epsilon}} + z\,\underline{\kappa} \tag{2.43}$$

Hook law for an isotropic material, under plane stress conditions.

$$\underline{\underline{D}} = \frac{E}{1-\nu^2} \begin{pmatrix} 1 & \nu & 0 \\ \nu & 1 & 0 \\ 0 & 0 & \frac{1-\nu}{2} \end{pmatrix} \tag{2.44}$$

Normal components for stress and strain, the latter for the isotropic material case only.

$$\sigma_z = 0 \tag{2.45}$$

$$\epsilon_z = -\frac{\nu}{1-\nu}\,(\epsilon_x + \epsilon_y) \tag{2.46}$$

Stresses at P.

$$\underline{\sigma} = \underline{\underline{D}}\,\underline{\epsilon} = \underline{\underline{D}}\,\bar{\underline{\epsilon}} + z\underline{\underline{D}}\,\underline{\kappa} \tag{2.47}$$

Membrane (direct and shear) stress resultants (stress flows).

$$\underline{q} = \begin{pmatrix} q_x \\ q_y \\ q_{xy} \end{pmatrix} = \int_h \underline{\sigma}\,dz \tag{2.48}$$

$$= \underbrace{\int_h \underline{\underline{D}}\,dz}_{\underline{\underline{A}}}\,\bar{\underline{\epsilon}} + \underbrace{\int_h \underline{\underline{D}}\,z dz}_{\underline{\underline{B}}}\,\underline{\kappa} \tag{2.49}$$

47

Figure 2.4:   Positive κ_{xy} torsional curvature for the plate element. Subfigure (a) shows the positive γ_{xy} shear strain at the upper surface, the (in-plane) undeformed midsurface, and the negative γ_{xy} at the lower surface; the point of sight related to subfigures (b) to (d) are also evidenced. θ and φ rotation components decrease with x and increase with y, respectively, thus leading to positive κ_{xy} contributions. As shown in subfigures (c) and (d), the torsional curvature of subfigure (b) evolves into two anticlastic bending curvatures if the reference system is aligned with the square plate element diagonals, and hence rotated by $45°$ with respect to z.
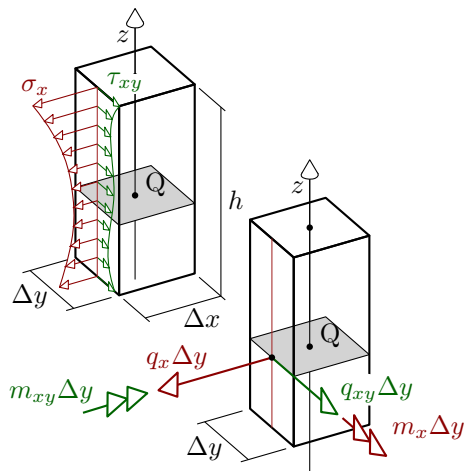
Figure 2.5: XXX

Bending and torsional moment stress resultants (moment flows).

$$\underline{m} = \begin{pmatrix} m_x \\ m_y \\ m_{xy} \end{pmatrix} = \int_h \underline{\sigma}\, z dz \tag{2.50}$$

$$= \underbrace{\int_h \underline{\underline{D}}\, z dz}_{\underline{\underline{B}} \equiv \underline{\underline{B}}^{\mathrm{T}}} \bar{\underline{\epsilon}} + \underbrace{\int_h \underline{\underline{D}}\, z^2 dz}_{\underline{\underline{C}}} \underline{\kappa} \tag{2.51}$$
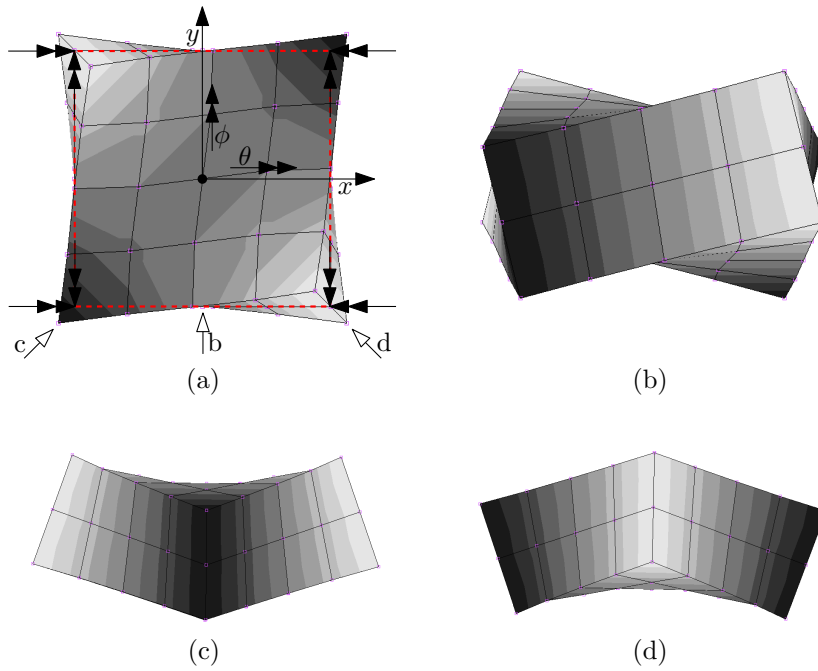
Cumulative generalized strain - stress resultants relations for the plate (or for the laminate)

$$\begin{pmatrix} \underline{q} \\ \underline{m} \end{pmatrix} = \begin{pmatrix} \underline{\underline{A}} & \underline{\underline{B}} \\ \underline{\underline{B}}^{\mathrm{T}} & \underline{\underline{C}} \end{pmatrix} \begin{pmatrix} \bar{\underline{\epsilon}} \\ \underline{\kappa} \end{pmatrix} \tag{2.52}$$

The $\underline{\underline{A}}$ and the $\underline{\underline{C}}$ matrices characterize the plate stiffness with respect to membrane and flexo-torsional load case families respectively; the membrane/flexo-torsional coupling stiffness term $\underline{\underline{B}}$ vanishes for symmetric laminates if the reference surface is made coincident with the midsurface.

Hook law for the orthotropic material in plane stress conditions,

with respect to principal axes of orthotropy;

$$\underline{\underline{D}}_{123} = \begin{pmatrix} \frac{E_1}{1-\nu_{12}\nu_{21}} & \frac{\nu_{21}E_1}{1-\nu_{12}\nu_{21}} & 0 \\ \frac{\nu_{12}E_2}{1-\nu_{12}\nu_{21}} & \frac{E_2}{1-\nu_{12}\nu_{21}} & 0 \\ 0 & 0 & G_{12} \end{pmatrix} \tag{2.53}$$

$$\begin{pmatrix} \sigma_1 \\ \sigma_2 \\ \tau_{12} \end{pmatrix} = \underline{\underline{T}}_1 \begin{pmatrix} \sigma_x \\ \sigma_y \\ \tau_{xy} \end{pmatrix} \qquad \begin{pmatrix} \epsilon_1 \\ \epsilon_2 \\ \gamma_{12} \end{pmatrix} = \underline{\underline{T}}_2 \begin{pmatrix} \epsilon_x \\ \epsilon_y \\ \gamma_{xy} \end{pmatrix} \tag{2.54}$$

where

$$\underline{\underline{T}}_1 = \begin{pmatrix} m^2 & n^2 & 2mn \\ n^2 & m^2 & -2mn \\ -mn & mn & m^2 - n^2 \end{pmatrix} \tag{2.55}$$

$$\underline{\underline{T}}_2 = \begin{pmatrix} m^2 & n^2 & mn \\ n^2 & m^2 & -mn \\ -2mn & 2mn & m^2 - n^2 \end{pmatrix} \tag{2.56}$$

α is the angle between 1 and x;

$$m = \cos(\alpha) \qquad\qquad n = \sin(\alpha) \tag{2.57}$$

The inverse transformations may be obtained based on the relations

$$\underline{\underline{T}}_1^{-1}(+\alpha) = \underline{\underline{T}}_1(-\alpha) \qquad\qquad \underline{\underline{T}}_2^{-1}(+\alpha) = \underline{\underline{T}}_2(-\alpha) \tag{2.58}$$

Finally

$$\underline{\sigma} = \underline{\underline{D}}\,\underline{\epsilon} \qquad\qquad \underline{\underline{D}} \equiv \underline{\underline{D}}_{xyz} = \underline{\underline{T}}_1^{-1}\underline{\underline{D}}_{123}\underline{\underline{T}}_2 \tag{2.59}$$

Notes:

- Midplane is ill-defined if the material distribution is not symmetric; the geometric midplane (i.e. the one obtained by ignoring the material distribution) exhibits no relevant properties in general. Its definition is nevertheless pretty straighforward.

- If the unsimmetric laminate is composed by isotropic layers, a reference plane may be obtained for which the $\underline{\underline{B}}$ membrane-to-bending coupling matrix vanishes; a similar condition may not be verified in the presence of orthotropic layers.

- In the present contribution, the *reference* plane is preferred to the usual geometric midplane for expressing the displacement field, even in the case of homogeneous material or symmetric laminates; in FE shell element implementation, in fact, the reference plane is uniquely defined by the position of the nodes, whereas an offset term may arbitrarily shift the geometrical midsurface.

- Thermally induced distortion is not self-compensated in an unsymmetric laminate even if the temperature is held constant through the thickness.
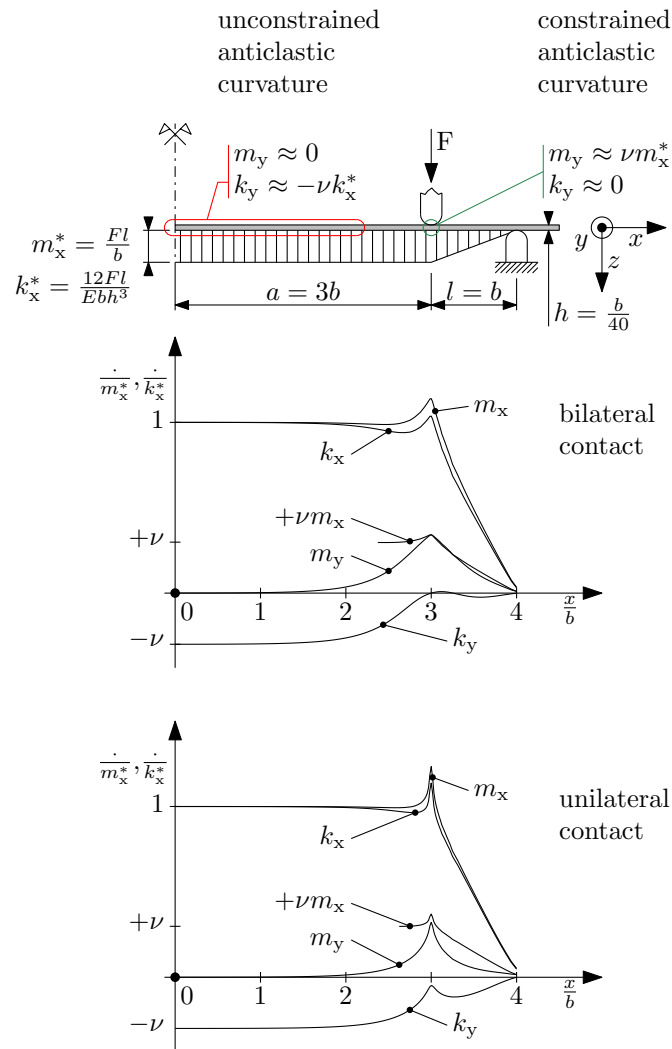
Figure 2.6: The *not-so-trivial* four point bending case. Moment fluxes and curvatures are sampled at the specimen midwidth, whereas they may vary while moving towards the flanks; the average value of m_x along the width must in fact coincide with m_x^* in correspondence with the load span.

2.3 The bilinear isoparametric shear-deformable shell element

This is a four-node, thick-shell element with global displacements and rotations as degrees of freedom. Bilinear interpolation is used for the coordinates, displacements and the rotations. The membrane strains are obtained from the displacement field; the curvatures from the rotation field. The transverse shear strains are calculated at the middle of the edges and interpolated to the integration points. In this way, a very efficient and simple element is obtained which exhibits correct behavior in the limiting case of thin shells. The element can be used in curved shell analysis as well as in the analysis of complicated plate structures. For the latter case, the element is easy to use since connections between intersecting plates can be modeled without tying. Due to its simple formulation when compared to the standard higher order shell elements, it is less expensive and, therefore, very attractive in nonlinear analysis. The element is not very sensitive to distortion, particularly if the corner nodes lie in the same plane. All constitutive relations can be used with this element.

<div style="text-align: right">— MSC.Marc 2013.1 Documentation, vol. B, Element library.</div>

2.3.1 Element geometry

Once recalled the required algebraic paraphernalia, the definition of a bilinear quadrilateral shear-deformable isoparametric shell element is straightforward.

The quadrilateral element geometry is defined by the position in space of its four vertices, which constitute the set of *nodal points*, or *nodes*, i.e. the set of locations at which field components are primarily, parametrically, defined; interpolation is employed in deriving the field values elsewhere.

A suitable interpolation scheme, named *bilinear*, has been introduced in paragraph 2.1.1; the related functions depend on the normalized coordinate pair $\xi, \eta \in [-1, 1]$ that spans the elementary quadrilateral of Figure 2.1.

A global reference system $OXYZ$ is employed for concurrently dealing with multiple elements (i.e. at a whole model scale); a more convenient, local $Cxyz$ reference system, z being locally normal to the shell, is used when a single element is under scrutiny – e.g. in the current paragraph.

Nodal coordinates define the element initial, undeformed, geometry[19] of the portion of shell reference surface pertaining to the currente element; spatial coordinates for each other element point may be retrieved by interpolation based on the associated pair of natural ξ, η coordinates.

In particular, the C centroid is the image within the physical space of the $\xi = 0, \eta = 0$ natural coordinate system origin.

The in-plane orientation of the local $Cxyz$ reference system is somewhat arbitrary and implementation-specific; the MSC.Marc approach is used as an example, and it is described in the following. The in-plane x, y axes are tentatively defined[20] based on the physical directions that are associated with the ξ, η natural axes, i.e. the oriented segments spanning a) from the midpoint of the n4-n1 edge to the midpoint of the n2-n3 edge, and b) from the midpoint of the n1-n2 edge to the midpoint of the n3-n4 edge, respectively; however, these two tentative axes are not mutually orthogonal in general. The mutual Cxy angle is then amended by rotating those interim axes with respect to a third, binormal axis Cz, while preserving their initial bisectrix.

The resulting quadrilateral shell element is in fact initially flat, apart from a (suggestedly limited) anticlastic curvature of the element diagonals, that is associated to the quadratic $\xi\eta$ term of the interpolation functions. The curve nature of a thin wall midsurface is thus represented by recurring to a plurality of basically flat, but mutually angled elements.

---

[19]They are however continuosly updated within most common nonlinear analysis frameworks, where *initial* usually refers to the last computed, aka *previous* step of an iterative scheme.

[20]The MSC.Marc element library documentation defines them as a normalized form of the

$$\left(\frac{\partial X}{\partial \xi}, \frac{\partial Y}{\partial \xi}, \frac{\partial Z}{\partial \xi}, \right)\Bigg|_{\xi=0,\eta=0}, \left(\frac{\partial X}{\partial \eta}, \frac{\partial Y}{\partial \eta}, \frac{\partial Z}{\partial \eta}, \right)\Bigg|_{\xi=0,\eta=0},$$

vectors, which are evaluated at the centroid. The two definitions may be proved equivalent based on the bilinear interpolation properties.

2.3.2 Displacement and rotation fields

The element degrees of freedom consist in the displacements and the rotations of the four quadrilateral vertices, i.e. *nodes*.

By interpolating the nodal values, displacement and rotation functions may be derived along the element as

$$\begin{bmatrix} u(\xi,\eta) \\ v(\xi,\eta) \\ w(\xi,\eta) \end{bmatrix} = \sum_{i=1}^{4} N_i(\xi,\eta) \begin{bmatrix} u_i \\ v_i \\ w_i \end{bmatrix} \tag{2.60}$$

$$\begin{bmatrix} \theta(\xi,\eta) \\ \varphi(\xi,\eta) \\ \psi(\xi,\eta) \end{bmatrix} = \sum_{i=1}^{4} N_i(\xi,\eta) \begin{bmatrix} \theta_i \\ \varphi_i \\ \psi_i \end{bmatrix} \tag{2.61}$$

with $i = 1 \ldots 4$ cycling along the element nodes.

2.3.3 Strains

By recalling Eqn. 2.13, we have e.g.

$$\begin{bmatrix} \frac{\partial u}{\partial x} \\ \frac{\partial u}{\partial y} \end{bmatrix} = \left(\underline{\underline{J}}' \right)^{-1} \underbrace{\begin{bmatrix} \cdots & \frac{\partial N_i}{\partial \xi} & \cdots \\ \cdots & \frac{\partial N_i}{\partial \eta} & \cdots \end{bmatrix}}_{\underline{\underline{L}}(\xi,\eta)} \begin{bmatrix} \vdots \\ u_i \\ \vdots \end{bmatrix} \tag{2.62}$$

for the x-oriented displacement component; the isoparametric differential operator $\underline{\underline{L}}(\xi,\eta)$ is also defined that extract the x, y directional derivatives from the nodal values of a given field component.

We now collect within the five column vectors

$$\underline{u} = \begin{bmatrix} \vdots \\ u_i \\ \vdots \end{bmatrix} , \quad \underline{v} = \begin{bmatrix} \vdots \\ v_i \\ \vdots \end{bmatrix} , \quad \underline{w} = \begin{bmatrix} \vdots \\ w_i \\ \vdots \end{bmatrix} , \quad \underline{\theta} = \begin{bmatrix} \vdots \\ \theta_i \\ \vdots \end{bmatrix} , \quad \underline{\varphi} = \begin{bmatrix} \vdots \\ \varphi_i \\ \vdots \end{bmatrix} \tag{2.63}$$

the nodal degrees of freedom; the $\underline{\psi}$ vector associated with the drilling degree of freedom is omitted.

A block defined $Q(\xi,\eta)$ matrix is thus obtained that cumulatively relates the in-plane displacement component derivatives to the associ-

ated nodal values

$$
\begin{bmatrix} \frac{\partial u}{\partial x} \\ \frac{\partial u}{\partial y} \\ \frac{\partial v}{\partial x} \\ \frac{\partial v}{\partial y} \end{bmatrix} = \underbrace{\begin{bmatrix} \underline{\underline{L}}(\xi, \eta) & \underline{\underline{0}} \\ \underline{\underline{0}} & \underline{\underline{L}}(\xi, \eta) \end{bmatrix}}_{\underline{\underline{Q}}(\xi, \eta)} \begin{bmatrix} \underline{u} \\ \underline{v} \end{bmatrix} \tag{2.64}
$$

An equivalent relation may then be obtained for the rotation field

$$
\begin{bmatrix} \frac{\partial \theta}{\partial x} \\ \frac{\partial \theta}{\partial y} \\ \frac{\partial \varphi}{\partial x} \\ \frac{\partial \varphi}{\partial y} \end{bmatrix} = \underline{\underline{Q}}(\xi, \eta) \begin{bmatrix} \underline{\theta} \\ \underline{\varphi} \end{bmatrix} \tag{2.65}
$$

By making use of two auxiliary matrices $H^{\dagger}$ and $H^{\ddagger}$ that collect the $\{0, \pm 1\}$ coefficients in Eqns. 2.41 and 2.42, we obtain

$$
\begin{bmatrix} \bar{\epsilon}_x \\ \bar{\epsilon}_y \\ \bar{\gamma}_{xy} \end{bmatrix} = \underbrace{\begin{bmatrix} +1 & 0 & 0 & 0 \\ 0 & 0 & 0 & +1 \\ 0 & +1 & +1 & 0 \end{bmatrix}}_{\underline{\underline{H}}^{\dagger}} \begin{bmatrix} \frac{\partial u}{\partial x} \\ \frac{\partial u}{\partial y} \\ \frac{\partial v}{\partial x} \\ \frac{\partial v}{\partial y} \end{bmatrix} = \underline{\underline{H}}^{\dagger} \underline{\underline{Q}}(\xi, \eta) \begin{bmatrix} \underline{u} \\ \underline{v} \end{bmatrix} \tag{2.66}
$$

$$
\begin{bmatrix} \kappa_x \\ \kappa_y \\ \kappa_{xy} \end{bmatrix} = \underbrace{\begin{bmatrix} 0 & 0 & +1 & 0 \\ 0 & -1 & 0 & 0 \\ -1 & 0 & 0 & +1 \end{bmatrix}}_{\underline{\underline{H}}^{\ddagger}} \begin{bmatrix} \frac{\partial \theta}{\partial x} \\ \frac{\partial \theta}{\partial y} \\ \frac{\partial \varphi}{\partial x} \\ \frac{\partial \varphi}{\partial y} \end{bmatrix} = \underline{\underline{H}}^{\ddagger} \underline{\underline{Q}}(\xi, \eta) \begin{bmatrix} \underline{\theta} \\ \underline{\varphi} \end{bmatrix}
$$

$$
\tag{2.67}
$$

The in plane strain tensor at each ξ, η, z point along the element may then be derived according to Eqn. 2.43 as a (linear) function of the nodal degrees of freedom

$$
\underline{\epsilon}(\xi, \eta, z) = \begin{bmatrix} \underline{\underline{H}}^{\dagger} \underline{\underline{Q}}(\xi, \eta) & \underline{\underline{0}} & z \underline{\underline{H}}^{\ddagger} \underline{\underline{Q}}(\xi, \eta) \end{bmatrix} \begin{bmatrix} \underline{u} \\ \underline{v} \\ \underline{w} \\ \underline{\theta} \\ \underline{\varphi} \end{bmatrix} \tag{2.68}
$$

56

where the transformation matrix is block-defined by appending to the 3x8 block introduced in Eqn. 2.66 a 3x3 zero block (the $\underline{w}$ out-of-plane displacements have no influence on the in-plane strain components), and then the 3x8 block presented in Eqn. 2.67.

By separating the terms of the above matrix based on their order with respect to z, we finally have.

$$\underline{\epsilon}(\xi, \eta, z) = \left(\underline{\underline{B}}_0(\xi, \eta) + \underline{\underline{B}}_1(\xi, \eta)z \right) \underline{d} \tag{2.69}$$

The out-of-plane shear strain components, as defined in Eqns. 2.35 and 2.36, become

$$\begin{bmatrix} \bar{\gamma}_{zx} \\ \bar{\gamma}_{yz} \end{bmatrix} = \underline{\underline{L}}(\xi, \eta) \underline{w} + \begin{bmatrix} 0 & +\underline{\underline{N}}(\xi, \eta) \\ -\underline{\underline{N}}(\xi, \eta) & 0 \end{bmatrix} \begin{bmatrix} \theta \\ \varphi \end{bmatrix}, \tag{2.70}$$

and thus, by employing a notation consistent with 2.69,

$$\begin{bmatrix} \bar{\gamma}_{zx} \\ \bar{\gamma}_{yz} \end{bmatrix} = \underbrace{\begin{bmatrix} \underline{0} & \underline{0} & \underline{\underline{L}}(\xi, \eta) & 0 & \underline{\underline{N}}(\xi, \eta) \\ & & & -\underline{\underline{N}}(\xi, \eta) & 0 \end{bmatrix}}_{\underline{\underline{B}}_{\bar{\gamma}}(\xi, \eta)} \underline{d} \tag{2.71}$$

where the transformation matrix that derives the out-of-plane, interlaminar strains from the nodal degrees of freedom vector is constituted by five 2×4 blocks.

2.3.4 Stresses

The plane stress relations discussed in Paragraph 2.2, see Eqns. 2.45, may be employed in deriving the in-plane stress components from the associated strains.

The G_{zx}, G_{yz} material shear moduli relate the out-of-plane shear stresses to the associated strain components only if the latter are assumed constant along the thickness, and thus equal to the average values $\bar{\gamma}_{zx}, \bar{\gamma}_{yz}$. A gross approximation, this, that may be overcome by extending the Jourawsky equilibrium considerations introduced for beams, to the plate realm. The actual treatise is however both complicated and, still, inexact[21].

In the case of homogeneous, linearly elastic plate material, an energetically consistent material law for the out-of-plane shear may be obtained by scaling the pointwise stress/strain relation[22]

$$\begin{bmatrix} \tau_{zx} \\ \tau_{yz} \end{bmatrix} = \underline{\underline{D}}_\gamma \begin{bmatrix} \gamma_{zx} \\ \gamma_{yz} \end{bmatrix}, \tag{2.72}$$

by a $6/5$ factor, thus obtaining the emended, average out-of-plane shear stress components

$$\begin{bmatrix} \bar{\tau}_{zx} \\ \bar{\tau}_{yz} \end{bmatrix} = \underbrace{\left(\frac{6}{5} \underline{\underline{D}}_\gamma \right)}_{\underline{\bar{\underline{D}}}_\gamma} \begin{bmatrix} \bar{\gamma}_{zx} \\ \bar{\gamma}_{yz} \end{bmatrix}, \tag{2.73}$$

Such relation is energetically consistent in the sense of the following equality

$$\frac{1}{2} \int_z \gamma_{zx} \tau_{zx} + \gamma_{yz} \tau_{yz} dz = \frac{1}{2} \begin{bmatrix} \bar{\gamma}_{zx} \\ \bar{\gamma}_{yz} \end{bmatrix}^\top \begin{bmatrix} \bar{\tau}_{zx} \\ \bar{\tau}_{yz} \end{bmatrix} h \tag{2.74}$$

$$= \frac{1}{2} \begin{bmatrix} \bar{\gamma}_{zx} \\ \bar{\gamma}_{yz} \end{bmatrix}^\top \underline{\bar{\underline{D}}}_\gamma \begin{bmatrix} \bar{\gamma}_{zx} \\ \bar{\gamma}_{yz} \end{bmatrix} h. \tag{2.75}$$

---

[21] See e.g. MSC.Marc 2013.1 Documentation, Vol. A, pp. 433-436

[22] As an example, the definition for $\underline{\underline{D}}_\gamma$ in the case of an orthotropic material whose out-of-plane shear moduli are G_{z1} and G_{2z} is

$$\underline{\underline{D}}_\gamma = \begin{bmatrix} n^2 G_{z1} + m^2 G_{2z} & mn G_{z1} - mn G_{2z} \\ mn G_{z1} - mn G_{2z} & m^2 G_{z1} + n^2 G_{2z} \end{bmatrix},$$

where $m = \cos\alpha$, $n = \sin\alpha$, and α is the angle between the first in-plane principal direction of ortotropy, namely 1, and the local x axis.

The definition of the $\bar{\underline{\underline{D}}}_\gamma$ matrix for composite laminates, or in the case of nonlinear material behaviour, is Beyond the Scope of the Present Contribution (BSPC).

2.3.5 The element stiffness matrix.

In this paragraph, the elastic behaviour of the finite element under scrutiny is derived.

The element is considered in its deformed configuration, being

$$\underline{d}^\top = \begin{bmatrix} \underline{u}^\top & \underline{v}^\top & \underline{w}^\top & \underline{\theta}^\top & \underline{\varphi}^\top \end{bmatrix} \tag{2.76}$$

the Degree of Freedom (DOF) vector associated with such condition.

A virtual displacement field perturbs such deformed configuration; as usual, those virtual displacements are infinitesimal, they do occur while time is held constant, and, being otherwise arbitrary, they respect the existing kinematic constraints.

Whilst, in fact, no external constrains are applied to the element, the motion of the pertaining material points is prescribed based on a) the assumed plate kinematics, and b) on the bilinear, isoparametric interpolation laws that propagate the generalized nodal displacements $\delta\underline{d}$ towards the quadrilateral's interior.

Since the element is supposed to elastically react to such deformed configuration, a set of external actions

$$\underline{F}^\top = \begin{bmatrix} \underline{U}^\top & \underline{V}^\top & \underline{W}^\top & \underline{\Theta}^\top & \underline{\Phi}^\top \end{bmatrix} \tag{2.77}$$

is applied at nodes[23] – one each DOF, that equilibrate the stretched element reactions.

The nature of each $\underline{F}$ generalized force component is defined based on the nature of the associated generalized displacement, such that the overall virtual work they perform on any $\delta\underline{d}$ motion is

$$\delta Q_e = \delta\underline{d}^\top\,\underline{F}. \tag{2.78}$$

The in-plane stress components that are induced by the $\underline{d}$ generalized displacements equal

$$\underline{\sigma} = \underline{\underline{D}}(z)\left(\underline{\underline{B}}_0(\xi,\eta) + \underline{\underline{B}}_1(\xi,\eta)z\right)\underline{d} \tag{2.79}$$

---

[23]There is no lack of generality in assuming the equilibrating external actions applied at DOFs only, as discussed in Par. XXX below.

according to the previous paragraphs. They perform (volumic) internal work on the

$$\delta \underline{\epsilon} = \left(\underline{\underline{B}}_0(\xi, \eta) + \underline{\underline{B}}_1(\xi, \eta) z \right) \delta \underline{d} \qquad (2.80)$$

virtual elongations.

The associate internal virtual work may be derived by integration along the element volume, i.e. along the thickness, and along the quadrilateral portion of reference surface that pertains to the element. We thus obtain a first contribution to the overall internal virtual work

$$
\begin{aligned}
\delta Q_{\mathrm{i}}^{\sigma} &= \iint_A \int_h \delta \underline{\epsilon}^{\top} \underline{\sigma} \, dz dA \\
&= \iint_A \int_h \left(\left(\underline{\underline{B}}_0 + \underline{\underline{B}}_1 z \right) \delta \underline{d} \right)^{\top} \underline{\underline{D}} \left(\underline{\underline{B}}_0 + \underline{\underline{B}}_1 z \right) \underline{d} \, dz dA \\
&= \delta \underline{d}^{\top} \left[\iint_A \int_h \left(\underline{\underline{B}}_0^{\top} + \underline{\underline{B}}_1^{\top} z \right) \underline{\underline{D}} \left(\underline{\underline{B}}_0 + \underline{\underline{B}}_1 z \right) dz dA \right] \underline{d} \\
&= \delta \underline{d}^{\top} \underline{\underline{K}}_{\sigma} \underline{d} \qquad (2.81)
\end{aligned}
$$

Integration along i) the reference surface, and ii) along the thickness is numerically performed through potentially distinct quadrature rules; in particular, contributions are collected along the surface according to the two points per axis (four points overall) Gaussian quadrature formula introduced in Par. 2.1.2, whilst a (composite) Simpson rule is applied in z, being each material layer sampled at its outer and middle points.

The two points per axis quadrature rule is the lowest order rule that returns an exact integral evaluation in the case of *distortion-free*[24] elements, i.e. planar elements whose peculiar (parallelogram) shape also determines a linear (vs. bilinear) isoparametric mapping. Since the associated Jacobian matrix is constant with respect to ξ, η, the $\underline{\underline{L}}$ matrix defined in 2.62 linearly varies with such isoparametric coordinates, and so do the $\underline{\underline{B}}_0$, $\underline{\underline{B}}_1$ matrices. The integrand of Eqn. 2.81 is thus a quadratic function of the ξ, η integration variables, as the Jacobian matrix determinant that scales the physical and the natural infinitesimal areas is also constant XXX.

A second contribution, which is due to the out-of-plane shear components, may be obtained with similar considerations, and based on

---

[24] Many distinct definitions are associated to the element distortion concept, being the one reported relevant for the specific dissertation passage.

Eqns. 2.71 and 2.75; such contribution may be cast as

$$
\begin{aligned}
\delta Q_{\mathrm{i}}^{\gamma} &= \iint_{A} \int_{h} \delta\,\underline{\bar{\gamma}}^{\top}\,\underline{\bar{\tau}}\,dz\,dA \\
&= \delta\,\underline{d}^{\top}\left[h \iint_{A} \underline{\underline{B}}_{\gamma}^{\top}\,\underline{\underline{\bar{D}}}_{\gamma}\,\underline{\underline{B}}_{\gamma}\,dA \right]\underline{d} \\
&= \delta\,\underline{d}^{\top}\,\underline{\underline{K}}_{\gamma}\,\underline{d}\,.
\end{aligned}
\tag{2.82}
$$

The overall internal work is thus

$$
\begin{aligned}
\delta Q_{\mathrm{i}} &= \delta Q_{\mathrm{i}}^{\sigma} + \delta Q_{\mathrm{i}}^{\gamma} \\
&= \delta\,\underline{d}^{\top}\left(\underline{\underline{K}}_{\sigma} + \underline{\underline{K}}_{\gamma}\right)\underline{d} \\
&= \delta\,\underline{d}^{\top}\,\underline{\underline{K}}\,\underline{d}\,.
\end{aligned}
\tag{2.83}
$$

The principle of virtual works states that the external and the internal virtual works are equal for a general virtual displacement $\delta\,\underline{d}$, namely

$$
\delta\,\underline{d}^{\top}\,\underline{G} = \delta Q_{\mathrm{e}} = \delta Q_{\mathrm{i}} = \delta\,\underline{d}^{\top}\,\underline{\underline{K}}\,\underline{d}, \quad \forall \delta\,\underline{d},
\tag{2.84}
$$

if and only if the applied external actions $\underline{G}$ are in equilibrium with the elastic reactions due to the displacements $\underline{d}$; the following equality thus holds

$$
\underline{G} = \underline{\underline{K}}\,\underline{d};
\tag{2.85}
$$

the $\underline{\underline{K}}$ *stiffness matrix* relates a deformed element configuration, which is defined the the generalized displacement vector $\underline{d}$, with the $\underline{G}$ generalized forces that have to be applied at the element nodes to keep the element in such a stretched state.

2.3.6 The shear locking flaw

Figure 2.17 rationalizes the shear locking phenomenon that plagues the bilinear isoparametric element in its mimicking the pure bending deformation modes, with both in-plane and out-of-plane constant curvature.

An ingenious sampling and interpolation technique has been developed in [3] that overcomes the locking effect due to the spurious transverse shear strain that develops when the element is subject to out-of-plane bending. Such technique, however, does not correct the element behaviour with respect to in-plane bending.

Eqn. 2.71 is employed in obtaining the tranverse shear strain components $\bar{\gamma}_{zx}$ and $\bar{\gamma}_{yz}$ at the edge midpoints; the edge-aligned component $\bar{\gamma}_{z\hat{ij}}$ is derived by projection along the $\hat{ij}$ direction, whereas the orthogonal component is neglected.

Figure 2.8a evidences that a null spurious tranverse shear is measured at the midpoint of the 12 and of the 41 edges when a constant, out-of-plane curvature is locally enforced that develops along the $\hat{12}$ and the $\hat{41}$ directions, respectively. Such property holds for all edges.

In Figure 2.8b, a differential out-of-plane displacement is added to the initial pure bending configuration of Fig. 2.8a, and in the absence of further rotations at nodes; a proper (vs. spurious) tranverse shear strain field is thus induced in the element, that the sampling scheme should properly evaluate.

The edge aligned, transverse shear components sampled at the side midpoints are then assigned to the whole edge, and in particular to both its extremal nodes.

As shown in Figure 2.8b (and in the related enlarged view), two independent transverse shear components $\bar{\gamma}_{z\hat{12}}$ and $\bar{\gamma}_{z\hat{41}}$ are associated to the n1 node, which is taken as an example.

A vector is uniquely determined, whose projections on the $\hat{12}$ and $\hat{41}$ directions coincide with the associated transverse shear components; the components of such vector with respect to the x, y axes define the $\bar{\gamma}_{zx,\text{n1}}$ and $\bar{\gamma}_{yz,\text{n1}}$ tranverse shear terms at the n1 node.

Such procedure is repeated for all the element vertices; the obtained nodal values for the transverse shear components are then interpolated to the element interior, according to the costumary bilinear scheme.

Due to the peculiarity of the initial sampling points, the obtained

a)

$+b$

$-a$ $+a$ x

$-b$

undeformed domain

b)

$\frac{\alpha}{2}$ $\frac{\alpha}{2}$

$\frac{\alpha}{2}$

C_{b}

$\epsilon_y > 0$

$\epsilon_y < 0$

exact solution,
pure in-plane bending

$\epsilon_x = -\frac{\alpha y}{2a}$

$\epsilon_y = \epsilon_z = \nu \frac{\alpha y}{2a}$

$\gamma_{xy} = 0$

$u = \frac{\alpha^2 E y^2}{8a^2}$

c)

$\frac{\theta}{2}$ $\frac{\theta}{2}$

C_{iso4}

four noded, isop. element,
in-plane trapezoidal mode

$\epsilon_x = -\frac{\alpha y}{2a}$

$\epsilon_y = 0, \ \epsilon_z = \frac{\nu}{1-\nu}\frac{\alpha y}{2a}$

$\gamma_{xy} = -\frac{\alpha x}{2a}$

$u = \left(1 + \frac{\nu^2}{1-\nu^2}\right)\frac{E\alpha^2 y^2}{8a^2} + \frac{G\alpha^2 x^2}{8a^2}$

d)

$\frac{\alpha}{2}$

residual (spurious)
shear deformation;

overall error assessment:

$\frac{C_{\mathrm{iso4}}}{C_{\mathrm{b}}} = \frac{1+\frac{1-\nu}{2}\left(\frac{a}{b}\right)^2}{1-\nu^2}$

≈ 1.48 if $\nu = 0.3, \frac{a}{b} = 1$

$\gamma_{xy} = \frac{\alpha}{2}$ $\gamma_{xy} = 0$ $\gamma_{xy} = -\frac{\alpha}{2}$
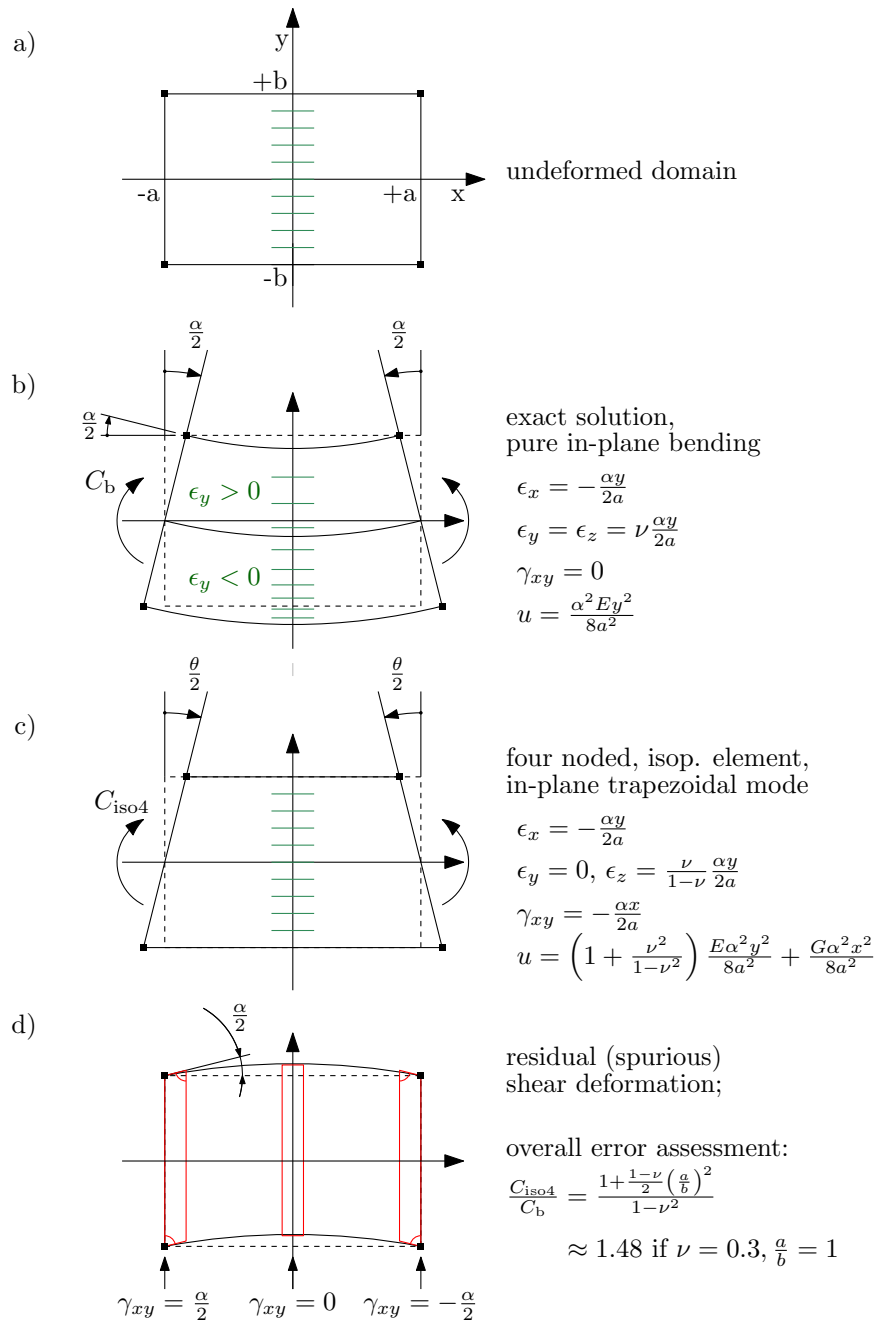
Figure 2.7: Rationalization of the shear locking phenomenon.
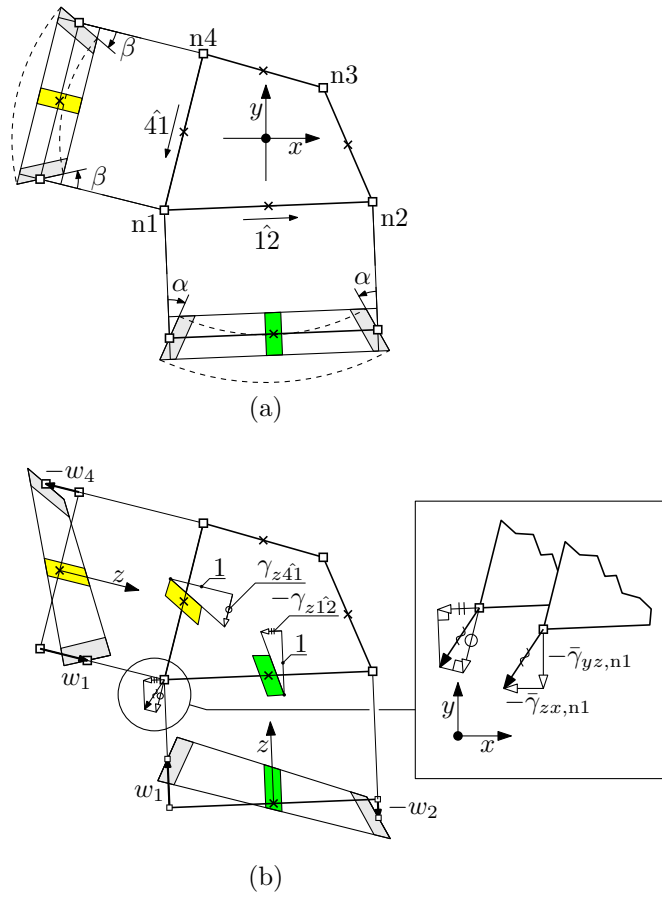
Figure 2.8: A tranverse shear sampling technique employed in the four-noded isoparametric element for preventing shear locking in the out-of-plane plate bending.

tranverse shear strain field is amended with respect to the spurious contribution that previously led to the shear locking effect; the usual quadrature scheme may now be employed.

Equation 2.71 still formalizes the passage from nodal DOFs to the out-of-plane shear field, since the procedure described in the present paragraph may be easily cast in the form of a revised $\underline{\underline{B}}_\gamma$ matrix.

2.4 Mass matrix for the finite element

2.4.1 Energy consistent formulation for the mass matrix

The Ω volume of material associated to a finite element is considered, along with the local, physical reference system (x, y, z), and its isoparametric counterpart that, for the quadrilateral plate element under scrutiny, is embodied by the (ξ, η, z) triad.

The *vector* shape function array

$$\underline{\underline{S}}(\xi, \eta, z) = \begin{bmatrix} \dots & \tilde{u}_i(\xi, \eta, z) & \dots \\ \dots & \tilde{v}_i(\xi, \eta, z) & \dots \\ \dots & \tilde{w}_i(\xi, \eta, z) & \dots \end{bmatrix} \tag{2.86}$$

is defined based on the elementary motions $\underline{\tilde{u}}_i \equiv [\tilde{u}_i, \tilde{v}_i, \tilde{w}_i]^\top$ induced to the element material points by imposing a unit value to the i-th degree of freedom d_i, while keeping the others fixed.

The displacement field is then defined as a linear combination of the elementary motions above, where the $\underline{d}$ element DOFs serve as coefficients, namely

$$\underline{u}(\xi, \eta, z) = \underline{\underline{S}}(\xi, \eta, z)\,\underline{d}\,. \tag{2.87}$$

Deriving with respect to time the equation above, the velocity field

$$\underline{\dot{u}}(\xi, \eta, z) = \underline{\underline{S}}(\xi, \eta, z)\,\underline{\dot{d}} \tag{2.88}$$

is obtained as a function of the first variation in time of element DOFs. Expression 2.88 is simplified by the constant-in-time nature of $\underline{\underline{S}}$.

The kinetic energy contribution associated to the deformable element material points may be integrated, thus obtaining

$$E_{\text{kin}} = \frac{1}{2} \iiint_\Omega \underline{\dot{u}}^\top \underline{\dot{u}}\, \rho d\Omega \tag{2.89}$$

where ρ is the material mass density, that may vary across the domain. By substituting the velocity field definition of Eq. 2.88 we obtain

$$E_{\text{kin}} = \frac{1}{2} \iiint_\Omega \left[\underline{\underline{S}}\,\underline{\dot{d}}\right]^\top \left[\underline{\underline{S}}\,\underline{\dot{d}}\right] \rho d\Omega, \tag{2.90}$$

and finally

$$E_{\text{kin}} = \frac{1}{2} \dot{\underline{d}}^\top \left[\iiint_\Omega \underline{\underline{S}}^\top \underline{\underline{S}} \rho d\Omega \right] \dot{\underline{d}} = \frac{1}{2} \dot{\underline{d}}^\top \underline{\underline{M}} \, \dot{\underline{d}}. \tag{2.91}$$

The integral term that defines the $\underline{\underline{M}}$ *mass* matrix is evaluated by resorting to the same quadrature technique introduced for its stiffness counterpart.

The actual nature of the mass matrix terms varies based on the type of the DOFs that are associated to the term row and column; in particular, the diagonal terms that are related to displacements and rotations are dimensionally consistent with a mass and a moment of inertia, respectively.

The mass matrix quantifies the inertial response of the finite element; according to its definition

$$\underline{\underline{M}} = \iiint_\Omega \underline{\underline{S}}^\top \underline{\underline{S}} \rho d\Omega, \tag{2.92}$$

it is merely a function of the material density, and of the kinematic laws that constrain the motion of the material particles within the element.

If a set of external (generalized) forces $\underline{G}$ is applied to the element DOFs in the fictitious absence of elastic reactions, a purely inertial response is expected. The $\dot{\underline{d}}$ vector defines the instantaneous first derivative in time of the DOFs (i.e. nodal translational and rotational velocities); the instantaneous power supplied by the external forces is then evaluated as $\dot{\underline{d}}^\top \underline{G}$, that induces an equal time derivative of the kinetic energy, quantified as [25]

$$\begin{aligned} \dot{\underline{d}}^\top \underline{G} = \frac{dE_{\text{kin}}}{dt} &= \frac{d}{dt} \left(\frac{1}{2} \dot{\underline{d}}^\top \underline{\underline{M}} \, \dot{\underline{d}} \right) \\ &= \frac{1}{2} \left(\ddot{\underline{d}}^\top \underline{\underline{M}} \, \dot{\underline{d}} + \dot{\underline{d}}^\top \underline{\underline{M}} \, \ddot{\underline{d}} \right) \\ &= \dot{\underline{d}}^\top \underline{\underline{M}} \, \ddot{\underline{d}}. \end{aligned}$$

---

[25]The symmetric matrix characterizing property

$$\underline{x}^\top \underline{\underline{A}} \, \underline{y} = \underline{y}^\top \underline{\underline{A}} \, \underline{x} \quad \forall \underline{x}, \underline{y} \in \mathbb{R}^n$$

is used in deriving the last passage.

Due to the general nature of $\underline{\dot{d}}$, equality

$$\underline{G} = \underline{\underline{M}}\, \underline{\ddot{d}} \tag{2.93}$$

is implied, which points out the mass matrix role in transforming the DOF vector second derivative in time (i.e. nodal translational and rotational accelerations) into the generalized force components that are to be applied in order to sustain such variation of motion.

2.4.2   Lumped mass matrix formulation

In a few applications, a diagonal form for the mass matrix is preferred at the expense of a) a strict adherence to energy consistency, and b) some arbitrariness in its definition.

The finite element volume is ideally partitioned into a set of influence domains, one each node. In the case of the four-noded quadrilateral, material points whose ξ, η isoparametric coordinates fall within the first, second, third and fourth quadrant are associated to nodes n3, n4, n1 and n2, respectively; those distributed masses are then ideally accumulated at the associated node.

A group of four concentrated nodal masses is thus defined, whose motion is defined based on single translational DOFs, and not on the plurality of weighted contributions that induces the nonzero, nondiagonal terms at the consistent mass matrix.

This undue material accumulation at the element periphery produces a spurious increase of the moment of inertia, condition, this, that may only be worsened if (positive) rotational inertias are introduced at nodes.

Those nodal rotational inertias are however required in associating a bounded angular acceleration to unbalanced nodal torques; solution methods based on the mass matrix inversion, e.g. explicit dynamic procedures, are precluded otherwise. Since there is no consensus on the quantification those inertial terms, the reader is addressed to specialized literature.

2.5   External forces

Energetically consistent external actions may be applied at the nodal DOFs, that may be interpreted as *concentrated* forces and moments;

their physical rationalization outside the discretized structure framework – and in particular back to the underlying elastic continua theory – is far from being trivial.

Surface tractions and volumetric loads are instead naturally tied with the continuum formulation, and are usually employed in formalizing the load condition of structural components.

The present paragraph derives the equivalent nodal representation of distributed actions acting on the domain of a single finite element; the inverse relation provides a finite, distributed traction counterpart to concentrated actions applied at the nodes of a discretized FE model.

The $\underline{\underline{S}}$ set of elementary deformation modes that is introduced in the context of the element mass matrix derivation, see Eqn. 2.86, is employed to define a virtual displacement field within the element domain based on the virtual variation $\delta \underline{d}$ of its nodal DOFs values, i.e.

$$\delta \underline{u}(\xi, \eta, z) = \underline{\underline{S}}(\xi, \eta, z)\delta \underline{d}, \qquad (2.94)$$

see also Eq. 2.87.

A volumetric external load is considered, whose components $\underline{q} = [q_x, q_y, q_z]$ are consistent with the $\underline{\underline{S}}$ matrix reference system, i.e. the local to the element, physical $Cxyz$ one. If external load components are defined in the context of a global reference system, straightforward reference frame transformations are to be applied.

The virtual work performed by those distributed actions is first integrated along the element domain, and then equalled to its nodal counterpart $\delta \underline{d}^\top \underline{G}$, thus leading to

$$\delta \underline{d}^\top \underline{G} = \iiint_\Omega (\delta \underline{u})^\top \underline{q} \, d\Omega$$

$$= \iiint_\Omega \left(\underline{\underline{S}} \, \delta \underline{d}\right)^\top \underline{q} \, d\Omega$$

$$= \delta \underline{d}^\top \iiint_\Omega \underline{\underline{S}}^\top \underline{q} \, d\Omega,$$

and finally to

$$\underline{G} = \iiint_\Omega \underline{\underline{S}}^\top \underline{q} \, d\Omega \qquad (2.95)$$

due to the general nature of $\delta \underline{d}$.

The quadrature along the domain is performed according to the methods introduced for deriving the element stiffness matrix. If a surface or an edge load are supplied in place of the volumetric load vector $\underline{q}$, equation 2.95 integral may be adapted to span each loaded element face, or edge.

In the case of low order isoparametric elements – e.g. the four-noded quadrilateral shell element, an alternative, simplified procedure for the consolidation of the distributed loads into nodal forces becomes viable. According to such procedure, the element domain is partitioned into influence volumes, one each node; the external load contributions are then accumulated within each partition, and the resultant force vector is applied to the associated node.

By moving such resultant force from the distribution Center of Gravity (COG) to the corner node, momentum balance is naively disregarded; the induced error however decreases with the load field variance across the element, and hence with the element size. Such error vanishes for uniform distributed loads.

In the presence of a better established, work consistent counterpart, such simplified procedure is mostly employed to set a rule-of-thumb equivalence between distributed and nodal loads; in particular, the stress-singular nature of a set of nodal loads may be easily pointed out if it is observed that a finite load resultant is applied to influence areas that cumulatively vanish with vanishing element size.

2.6 Joining elements into structures.

2.6.1 Displacement and rotation field continuity

Displacement and rotation fields are continuous at the isoparametric quadrilateral inter-element interfaces; they are in fact continuous at nodes since the associated nodal DOFs are shared by adjacent elements, and the field interpolations that occur within each quadrilateral domain a) they both reduce to the same linear relation along the shared edge, and b) they are performed in the absence of any contributions related to unshared nodes or DOFs.

2.6.2 Expressing the element stiffness matrix in terms of global DOFs

As seen in Par. 2.3.5, the stiffness matrix of each j-th element defines the elastic relation between the associated generalized forces and displacements, i.e.

$$\underline{G}_{ej} = \underline{\underline{K}}_{ej}\,\underline{d}_{ej} \tag{2.96}$$

where the DOFs definition is local with respect to the element under scrutiny.

In order to investigate the mutual interaction between elements in a structure, a common set of *global* DOFs is required; in particular, generalized displacement DOFs are defined at each l-th global node, i.e., for nodes interacting with the shell element formulation under scrutiny,

$$\underline{d}_{gl} = \begin{bmatrix} u_{gl} \\ v_{gl} \\ w_{gl} \\ \theta_{gl} \\ \varphi_{gl} \\ \psi_{gl} \end{bmatrix}. \tag{2.97}$$

The global reference system $OXYZ$ is typically employed in projecting nodal vector components. However, each l-th global node may be supplied with a specific reference system, whose unit vectors are $\hat{\imath}_{gl}, \hat{\jmath}_{gl}, \hat{k}_{gl}$, thus permitting the employment of non uniformly aligned (e.g. cylindrical) global reference systems.

Those nodal degrees of freedom may be collected in a global DOFs vector

$$\underline{d}_g^\top = \begin{bmatrix} \underline{d}_{g1}^\top & \underline{d}_{g2}^\top & \cdots & \underline{d}_{gl}^\top & \cdots & \underline{d}_{gn}^\top \end{bmatrix} \qquad (2.98)$$

that parametrically defines any deformed configuration of the structure.

Analogously, a global, external (generalized[26]) forces vector may be defined, that assumes the form

$$\underline{F}_g^\top = \begin{bmatrix} \underline{F}_{g1}^\top & \underline{F}_{g2}^\top & \cdots & \underline{F}_{gl}^\top & \cdots & \underline{F}_{gn}^\top \end{bmatrix} ; \qquad (2.99)$$

since *external* (single DOF or *"to ground"*) and *internal* (multi DOF) kinematic constraints are expected to be applied to the structure DOFs, the following vector of reaction forces

$$\underline{R}_g^\top = \begin{bmatrix} \underline{R}_{g1}^\top & \underline{R}_{g2}^\top & \cdots & \underline{R}_{gl}^\top & \cdots & \underline{R}_{gn}^\top \end{bmatrix} \qquad (2.100)$$

is introduced. Many FE softwares – and MSC.Marc in particular – treat external and internal constraints separately, thus leading to two set of constraint actions, namely the (strictly named) *reaction forces*, and the *tying forces*, respectively; for the sake of simplicity, the constraint treatise is unified in the present contribution.

The simple four element, roof-like structure of Fig. 2.9 is employed in the following to discuss the procedure that derives the elastic response characterization for the structure from its elemental counterparts.

The structure comprises nine nodes, whose location in space is defined according to a global reference system $OXYZ$, see Table 2.2.

The structure is composed by four, identical, four noded isoparametric shell elements, whose formulation is described in the preceding section 2.3.

A grayscale, normalized representation of the element stiffness matrix is shown in Figure 2.10, where the white to black colormap spans from zero to the maximum in absolute value term.

The mapping between local, element based node numbering and the global node numbering is reported in the connectivity Table 2.3.

Such i) local to global node numbering mapping, together with ii) the change in reference system mentioned above, defines a set of

---

[26]Unless otherwise specified, the *displacement* and *force* terms refer to the DOFs, and the suitable actions that perform work with their variation, respectively. They are in fact *generalized* forces and displacements.

$$w_{e1n2}\,\hat{k}_{e1} = u_{g2}\,\hat{i}_{g2} + v_{g2}\,\hat{j}_{g2} + w_{g2}\,\hat{k}_{g2}$$
$$\theta_{e1n1}\,\hat{i}_{e1} = \theta_{g1}\,\hat{i}_{g1} + \varphi_{g1}\,\hat{j}_{g1} + \psi_{g1}\,\hat{k}_{g1}$$
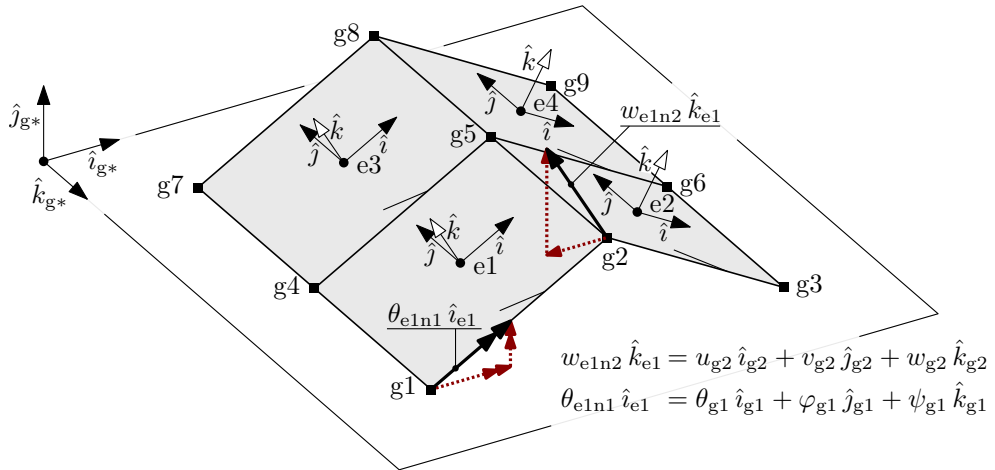
Figure 2.9: A simple four-element, roof-like structure employed in discussing the assembly procedures. The elements are square, thick plates whose angle with respect to the global XY plane is $30°$

node	X	Y	Z
g1	$-lc$	0	$+l$
g2	0	$+ls$	$+l$
g3	$+lc$	0	$+l$
g4	$-lc$	0	0
g5	0	$+ls$	0
g6	$+lc$	0	0
g7	$-lc$	0	$-l$
g8	0	$+ls$	$-l$
g9	$+lc$	0	$-l$

Table 2.2: Nodal coordinates for the roof-like structure of Figure 2.9. l is the element side length, $c = \cos 30°$ and $s = \sin 30°$
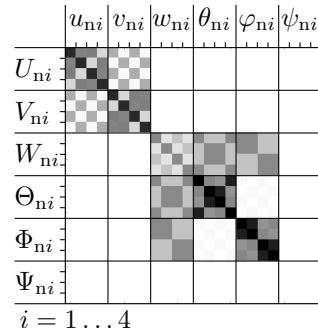
Figure 2.10: A representation of the stiffness matrix terms for each element in the example structure; the term magnitude is represented through a linear grayscale, spanning from zero (white) to the peak value (black).

	n1	n2	n3	n4
e1	g1	g2	g5	g4
e2	g2	g3	g6	g5
e3	g4	g5	g8	g7
e4	g5	g6	g9	g8

Table 2.3: Element connectivity for the roof-like structure of Figure 2.9. As an example, the node described by the local numbering e3n2 is mapped to the global node g5.
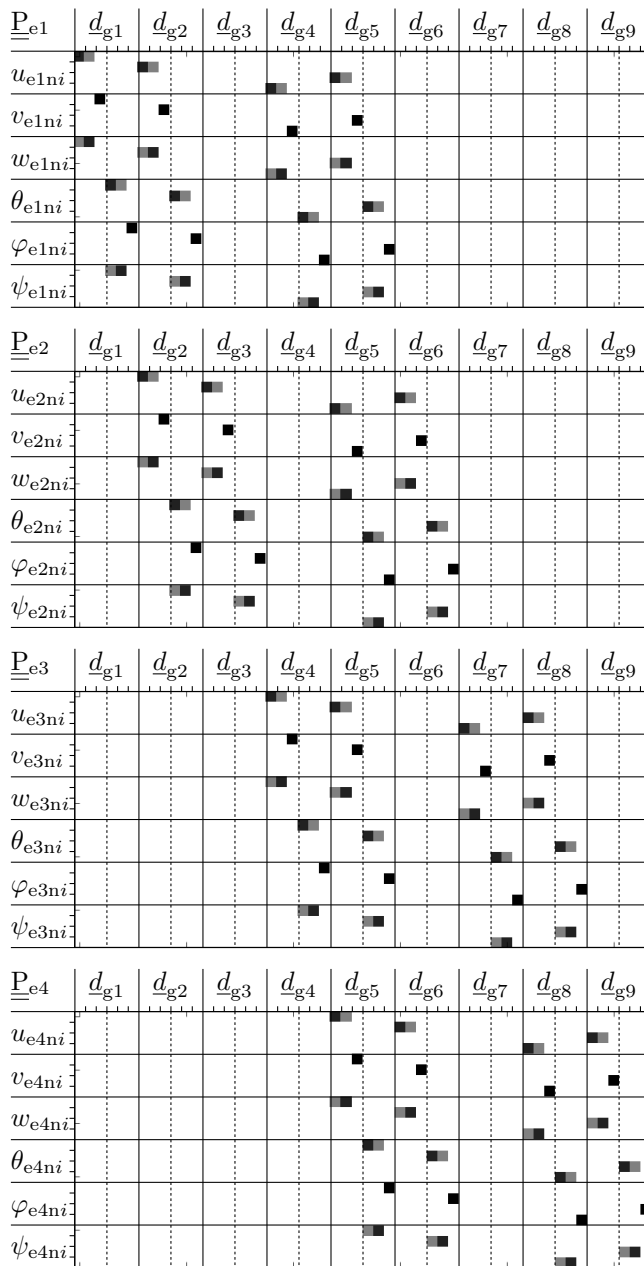
Figure 2.11: A grayscale representation of the terms of the four $\underline{\underline{\mathrm{P}}}_{\mathrm{e}j}$ mapping matrices associated the elements of Fig. 2.9. The colormap spans from white (zero) to black (one); the lighter and the darker grey colors represent terms that equate in modulus $\sin 30°$ and $\cos 30°$, respectively.

elemental DOF mapping matrices, $\underline{\underline{P}}_{ej}$, one each j-th element. Such matrices are defined as follows: the i-th row the $\underline{\underline{P}}_{ej}$ matrix contains the coefficients of the linear combination of global DOFs that equates the i local DOF of the j-th element; an example is proposed in the following to illustrate such relation.

With reference to the structure of Figure 2.9, w_{e1n2} and θ_{e1n1} respectively represent the 10th and the 13th local degrees of freedom of element 1.

Their global representation involves a subset of the g2 and g1 global nodes DOFs, respectively, namely

$$w_{e1n2} = \langle \hat{k}_{e1}, \hat{\imath}_{g2} \rangle u_{g2} + \langle \hat{k}_{e1}, \hat{\jmath}_{g2} \rangle v_{g2} + \langle \hat{k}_{e1}, \hat{k}_{g2} \rangle w_{g2} \qquad (2.101)$$

$$\theta_{e1n1} = \langle \hat{\imath}_{e1}, \hat{\imath}_{g1} \rangle \theta_{g1} + \langle \hat{\imath}_{e1}, \hat{\jmath}_{g1} \rangle \phi_{g1} + \langle \hat{\imath}_{e1}, \hat{k}_{g1} \rangle \psi_{g1} \qquad (2.102)$$

where $\hat{\imath}_{e1}, \hat{\jmath}_{e1}, \hat{k}_{e1}$ are the orientation vectors of the element 1 local reference system, $\hat{\imath}_{g1}, \hat{\jmath}_{g1}, \hat{k}_{g1}$ and $\hat{\imath}_{g2}, \hat{\jmath}_{g2}, \hat{k}_{g2}$ are the orientation vectors of the global nodes 1 and 2 reference systems, and $\langle \cdot, \cdot \rangle$ represents their mutual scalar product, or, equivalently, the cosinus of the angle between two unit vectors.

The 10th and the 13th row of the $\underline{\underline{P}}_{e1}$ mapping matrix are defined based on Eqs.2.101 and 2.102, respectively, and they are null except for the elements

$$\left[\underline{\underline{P}}_{e1} \right]_{10,7} = \langle \hat{k}_{e1}, \hat{\imath}_{g2} \rangle \qquad\qquad \left[\underline{\underline{P}}_{e1} \right]_{13,4} = \langle \hat{\imath}_{e1}, \hat{\imath}_{g1} \rangle$$

$$\left[\underline{\underline{P}}_{e1} \right]_{10,8} = \langle \hat{k}_{e1}, \hat{\jmath}_{g2} \rangle \qquad\qquad \left[\underline{\underline{P}}_{e1} \right]_{13,5} = \langle \hat{\imath}_{e1}, \hat{\jmath}_{g1} \rangle$$

$$\left[\underline{\underline{P}}_{e1} \right]_{10,9} = \langle \hat{k}_{e1}, \hat{k}_{g2} \rangle \qquad\qquad \left[\underline{\underline{P}}_{e1} \right]_{13,6} = \langle \hat{\imath}_{e1}, \hat{k}_{g1} \rangle,$$

being $u_{g2}, v_{g2}, w_{g2}, \theta_{g1}, \phi_{g1}$ and ψ_{g1} the 7th, 8th, 9th, 4th, 5th and 6th global degrees of freedom according to their position in $\underline{d}_g$.

Figure 2.11 presents a grayscale representation of the four $\underline{\underline{P}}_{ej}$ matrices; please note the extremely sparse nature of those matrices, whose number of nonzero terms scales with the single element DOF cardinality, whereas the total number of terms scale with the whole structure DOF cardinality.

The rows of the rectangular $\underline{\underline{P}}_{ej}$ mapping matrix are mutually orthonormal; the mapping matrix is orthogonal in the sense of the Moore-Penrose pseudoinverse, since its transpose and its pseudoinverse coincide.

$$V_{g8\leftarrow e3}\,\hat{j}_{g8} = U_{e3n3}\,\hat{i}_{e3} + V_{e3n3}\,\hat{j}_{e3} + W_{e3n3}\,\hat{k}_{e3}$$
$$V_{g8\leftarrow e4}\,\hat{j}_{g8} = U_{e4n4}\,\hat{i}_{e4} + V_{e4n4}\,\hat{j}_{e4} + W_{e4n4}\,\hat{k}_{e4}$$
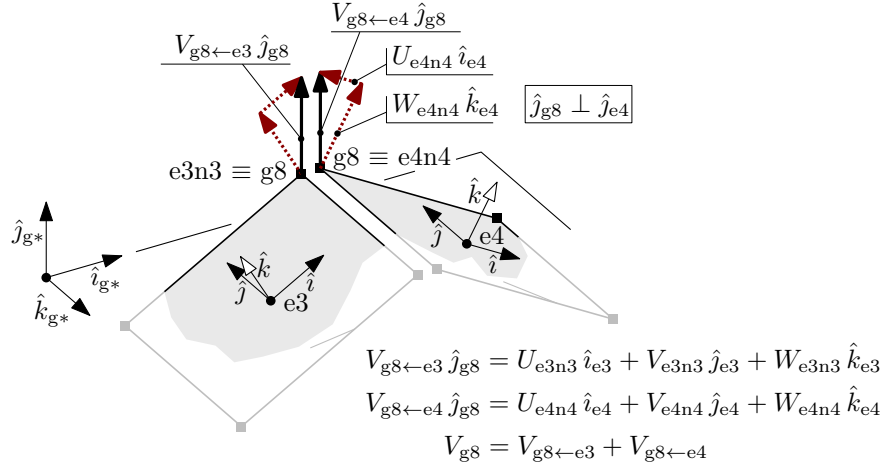$$V_{g8} = V_{g8\leftarrow e3} + V_{g8\leftarrow e4}$$

Figure 2.12: Accumulation of elemental nodal actions at global nodes.

The elemental mapping $\underline{\underline{P}}_{ej}$ matrices constitute an artifice that plays a double role in the local to global DOF mapping; if on one side the j-th element DOFs may be derived from their global counterpart as

$$\underline{d}_{ej} = \underline{\underline{P}}_{ej}\,\underline{d}_g, \quad \forall j \tag{2.103}$$

on the other, the nodal actions required to oppose the elastic reactions at each j-th element, as evaluated as in Eq. 2.96 according to the local DOF system, may be collected at global nodes.

Such collection is illustrated in Figure 2.12 for the second DOF of the global node g8, and in particular the force component V_{g8}, namely the 44-th component of $\underline{G}_g$; such a force component collects the contributions aligned with the $\hat{j}_{g8}$ unit vector from element 3, local node 3, and element 4, local node 4, named $V_{g8\leftarrow e3}$ and $V_{g8\leftarrow e4}$, respectively.

Figure 2.12 equations relate the nodal force components expressed with respect to the element reference systems with the global force component under scrutiny; in particular we have

$$V_{g8\leftarrow e3} = U_{e3n3}\langle\hat{i}_{e3}, \hat{j}_{g8}\rangle + V_{e3n3}\langle\hat{j}_{e3}, \hat{j}_{g8}\rangle + W_{e3n3}\langle\hat{k}_{e3}, \hat{j}_{g8}\rangle \tag{2.104}$$

$$V_{g8\leftarrow e4} = U_{e4n4}\langle\hat{i}_{e4}, \hat{j}_{g8}\rangle + V_{e4n4}\langle\hat{j}_{e4}, \hat{j}_{g8}\rangle + W_{e4n4}\langle\hat{k}_{e4}, \hat{j}_{g8}\rangle. \tag{2.105}$$

If we want to collect the contribution along the global DOFs of the

forces collected on element 4 in the algebraic relation

$$\underline{G}_{g \leftarrow e4} = \underline{\underline{P}}'_{e4}\, \underline{G}_{e4} \tag{2.106}$$

the 44-th row of the $\underline{\underline{P}}'$ - whose row and column cardinality equates that of the global and the elemental DOF, respectively - may be compiled based on 2.105; in particular, its nonzero terms are

$$\left[\underline{\underline{P}}'_{e4}\right]_{44,4} = \langle \hat{j}_{g8}, \hat{i}_{e4} \rangle \qquad\qquad \left[\underline{\underline{P}}'_{e4}\right]_{44,12} = \langle \hat{j}_{g8}, \hat{k}_{e4} \rangle$$
$$\left[\underline{\underline{P}}'_{e4}\right]_{44,8} = \langle \hat{j}_{g8}, \hat{j}_{e4} \rangle$$

being 4,8,12 the index locations of $U_{e4n4}, V_{e4n4}, W_{e4n4}$ within $\underline{G}_{e4}$.

By repeating the procedure for each global DOF, and for each element, it is found that the $\underline{\underline{P}}'_{ej}$ matrices equate the transpose of the $\underline{\underline{P}}_{ej}$ matrices associated to the same element, and hence Eq. 2.105 may be recast for each element as

$$\underline{G}_{g \leftarrow ej} = \underline{\underline{P}}^{\top}_{ej}\, \underline{G}_{ej}, \quad \forall j \tag{2.107}$$

thus obtaining a transformation from element DOFs to their contributes to global counterparts.

The role of $\underline{\underline{P}}^{\top}_{ej}$ in such a local-to-global mapping Eq. pairs the role of $\underline{\underline{P}}_{ej}$ in the global-to-local relation expressed in Eq. . A strict inverse relation may not be defined due to the different cardinality of the two DOF sets, and $\underline{\underline{P}}_{ej}$ lacks of a proper inverse, being in fact a rectangular matrix.

However, due to the mutually orthonormal nature of the $\underline{\underline{P}}_{ej}$ matrix columns, such a matrix may be defined *orthonormal* in the sense of the Moore-Penrose pseudoinverse; the $\underline{\underline{P}}^{\top}_{ej}$ matrixes that, for each element, control the local-to-global mapping are the pseudoinverses of the $\underline{\underline{P}}_{ej}$ matrixes that regulate the global-to-local mapping.

Based on 2.96, 2.103 and 2.107, the contribution of the j-th element to the elastic response of the structure may finally be described as the vector of global force components

$$\underline{G}_{g \leftarrow ej} = \underline{\underline{P}}^{\top}_{ej}\, \underline{\underline{K}}_{ej}\, \underline{\underline{P}}_{ej}\, \underline{d}_{g}; \tag{2.108}$$

that have to be applied at the structure DOFs in order to equilibrate the elastic reactions that arise at the nodes of the j-th element, if a

deformed configuration is prescribed for the latter according to the $\underline{d}_g$ global displacement mode.

By accumulating the contribution of the various elements in a structure, the overall relation is obtained

$$\underline{G}_g = \sum_j \underline{G}_{g \leftarrow ej} = \left(\sum_j \underline{\underline{P}}_{ej}^\top \underline{\underline{K}}_{ej} \underline{\underline{P}}_{ej} \right) \underline{d}_g = \underline{\underline{K}}_g \underline{d}_g, \qquad (2.109)$$

that defines the $\underline{\underline{K}}_g$ global stiffness matrix as an assembly of the elemental contributions. The contribute accumulation at each summatory step is graphically represented in Fig. 2.13, in the case of the example structure of Fig. 2.9.

The global stiffness matrix is symmetric, and it shows nonzero terms at cells whose row and column indices are associate to two DOFs that are bridged by a direct elastic link – i.e., an element exists, that insists on both the nodes those DOFs pertain; since only a limited number of elements insist on each given node, the matrix is sparse, as shown in Fig. 2.13d.

An favourable numbering of the global nodes may be searched for, such that the nonzero terms are clustered within a (possibly) narrow band around the diagonal; the resulting stiffness matrix is hence *banded*, condition this that reduces both the storage memory requirements, and the computational effort in applying the various algebraic operators to the matrix.

The stiffness matrix (half-)bandwidth may be predicted by evaluating the bandwidth required for storing each element contribution

$$b_{ej} = (i_{\max} - i_{\min} + 1)\, l, \qquad (2.110)$$

and retaining the

$$b = \max_{ej} b_{ej} \qquad (2.111)$$

peak value; in the formula 2.110, l is the number of DOF per element node, whereas $i_{\max}$ and $i_{\max}$ are the extremal integer labels associated to the element nodes, according to the global numbering.
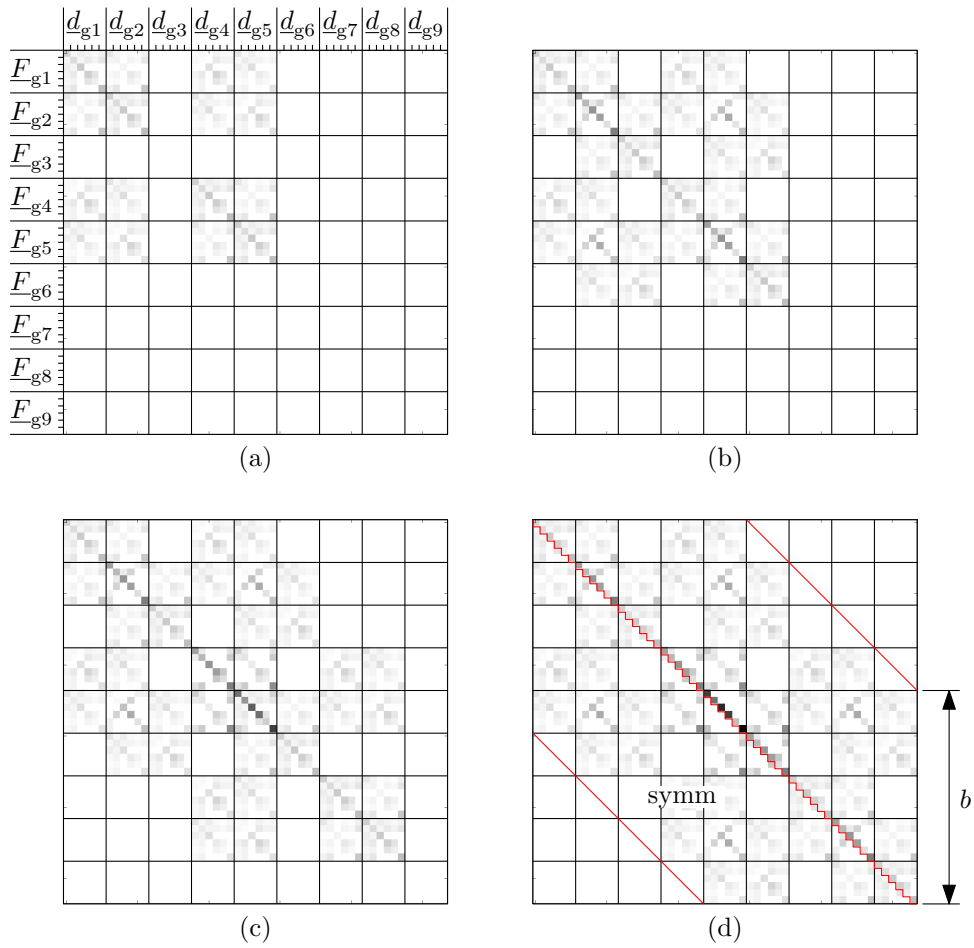
Figure 2.13: Graphical representation of the assembly steps for the stiffness matrix of the Fig. 2.9 structure. The zero-initialized form for the matrix that precedes the (a) step is omitted.

2.6.3 External forces assembly

The element vector forces are accumulated to derive global external forces vector $\underline{F}_g$, as in

$$\underline{F}_g = \sum_j \underline{\underline{P}}_{ej}^\top \underline{F}_{ej};$$
<div align="right">(2.112)</div>

the transposed $\underline{\underline{P}}_{ej}^\top$ mapping matrix is employed to translate the actions on the local DOFs to their global counterpart.

2.7 Constraints.

2.7.1 A pedagogical example.

Figure 2.14 represents a simple, pedagogical example of a three d.o.f. elastic system subject to a set of two kinematic constraints. The first, I, embodies a typical multi d.o.f. constraint[27], namely a 3:1 leverage between the vertical displacements d_3 and d_1 The second, II, consists in a single d.o.f., inhomogeneous constraint that imposes a fixed value to the d_2 vertical displacement.

Both the kinematic constraint may be cast in the same algebraic form

$$\sum_i \alpha_{ji}\, \underline{d}_i = \underline{\alpha}_j^\top \underline{d} = \Delta_j \qquad (2.113)$$

where $j = I, II$ and $i = 1 \dots 3$ the indexes span through the constraints and the model d.o.f.s, respectively, and the $\underline{\alpha}_j$ equation coefficient vectors and inhomogeneous terms are

$$\underline{\alpha}_I^\top = \begin{bmatrix} 3 & 0 & 1 \end{bmatrix} \qquad \Delta_I = 0$$
$$\underline{\alpha}_{II}^\top = \begin{bmatrix} 0 & 1 & 0 \end{bmatrix} \qquad \Delta_{II} = 0.2$$

In the absence of constraints, viable system configurations span the whole $\mathbb{R}^3$ space of Fig. 2.15 (a); viable configurations with respect to the first constraint alone span the *hyper*-plane/subspace[28] I, whereas the subspace II collects the feasible configurations with respect to the second constraint.

It is relevant to underline that the feasible configuration hyperplanes I and II are normal to the associated coefficient vectors $\underline{\alpha}_I$ and $\underline{\alpha}_{II}$, respectively.

The $I \cap II$ intersection subspace collects the configurations that satisfies both the constraints; such subspace is orthogonal to both $\underline{\alpha}_I$ and $\underline{\alpha}_{II}$.

If the constraints are assumed as ideal[29], the exerted reactions are orthogonal to the allowed displacements; reaction forces are confined on

---

[27]usually, and rather improperly, named *multipoint* constraint (MPC)

[28]The subspace of the feasible configurations with respect to a single, scalar linear equation is an hyperplane in the configuration space; due to the limited d.o.f. set cardinality, Figure 2.15 (a) represents a 2d plane within a 3d space. The *hyper*-nomenclature is preserved to

[29]or, namely, frictionless

$$\begin{array}{ll}
\text{I:} & 3\,d_1 - 0\,d_2 + 1\,d_3 = 0 \\
\text{II:} & 0\,d_1 + 1\,d_2 + 0\,d_3 = 0.2
\end{array}$$
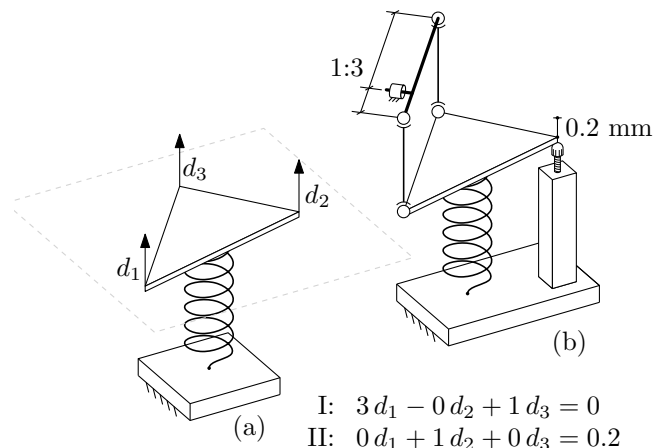
Figure 2.14: A pedagogical elastic three d.o.f. system, (a), subject to a few kinematic constraints (b).

a subspace of the reaction space that corresponds to[30] the orthogonal complement of the feasible subspace of the configuration space.

By moving on the constraint reaction space shown in 2.15 (b), the reaction forces associated to constraint I and II are thus proportional to the $\underline{\alpha}_{\mathrm{I}}$ and $\underline{\alpha}_{\mathrm{II}}$ vectors, respectively; the cumulative constraint reactions lie on the linear span of those two vectors, namely $\mathcal{L}(\alpha_{\mathrm{I}}, \alpha_{\mathrm{II}})$.

With reference to some concepts anticipated from the next paragraph, we may set d_1 as the only retained[31] DOF, thus leading to $\underline{\underline{\Lambda}}$ and $\underline{\Delta}$ terms equal to, respectively,

$$\underline{\underline{\Lambda}} = \begin{bmatrix} 1 \\ 0 \\ -3 \end{bmatrix} \qquad\qquad \underline{\Delta} = \begin{bmatrix} 0 \\ 0.2 \\ 0 \end{bmatrix}.$$

2.7.2 General formulation

A set of m constraints

$$d_j = \sum_{d_i \in \underline{d}_{\mathrm{R}}} \lambda_{ji} d_i + \Delta_j \tag{2.114}$$

---

[30]i.e. the two subspaces share, with adjusted physical dimensions, the same generator vectors.

[31]alternatively, d_3 may be chosen for such a role.

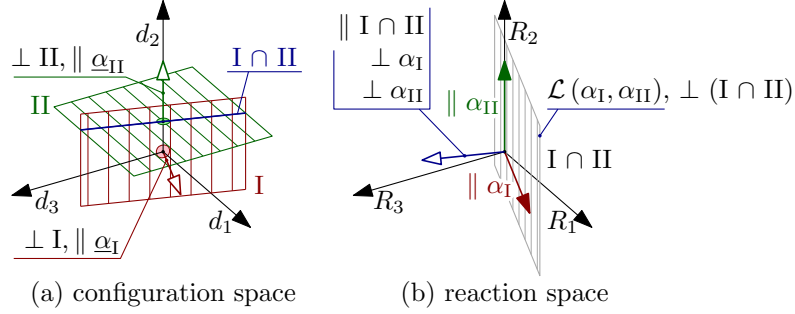Figure 2.15: Allowed system configurations and constraint reactions for the pedagogical example of Fig. 2.14. The allowed displacement sets are easily derived as the homogenous counterpart of (a), and are not represented here.

is defined that states the linear[32] dependence of a partition subset of the $\underline{d}$ DOFs vector terms, the *tied* ones, on the remaining d_i terms, that retain their independent nature. The independent terms are collected within a reduced cardinality DOF vector $\underline{d}_R$, and they are referred to as the *retained* ones[33].

Also the inhomogeneous Δ_j term is provided for in Eqn. 2.114 to accomodate constraints of the nonzero fixed displacement kind.

The following algebraic relation may then be derived, that defines the initial, unabridged $\underline{d}$ DOF vector terms based on the subset that produces the retained DOF vector $\underline{d}_R$

$$\underline{d} = \underline{\underline{\Lambda}}\,\underline{d}_R + \underline{\Delta}\,; \qquad (2.115)$$

the $\underline{\Delta}$ n-sized column vector collects the various Δ_j terms of the 2.114 constraint equations, and the n rows, $n-m$ columns $\underline{\underline{\Lambda}}$ matrix collects

- the identity relations between corresponding retained DOFs terms that appear in both $\underline{d}$ and $\underline{d}_R$, and

---

[32] more precisely, *linear variation* dependence, due to the presence of the inhomogeneous term.

[33] Here, the definition of the overall, retained, and tied DOF vectors, ($\underline{d}$, $\underline{d}_R$, $\underline{d}_T = \underline{d} \setminus \underline{d}_R$, respectively) is overloaded with both its DOF and DOF index (ordered) set counterparts, thus allowing e.g. the $d_i \in \underline{d}_R$ notation in a vector element context, and the $i \in \underline{d}_R$ notation in an integer index context.

Figure 2.16: Graphical representation for the $\underline{\underline{\Lambda}}$ matrix in Eq. 2.115; representative matrix rows are illustrated for a retained DOF, and for two tied DOFs, namely a fixed displacement subcase, and the general case.

- the λ_{ji} coefficients that define the linear variation dependence of the tied d_j DOF on the retained d_i DOF.

Figure 2.16 illustrates a few representatives of the rows whose assembly defines the $\underline{\underline{\Lambda}}$. In the case of a retained global DOF, d_l, which finds a counterpart in the h-th element of $\underline{d}_{\mathrm{R}}$, $= d_h^{\mathrm{R}}$, the associated row contains a single unit term at of the intersection of the l-th row with the h-th column, being zero elsewhere. In the case of a tied DOF of the plain fixed displacement kind (single DOF constraint), the associated row in $\underline{\underline{\Lambda}}$ is null, and the associated inhomogeneous term in $\underline{\Delta}$ equates the imposed value for the displacement. In the case of a tied DOF of the general kind, see Eq. 2.115, the associated row in the $\underline{\underline{\Lambda}}$ matrix is build upon the λ_{ji} linear relation coefficients.

It is finally worth to mention that the virtual displacements in the neighborhood of a feasible constrained configuration are restricted to the linear combinations of the $\underline{\underline{\Lambda}}$ matrix columns $\underline{\Lambda}_j$, i.e.

$$\delta \underline{d} = \underline{\underline{\Lambda}} \, \delta \underline{d}_R = \underline{\Lambda}_1 \, \delta \underline{d}_1^R + \underline{\Lambda}_2 \, \delta \underline{d}_2^R + \ldots \qquad (2.116)$$

with arbitrary virtual displacement values $\delta \underline{\mathrm{d}}_j^R$ for the retained DOF alone.

The ideal constraint hypothesis requires the reaction force vector $\underline{\mathrm{R}}$ to be orthogonal to a generic virtual displacement, and such condition hods if and only if $\underline{\mathrm{R}}$ is orthogonal to each the $\underline{\underline{\Lambda}}$ matrix columns, i.e.

$$\langle \underline{\Lambda}_j, \underline{\mathrm{R}} \rangle = 0 \quad \forall j, \tag{2.117}$$

or, equivalently,

$$\underline{\underline{\Lambda}}^\top \underline{\mathrm{R}} = \underline{0}. \tag{2.118}$$

2.8 The system of constrained equilibrium equations, and its solution.

The nodal DOF equilibrium equations derived by pairing i) the $\underline{\underline{\mathrm{K}}}\,\underline{\mathrm{d}}$ external forces required to keep the structure in a $\underline{\mathrm{d}}$ deformed configuration, see Eq. 2.109, ii) the actual external forces $\underline{\mathrm{F}}$ which are applied to the elements as distributed loads, see Eq. 2.112, or directly at nodes in form of concentrated loads, and iii) the reaction forces $\underline{\mathrm{R}}$ may be cast as

$$\underline{\underline{\mathrm{K}}}\,\underline{\mathrm{d}} = \underline{\mathrm{F}} + \underline{\mathrm{R}}. \tag{2.119}$$

Here, $\underline{\mathrm{d}}$ and $\underline{\mathrm{R}}$ are both unknown.

If constraints are applied, we have

$$\underline{\underline{\mathrm{K}}} \left(\underline{\underline{\Lambda}}\,\underline{\mathrm{d}}_{\mathrm{R}} + \underline{\Delta} \right) = \underline{\mathrm{F}} + \underline{\mathrm{R}} \tag{2.120}$$

and

$$\underline{\underline{\mathrm{K}}}\,\underline{\underline{\Lambda}}\,\underline{\mathrm{d}}_{\mathrm{R}} = \left(\underline{\mathrm{F}} - \underline{\underline{\mathrm{K}}}\,\underline{\Delta} \right) + \underline{\mathrm{R}}, \tag{2.121}$$

where the inhomogeneous part of the constraint equations is *de facto* assimilated to a further contribution to the external loads.

By projecting the equations on the subspace of allowed configurations

$$\underbrace{\underline{\underline{\Lambda}}^\top \underline{\underline{\mathrm{K}}}\,\underline{\underline{\Lambda}}}_{\underline{\underline{\mathrm{K}}}_{\mathrm{R}}} \underline{\mathrm{d}}_{\mathrm{R}} = \underbrace{\underline{\underline{\Lambda}}^\top \left(\underline{\mathrm{F}} - \underline{\underline{\mathrm{K}}}\,\underline{\Delta} \right)}_{\underline{\mathrm{F}}_{\mathrm{R}}} + \underbrace{\underline{\underline{\Lambda}}^\top \underline{\mathrm{R}}}_{=0}, \tag{2.122}$$

the contribution of the unknown reaction forces, that are normal to such a subspace – see Eq. 2.118, vanishes.

The linear system of *constrained* nodal DOF equilibrium equations is then set as

$$\underline{\underline{K}}_R \, \underline{d}_R = \underline{F}_R \tag{2.123}$$

and it may be solved for the retained DOF vector $\underline{d}_R$.

Once the solution vector $\underline{d}_R^*$ is found in terms of displacements at retained DOFs, the overall displacement vector and the unknown reaction forces may be derived as

$$\underline{d}^* = \underline{\underline{\Lambda}} \, \underline{d}_R^* + \underline{\Delta}; \tag{2.124}$$

and

$$\underline{R}^* = \underline{\underline{K}} \left(\underline{\underline{\Lambda}} \, \underline{d}_R^* + \underline{\Delta} \right) - \underline{F}. \tag{2.125}$$

Then, for each j-th element, the local DOFs vector may be derived based on

$$\underline{d}_{ej}^* = \underline{\underline{P}}_{ej} \, \underline{d}^*, \tag{2.126}$$

and consequently its in-plane

$$\underline{\epsilon} = \left(\underline{\underline{B}}_{ej}^0(\xi,\eta) + \underline{\underline{B}}_{ej}^1(\xi,\eta)z \right) \underline{d}_{ej}^* \tag{2.127}$$

and out-of-plane strain fields

$$\underline{\bar{\gamma}} = \underline{\underline{B}}_{ej}^{\bar{\gamma}}(\xi,\eta) \, \underline{d}_{ej}^*, \tag{2.128}$$

from which the stress components may be easily derived.

2.8.1   Rigid body link RBE2

A master (or retained, control, independent, etc.) C node is considered, whose coordinates are defined as x_C, y_C, z_C in a (typically) global reference system, along with a set of n P_i nodes whose coordinates are x_i, y_i, z_i.

A kinematic link is to be established such that the DOFs – or a subset of them – associated to the P_i nodes follow the rototranslations of the C control according to the rigid body motion laws.

In the case of a fully constrained P_i node we have

$$
\begin{bmatrix} u_i \\ v_i \\ w_i \\ \theta_i \\ \phi_i \\ \psi_i \end{bmatrix} = \underbrace{\begin{bmatrix} 1 & 0 & 0 & 0 & +(z_i - z_C) & -(y_i - y_C) \\ 0 & 1 & 0 & -(z_i - z_C) & 0 & +(x_i - x_C) \\ 0 & 0 & 1 & +(y_i - y_C) & -(x_i - x_C) & 0 \\ 0 & 0 & 0 & 1 & 0 & 0 \\ 0 & 0 & 0 & 0 & 1 & 0 \\ 0 & 0 & 0 & 0 & 0 & 1 \end{bmatrix}}_{\underline{\underline{L}}_i} \cdot \begin{bmatrix} u_C \\ v_C \\ w_C \\ \theta_C \\ \phi_C \\ \psi_C \end{bmatrix}
$$

$$(2.129)$$

where u, v, w (θ, ϕ, ψ) are the translation (rotation) vector components with respect to the x, y, z cartesian reference system. A subset of the above DOF dependency relations may be cast to obtain a partial constraining of the P_i node; a free relative motion of such node with respect to the rigid body is allowed at the unconstrained DOFs.

External actions that are applied to tied P_i DOFs are reduced to the master node in form of a statically equivalent counterpart; the contributions deriving from each P_i node are finally accumulated.

2.9   Advanced modeling tools

2.9.1   Inertia relief

Inertia relief[34] refers to an analysis procedure that allows unconstrained systems – or systems otherwise susceptible to stress-free motions – to be subjected to a quasi-static analysis by taking rigid body inertia forces into account.

Conventional static analysis cannot be performed for such systems since, in the absence of constraints, the stiffness matrix is singular. The structure response is measured relative to a steady state accelerating frame, whose motion is induced by the (usually nonzero) external load resultants.

The inertia relief solution procedure provides for three steps, namely i) the rigid body mode evaluation, ii) the assessment of the inertia relief loads, and iii) the solution of a supported, self-equilibrated static loadcase within the moving frame.

A set of nodal DOFs is supplied, one each expected rigid body motion, whose *imposed* displacements values uniquely define the structure positioning in space; also, they may be employed in supporting the structure to untangle the stiffness matrix rank-deficiency.

The $\underline{t}_l$ rigid body modes are evaluated by sequentially setting each of these *support* DOF to unity, while retaining the others to zero, and solving for the system of nodal equilibrium equations

$$\underline{\underline{K}} \, \underline{d} \, = \, \underline{F} \,, \tag{2.130}$$

where $\underline{\underline{K}}$ is the structure stiffness matrix, in the absence of further external loads, i.e. $\underline{F} = 0$. Since the tied/retained condition of the structure DOFs does not vary throughout the sequence of aforementioned loadcases, comprised of the final step introduced in the following, a single $\underline{\underline{L}} \, \underline{\underline{L}}^{\top}$ Cholesky system matrix decomposition is required by the procedure, whose computational burden is thus not significantly increased with respect to the usual static solution.

A rigid body, steady state acceleration field is defined as the linear

---

[34]XXX some cut and paste from the MSC.Marc vol A manual, please rewrite as required to avoid copyright infringement.

combination of the so defined $\underline{t}_l$ rigid body modes

$$\ddot{\underline{d}} = \underbrace{\begin{bmatrix} \cdots & \underline{t}_l & \cdots \end{bmatrix}}_{\underline{\underline{T}}} \underbrace{\begin{bmatrix} \vdots \\ \alpha_l \\ \vdots \end{bmatrix}}_{\underline{\alpha}}, \qquad (2.131)$$

whose α_l coefficients define the modal acceleration vector $\underline{\alpha}$. Those acceleration terms are then evaluated according to the inertial equilibrium of the structure under the applied $\underline{F}$ external loads, condition, this, that may be stated as

$$\underline{\underline{T}}^\top \underline{\underline{M}}\, \underline{\underline{T}}\, \underline{\alpha} = \underline{\underline{T}}^\top \underline{F} \qquad (2.132)$$

The projection of the equilibrium equations onto the subspace defined by the linear span of the $\underline{t}_l$ rigid body mode vectors – i.e. the left multiplication of both the equation sides by the $\underline{\underline{T}}^\top$ matrix, is solved in place of the overdetermined linear system

$$\underline{\underline{M}}\, \underline{\underline{T}}\, \underline{\alpha} = \underline{F}\, [+ \underline{R}_l]$$

since the $\underline{R}_l$ reaction forces associated to the rigid body constraints balance the equilibrium residual components that are orthogonal to such allowed configuration subspace.

The inertia relief forces may then be quantified as $\underline{\underline{M}}\, \underline{\underline{T}}\, \underline{\alpha}$, and superposed to the initial external loads, thus leading to a self equilibrated loading condition in the context of the steady state accelerating frame; by employing the support DOFs to establish a positioning constraint set, the elastic problem may finally be solved in the form

$$\underline{\underline{K}}\, \underline{d} = \underline{F} - \underline{\underline{M}}\, \underline{\underline{T}}\, \underline{\alpha}, \qquad (2.133)$$

The $\underline{d}$ displacement components are expressed with respect to a reference frame that clings to the possibly accelerating structure through the support DOFs; due to the self-equilibrated nature of the applied loads in the moving frame, reaction forces at supports are zero.

As a closing comment, the MSC.Marc solver employs a lumped definition for the system mass matrix for evaluating inertia relief forces.

2.9.2 Harmonic response analysis

The equilibrium equations of a multiple DOF system subject to elastic, inertial and viscous actions may be stated in the general form

$$\underline{\underline{M}}\,\ddot{\underline{d}} + \underline{\underline{C}}\,\dot{\underline{d}} + \underline{\underline{K}}\,\underline{d} = \underline{f}(t), \quad \underline{d} = \underline{d}(t) \tag{2.134}$$

where:

- $\underline{\underline{M}}$ is the mass matrix, which is symmetric and positive definite;

- $\underline{\underline{C}}$ is the viscous damping matrix, which is symmetric and positive semidefinite;

- $\underline{\underline{K}}$ is the elastic stiffness matrix, which is symmetric and positive semidefinite: complex terms may appear within the stiffness matrix to represent structural damping contributions;

- $\underline{f}(t)$ is the vector of the external (generalized) forces;

- $\underline{d}(t)$ collects the system DOFs, which vary in time.

The system response is assumed linear – a strong assumption, this, that hardly holds in complex structures as the automotive chassis under scrutiny. The lack of nonlinear analysis tools whose modeling and computational effort is comparable with respect to the one presented in the present section, pushes for some laxity in the linearity prerequisite check, and for the acceptance of a certain extent of error.

The applied force is assumed periodic in time, and so is the long term solution, if linearity holds. Moreover, Fourier decomposition may be applied, and there is no lack in generality in further assuming an harmonic forcing term, and hence an harmonic solution. We have

$$\underline{f}(t) = \frac{\bar{\underline{f}}\,e^{j\omega t} + \bar{\underline{f}}^{*}e^{-j\omega t}}{2} = \mathrm{Re}(\bar{\underline{f}}\,e^{j\omega t}) \tag{2.135}$$

where the asterisk superscript denotes the complex conjugate variant of the base vector. We recall that the compact notation

$$\underline{f}(t) = \bar{\underline{f}}\,e^{j\omega t} \tag{2.136}$$

extensively employed below defines a complex form for the driving force, whose real part is the portion which is physically applied to the nodes over time, i.e.

$$\text{Re}(\bar{\underline{f}}\, e^{j\omega t}) = \text{Re}(\bar{\underline{f}}\,)\cos\omega t - \text{Im}(\bar{\underline{f}}\,)\sin\omega t \qquad (2.137)$$

This compact formalism is not rigorous but still it is effective, and hence commonly employed. Any phase difference amongst the applied nodal excitations may be described by resorting to the complex nature of the $\bar{\underline{f}}$ vector terms.

In the neglection of the transient response, the harmonic tentative solution

$$\underline{d}\,(t) = \bar{\underline{d}}\, e^{j\omega t} \qquad (2.138)$$

is substituted within Eq. 2.134, thus obtaining

$$\left(-\omega^2\,\underline{\underline{M}} + j\omega\,\underline{\underline{C}} + \underline{\underline{K}}\right)\bar{\underline{d}} = \bar{\underline{f}} \qquad (2.139)$$

where the $e^{j\omega t}$ time varying, generally nonzero factors are simplified away.

Expression 2.140 defines a system of linear complex equations, one each DOF, in the complex unknown vector $\bar{\underline{d}}$; equivalently, each complex equation and each unknown term may be split into the associated real and imaginary parts, thus leading to a system of linear, real equations whose order is twice the number of the discretized structure DOFs.

The system matrix varies with the ω parameter, and in particular its stiffness contribute $\underline{\underline{K}}$ is dominant for low ω values, whereas the $\underline{\underline{C}}, \underline{\underline{M}}$ terms acquire relevance with growing ω.

In distributed inertia systems, however, it is a misleading claim that the stiffness matrix contribution becomes negligible with high ω values, since – with the notable exception of external loads that are directly applied to concentrated masses or rigid bodies – the pulsation is unphysically high above which such behaviour arises.

Since Eqns. 2.140 are independently solved for each ω value, it constitutes no added complexity to let $\underline{\underline{M}}$, $\underline{\underline{C}}$, $\underline{\underline{K}}$ and $\bar{\underline{f}}$ vary according to the same parameter.

Finally, in the absence of the damping-related imaginary terms within the system matrix, the Eq. 2.140 problem algebraic order is led back to the bare number of system DOFs; in fact, two independent

real system of equations – that share a common $\underline{\underline{L}}\,\underline{\underline{L}}^{\top}$ matrix decomposition – may be cast for the real and the imaginary parts of $\bar{\underline{d}}$ and $\bar{\underline{f}}$.

2.9.3   Modal analysis

The present paragraph briefly deals with the structure's natural modes, i.e. those periodic[35] motions that are allowed according to Eq. 2.134, in the further absence of externally applied loads.

A necessary condition for a motion to endure in the absence of a driving load is the absence of dissipative phenomena; it is hence necessary to have a zero $\underline{\underline{C}}$ damping matrix, whereas the $\underline{\underline{K}}$ stiffness matrix must be free of imaginary terms. This hypothesis holding, Eq. 2.140 is reduced to the following real-term algebraic form

$$\left(-\omega^2\,\underline{\underline{M}} + \underline{\underline{K}}\right)\bar{\underline{d}} = \underline{0} \tag{2.140}$$

whose nontrivial solutions constitute a set of $(\omega_i^2, \hat{\underline{d}}_i)$ *generalized* eigenvalue/eigenvector pairs, one each system DOF, if eigenvalue multiplicity is taken into account.

In the context of each $(\omega_i^2, \hat{\underline{d}}_i)$ pair, ω_i is the natural pulsation ($\omega_i = 2\pi f_i$, where f_i is the natural frequency), whereas the $\hat{\underline{d}}_i$ vector of generalized displacemts is named natural mode.

The extraction of the Eq. 2.140 nontrivial solutions reduces to a *standard* eigenvalue problem is the algebraic form is left-multiplied by the mass matrix inverse, i.e.

$$\left(\underline{\underline{M}}^{-1}\,\underline{\underline{K}} - \omega^2\,\underline{\underline{I}}\right)\hat{\underline{d}} = \underline{0}\,; \tag{2.141}$$

the availability of solvers that specifically approach the generalized problem avoid such computationally uneconomical preliminary.

It is worth to recall that in the case of eigenvalues with non-unit multiplicity – concept, this, that is to be contextualized within the limited precision floating point arithmetics[36] – the associated eigenvectors must be considered only through their linear combination; the specific selection of the base elements for representing such a subspace (i.e.,

---

[35]*harmonic* in the context of linearly behaving systems
[36]XXX

each single eigenvector) derives in fact from the unpredictable inter-action between the truncation error and the inner mechanics of the numerical procedure.

Also, the eigenvectors that are associated to eigenvalues of unit mul-tiplicity are returned by the numerical solver in the misleading form of a definite vector, whereas an arbitrary (both in sign and magnitude) scaling factor has to be prepended.

In particular, any speculation which is not robust with respect to such arbitrary scaling (or combination) is of no engineering relevance, and must be avoided.

Finally, in continuous elasticity, no upper bound exists for natural frequencies; in Finite Element (FE) discretized structure, an apparent upper bound exists, which depends on local element size[37].

A common normalizing rule for the natural modes is the one that produces a unit modal mass m_i, i.e.

$$m_i = \hat{\underline{d}}_i^\top \underline{\underline{M}} \, \hat{\underline{d}}_i = 1 \tag{2.142}$$

this rule is e.g. adopted by the MSC.Marc solver in its default config-uration.

The resonant behaviour of the system in correspondence with a natural frequency may be investigated by substituting the following tentative solution

$$\underline{x}(t) = a \, \hat{\underline{d}}_i \sin(\omega_i t) \tag{2.143}$$

within the dynamic equilibrium equations 2.134, with

$$f(t) = \hat{\underline{f}} \cos(\omega_i t), \tag{2.144}$$

and thus obtaining

$$\underbrace{\left(-\omega_i^2 \, \underline{\underline{M}} + \underline{\underline{K}}\right) \hat{\underline{d}}_i}_{= \underline{0}} a_i \sin(\omega_i t) + \omega_i a_i \, \underline{\underline{C}} \, \hat{\underline{d}}_i \cos(\omega_i t) = \bar{\underline{f}} \cos(\omega_i t). \tag{2.145}$$

By simplifying away the generally nonzero time modulating factors, and by left-multiplying both equation sides by $\hat{\underline{d}}^\top$ – i.e. by projecting

---

[37]In particular, the natural oscillation period for the highest dynamic mode is estimated with order of magnitude precision as the minimum time it takes a pressure wave to travel between two different nodes in the discretized structure.

the equation residual along the subspace defined by the eigenvector itself, we obtain an amplitude term in the form

$$a_i = \frac{\hat{\underline{d}}^\top \bar{\underline{f}}}{\omega_i \, \hat{\underline{d}}^\top \, \underline{\underline{C}} \, \hat{\underline{d}}_i} \qquad (2.146)$$

whose singularity is prevented only a) in the presence of a damping matrix that associates nonzero and non-orthogonal viscous reactions to the motion described by the natural mode under scrutiny, or b) if the driving load is orthogonal to such natural mode, i.e. it unable to perform periodic work on such a motion. The nature of the expression 2.146 numerator will be further discussed in the following paragraph.

2.9.4 Harmonic response through mode superposition

In the case the eigenvalues associated with the dynamic modes are all distinct[38], the following orthogonality conditions hold

$$\hat{\underline{d}}_j^\top \, \underline{\underline{M}} \, \hat{\underline{d}}_i = m_i \delta_{ij} \qquad\qquad \hat{\underline{d}}_j^\top \, \underline{\underline{K}} \, \hat{\underline{d}}_i = m_i \omega_i^2 \delta_{ij} \qquad (2.147)$$

where δ_{ij} is the Kroneker delta function, and $m_i = 1$ is the i-th modal mass, which is unitary due to the the $\hat{\underline{d}}_i$ unit modal mass normalization.

It is further assumed that it is possible to describe the elastic body motion through a linear combination of a (typically narrow) subset of the dynamic natural modes. Such assumption may be rationalized in two equivalent ways: on one hand, the contribution of the neglected modes is assumed negligible, and hence ignored; on the other hand, it is imagined that a set of kinematic constraints is imposed, that rigidly impede any additional system motion with respect to the chosen set. According to this latter explanation, reaction forces will be raised that absorb any equilibrium residual term which is orthogonal with respect to the allowed displacements.

The subset defined by the first m eigenvectors $(1 \leq m \ll n)$ are commonly employed, whereas different assortments are possible; a control calculation perfomed with a wider base may be employed for error estimation.

---

[38]condition, this, that is assumed to hold; a slightly perturbed FE discretization may be effective in separating the instances of a theoretically multiple natural frequency.

By stacking those first m normalized column eigenvectors into the $\underline{\underline{\Xi}}$ matrix below,

$$\underline{\underline{\Xi}} = \begin{bmatrix} \hat{\underline{d}}_1 & \cdots & \hat{\underline{d}}_l & \cdots & \hat{\underline{d}}_m \end{bmatrix}, \qquad (2.148)$$

any $\underline{\bar{d}}$ configuration belonging to the linear span of the selected modes may be expressed through a vector of m *modal* coordinates $\bar{\xi}_l$, as in

$$\underline{\bar{d}} = \underline{\underline{\Xi}} \, \underline{\bar{\xi}} \qquad (2.149)$$

.

Due to the natural modes orthogonality conditions 2.147, the $\underline{\underline{\Xi}}$ tranformation matrix diagonalizes both the mass and the stiffness matrices, since

$$\underline{\underline{\Xi}}^{\top} \underline{\underline{M}} \, \underline{\underline{\Xi}} = \underline{\underline{I}} \qquad \underline{\underline{\Xi}}^{\top} \underline{\underline{K}} \, \underline{\underline{\Xi}} = \underline{\underline{\Omega}} = \mathrm{diag}(\omega_l^2); \qquad (2.150)$$

by appling such transformation to the damping matrix, however, a dense matrix is generally obtained.

The *Rayleigh* or *proportional* damping matrix definition assumes that the latter may be passably represented as a linear combination of the mass matrix and of the stiffness matrix: in particular

$$\underline{\underline{C}} = \alpha \underline{\underline{M}} + \beta \underline{\underline{K}} \qquad (2.151)$$

where α and β are commonly named *mass* and *stiffness matrix multipliers*, respectively; according to such assumption, the damping matrix is also diagonalized by the $\underline{\underline{\Xi}}$ tranformation matrix.

Equation 2.140 algebraic problem may be cast in terms of the m ξ_l modal unknowns, thus obtaining

$$\underline{\underline{\Xi}}^{\top} \left(-\omega^2 \underline{\underline{M}} + j\omega \underline{\underline{C}} + \underline{\underline{K}} \right) \underline{\underline{\Xi}} \, \underline{\bar{\xi}} = \underline{\underline{\Xi}}^{\top} \underline{\bar{f}} \qquad (2.152)$$

which reduces to the diagonal form

$$\left(-\omega^2 \underline{\underline{I}} + j\omega \left(\alpha \underline{\underline{I}} + \beta \underline{\underline{\Omega}} \right) + \underline{\underline{\Omega}} \right) \underline{\bar{\xi}} = \underline{\underline{\Xi}}^{\top} \underline{\bar{f}}, \qquad (2.153)$$

or, equivalently, to the set of m independent complex equations

$$\left(-\omega^2 + j\omega \left(\alpha + \beta \omega_l^2 \right) + \omega_l^2 \right) \xi_l = q_l, \quad j = 1 \ldots m \qquad (2.154)$$

where $q_l = \left\langle \underline{\hat{d}}_l, \underline{\bar{f}} \right\rangle$ is the coupling factor between the external load and the l-th natural mode.

The algebraic equation above may be interpreted as the characteristic equation of an harmonically driven single DOF oscillator that exhibits the following properties:

- its mass is unity;

- its natural frequency equals that of the l-th natural mode ω_l;

- its damping ratio ζ_l is a combination of the two Rayleigh damping coefficients, i.e.

$$\zeta_l = \frac{1}{2}\left(\frac{\alpha}{\omega_l} + \beta\omega_l\right);$$

- the external load real(imaginary) term is defined as the cyclic work that the external load performs upon a system motion described as the sinusoidal (cosinusoidal) modulation in time of the l-th modal shape, divided by π.[39]

The uncoupled equations 2.154 may be solved resorting to complex division arithmetics, thus leading to the definition of the $\bar{\xi}_l$ modal amplitude and phase terms; in particular we have that the l-th modal shape is modulated in time according to the function

$$\begin{aligned}
\xi_l(t) &= \mathrm{Re}(\bar{\xi}_l)\cos\omega t - \mathrm{Im}(\bar{\xi}_l)\sin\omega t \\
&= \left|\bar{\xi}_l\right|\cos\left(\omega t + \psi_l - \phi_l\right)
\end{aligned}$$

whose terms are detailed in the following.

The auxiliary parameters

$$a_l = 1 - r_l^2 \qquad\qquad b_l = 2\zeta_l r_l \qquad\qquad r_l = \frac{\omega}{\omega_l}$$

are first defined; we then have the oscillation amplitude and phase

---

[39]In the case of a concentrated load that act on a single DOF, q_j equates the product of the load magnitude with the associated component in $\underline{\hat{d}}_l$, i.e. the generalized displacement at the specific node, as shown by the FE postprocessor.

terms

$$|\bar{\xi}_l| = \frac{|\bar{q}_l|}{\omega_l^2} \frac{1}{\sqrt{a_l^2 + b_l^2}}$$

$$\psi_l = \arg(\bar{q}_l)$$

$$\phi_l = \arg(a_l + jb_l)$$

or, equivalently, the real and imaginary parts

$$\mathrm{Re}(\bar{\xi}_l) = \frac{1}{\omega_l^2} \frac{a_l \, \mathrm{Re}(\bar{q}_l) + b_l \, \mathrm{Im}(\bar{q}_l)}{a_l^2 + b_l^2}$$

$$\mathrm{Im}(\bar{\xi}_l) = \frac{1}{\omega_l^2} \frac{a_l \, \mathrm{Im}(\bar{q}_l) - b_l \, \mathrm{Re}(\bar{q}_l)}{a_l^2 + b_l^2}.$$

2.9.5 Linearized pre-buckling analysis

A few notes.

According to the linearized pre-buckling analysis, the structure is considered in an oxymoronic configuration which is both *pre-stressed* and *undeformed*.

The $\underline{\sigma}^0$ *pre-stress* condition is evaluated through a linear preliminary analysis of the structure subject to a set of applied loads, and potentially inhomogeneous constraints; both the preload and the associate stress field may be scaled by a common λ amplification factor, and the structure behaviour is parametrically examined with varying λ.

The displacement and rotation fields associated this preliminary analysis are not however retained in the subsequent step, in contrast to the pre-stress; such looseness is commonly justified based on the assumed smallness of such deflections.

For each element of the structure, the stiffness matrix is derived by a) taking into account the contribution of the $\underline{\sigma}^0$ pre-stress to the internal virtual work, and b) by employing a second order, nonlinear, *large rotation* formulation for the $\underline{B}$ matrix that derives the strain tensor from nodal DOFs. Details are here omitted[40], and only the following placeholder formula for the internal virtual work is proposed

$$
\begin{aligned}
\delta U_{\mathrm{i}} &= \iiint_V \delta\,\underline{\epsilon}^\top \left(\underline{\sigma}_0 + \underline{\underline{D}}\,\underline{\epsilon}\right) dV \\
&= \iiint_V \left[\underline{\underline{B}}\,(\underline{d})\delta\,\underline{d}\right]^\top \left(\underline{\sigma}_0 + \underline{\underline{D}}\,\underline{\underline{B}}\,(\underline{d})\,\underline{d}\right) dV \\
&= \ldots \\
&= \delta\,\underline{d}\left(\left(\underline{\underline{K}}_{\mathrm{ej}}^{\mathrm{M}} + \underline{\underline{K}}_{\mathrm{ej}}^{\mathrm{G}}\right)\underline{d} + \mathrm{o}\,(\underline{d})\right).
\end{aligned}
$$

The resulting element stiffness matrix is obtained as the sum of two distinct contributions; the first contribution $\underline{\underline{K}}_{\mathrm{ej}}^{\mathrm{M}}$ is named *material* stiffness matrix and, in the absence of large element reorientation in space, it coincides with the customary definition of element stiffness matrix. The second contribution $\underline{\underline{K}}_{\mathrm{ej}}^{\mathrm{G}}$ is named *geometric* stiffness matrix and it embodies the corrective terms due to the interaction of the pre-stress with the rotations; such term is invariant with the

---

[40]see e.g. reference [4]

material properties, and it scales with the pre-stress itself, i.e. with the λ amplification factor. This second contribution embodies the *stress stiffening* and *stress softening* effects.

Both the two terms are obtained by relying on the initial coordinates of the element nodes, thus effectively neglecting the preload-induced deflections.

The elemental material and geometric stiffness matrix are then assembled into their global counterparts, and contraints are applied that are consistent[41] with the ones employed in deriving the pre-stress.

The following relation is thus obtained in the neighborhood of a λ-scaled, pre-stressed configuration

$$\left(\underline{\underline{K}}^{\,M} + \lambda \underline{\underline{K}}^{\,G} \right) \delta \underline{d} = \delta \underline{F} \tag{2.155}$$

that relates a small variation in the externally applied actions $\delta \underline{F}$ with the required adjustments in the structure configuration $\delta \underline{d}$ for the sake of equilibrium; the cumulative $\underline{\underline{K}}^{\,m} + \lambda \underline{\underline{K}}^{\,g}$ term is named *tangent* stiffness matrix upon its role in locally orienting the equilibrium path.

Of a particular interest is the case of a nonzero variation in configuration for which equilibrium is preserved in the absence of external load variation; such condition is a prerequisite for a bifurcation of the equilibrium path. We have in particular an homogenous system of equations

$$\left(\underline{\underline{K}}^{\,M} + \lambda_i \underline{\underline{K}}^{\,G} \right) \delta \hat{\underline{d}}_i = 0 \tag{2.156}$$

whose nontrivial solutions are in form of generalized[42] eigenpairs $(\lambda_i, \delta \hat{\underline{d}}_i)$, with λ_i values that zero the determinant of the tangent stiffness matrix, and are hence named *critical* pre-stress (or preload, or load) amplification factor.

---

[41]not stricty equal in theory, since some variations are allowed with respect in particular positioning and symmetry constraints. FE packages may however limit such theoretically allowed redefinition of constraints.

[42]an equivalent, standard

$$\left(\underline{\underline{A}} - \eta_i \underline{\underline{I}} \right) \underline{v}_i = 0$$

eigenproblem may be defined with

$$\underline{\underline{A}} = \left[\underline{\underline{K}}^{\,M} \right]^{-1} \underline{\underline{K}}^{\,G}, \quad \lambda_i = -1/\eta_i, \quad \underline{v}_i = \delta \hat{\underline{d}}_i.$$

$$N_{AB} = N_{CA} = +\frac{F}{\sqrt{3}}$$

$$N_{BC} = -\frac{F}{2\sqrt{3}}$$

$$N_{\mathrm{crit},i} = -\frac{\pi^2 i^2 EJ}{l^2}$$

$$\lambda_1 = -\frac{\pi^2 EJ}{l^2}\frac{\sqrt{3}}{F}$$

moltepl. 2

minimum λ_i in absolute value

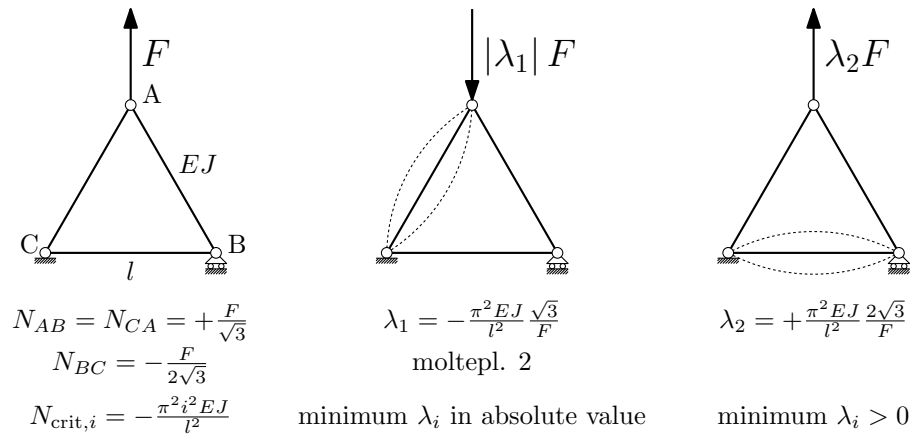$$\lambda_2 = +\frac{\pi^2 EJ}{l^2}\frac{2\sqrt{3}}{F}$$

minimum $\lambda_i > 0$

Figure 2.17: In the case the load that induces the pre-stress state is subject to inversion, the minimum amplification factor in modulus is to be considered. On the other hand, if a load inversion may be excluded, the minimum among the positive amplification factors is to be considered.

In correspondence of critical λ_i values, the elastic reactions are unable to restrain an arbitrary scaled $\delta\,\hat{\underline{\mathrm{d}}}_i$ perturbation of the structure configuration, and the related variation in stress/strain values, thus obtaining a *indifferent equilibrium* condition.

Chapter 3

Miscellaneous
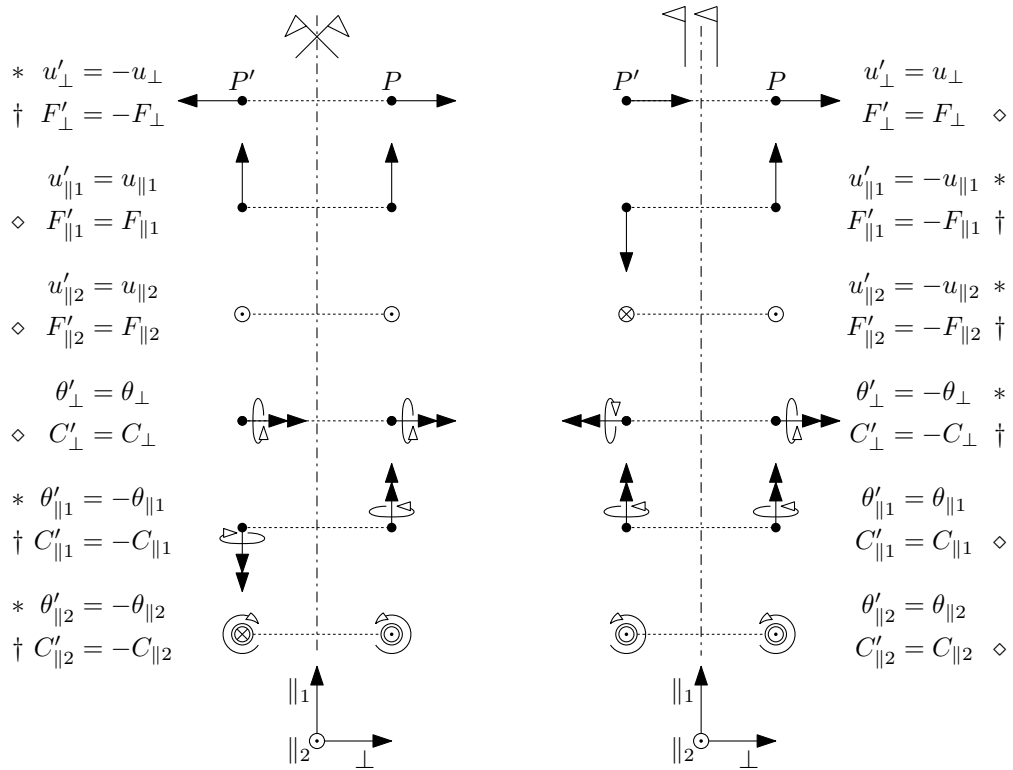
Figure 3.1: An overview of symmetrical and skew-symmetrical (generalized) loading and displacements.

3.1 Symmetry and skew-symmetry conditions

Symmetric and skew-symmetric loading conditions are mostly relevant for linearly-behaving systems; a nonlinear system may develop an asymmetric response to symmetric loading (e.g. column buckling).

Figure 3.1 collects symmetrical and skew-symmetrical pairs of vectors and moment vectors (moments); those (generalized) vectors are applied at symmetric points in space with respect to the reference plane. Normal and parallel to the plane vectors are considered, that may embody the same named components of a general vector.

The pair members may be moved towards the reference plane up to a vanishing distance ϵ; a point on the reference plane coincides with its image. In the case different (in particular, opposite and nonzero)

104
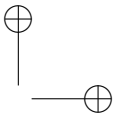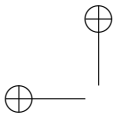
field vectors are associated to the two coincident pair members, single valuedness does not hold at the reference plane; such condition deserves an attentive rationalization whenever a physical field (displacement field, applied force field, etc.) is to be represented.

Those vector and moment pairs may represent generalized forces (both internal and external) and displacements.

The $*$ (generalized) displacement components may induce material discontinuity at points laying on the [skew-]symmetry plane, if nonzero. They have to be constrained to zero value at those points, thus introducing [skew-]symmetry constraints.

These constraints act in place of the portion of the structure that is omitted from our model, since the results for the whole structure may be derived from the modeled portion alone, due to [skew-]symmetry.

In case of symmetry, a constraint equivalent to a planar joint is to be applied at points laying on the symmetry plane for ensuring displacement/rotation continuity between the modeled portion of the structure, and its image. In case of skew-symmetry, a constraint equivalent to a *doweled sphere - slotted cylinder* joint (see Figure 3.1), where the guide axis is orthogonal to the skew-symmetry plane, is applied at the points belonging to the intersection between the deformable body and the plane.

The $\diamond$ internal action components are null at points pertaining to the [skew-]symmetry plane, since they would otherwise violate the action-reaction law. The complementary $\dagger$ internal action components are generally nonzero at the [skew-]symmetry plate.

The $\dagger$ external action components are not allowed at points along the [skew-]symmetry plane; instead, the complementary $\diamond$ generalized force components are allowed, if they are due to external actions.

In the case of a symmetric structure, generally asymmetric applied loads may be decomposed in a symmetric part and in a skew-symmetric part; the problem may be solved by employing a half structure model for both the loadcases; the results may finally be superposed since the system is assumed linear.
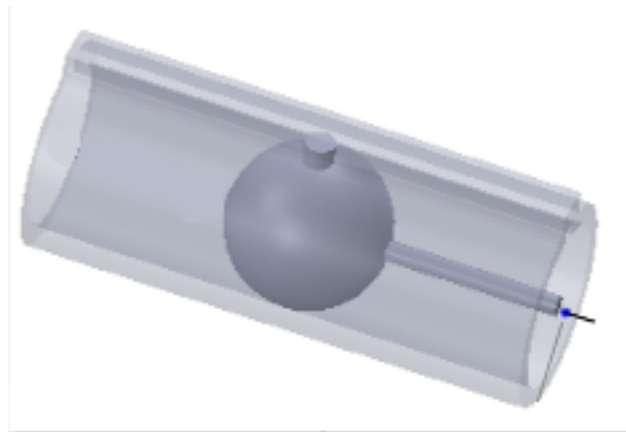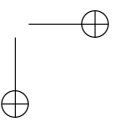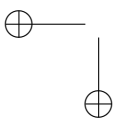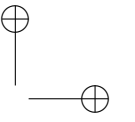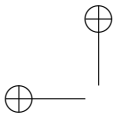
3.2 Periodicity conditions

TODO, if needed.
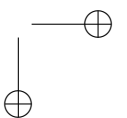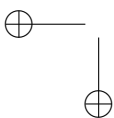
Figure 3.2: The doweled sphere - slotted cylinder joint, which is associated to the skew-symmetry constraint. In this particular application, the cylindrical guide may be considered as grounded.

Bibliography

[1] A. E. H. Love, *A treatise on the mathematical theory of elasticity*. Cambridge university press, 2013.

[2] C. Hua, "An inverse transformation for quadrilateral isoparametric elements: analysis and application," *Finite elements in analysis and design*, vol. 7, no. 2, pp. 159–166, 1990.

[3] T. J. Hughes and T. Tezduyar, "Finite elements based upon mindlin plate theory with particular reference to the four-node bilinear isoparametric element," *Journal of applied mechanics*, vol. 48, no. 3, pp. 587–596, 1981.

[4] J. Oden, "Calculation of geometric stiffness matrices for complex structures.," *AIAA Journal*, vol. 4, no. 8, pp. 1480–1482, 1966.